DESIGN OF PVDF TRANSDUCERS FOR ACOUSTIC REFLECTOMETRY APPLICATIONS

By

Maria Fernanda Naranjo-Bueno

A thesis submitted in partial fulfillment of the requirements for the degree of

MASTER OF SCIENCE
IN
ELECTRICAL ENGINEERING

UNIVERSITY OF PUERTO RICO
MAYAGÜEZ CAMPUS
2007

Approved by:

Miguel Vélez-Reyes, Ph.D. Member, Graduate Committee	Date
Rafael Rodríguez-Solís, Ph.D. Member, Graduate Committee	Date
Eduardo J. Juan-García, Ph.D. President, Graduate Committee	Date
Ricky Valentin, Ph.D. Representative of Graduate Studies	Date
Isidoro Couvertier, Ph.D. Chairperson of the Department	Date

ABSTRACT

Nine polyvinylidene fluoride (PVDF) membrane transducers were developed to be used as receivers and transmitters in underwater applications, such as in acoustic reflectometry. The design requirements were oriented to comply with a bandwidth of 10 to 160 kHz, minimize the transducer size and generate construction techniques that will allow future researchers to modify the transducers and adapt them to different geometries. They represent a novel concept because of their working frequency range and their physical construction, easily shaped to customized applications. The nine transducers were created through the combination of three different PVDF film thicknesses (28, 52 and 110 μm) and three circular active areas (with radius 2, 3 and 4 mm). The receiving and transmitting sensitivities were studied through computer simulations and experimental tests, with respect to three main parameters: frequency, active area and film thickness. The receiving sensitivity increased as function of active area, and did not reveal any clear trend with respect to thickness or frequency. The transmitting sensitivity increased its magnitude with increasing frequency or the active area, but did not depend considerably on thickness. The final construction technique selected was to attach the PVDF film to a pre-engraved conductive base, with a case molded with an epoxy material. It offers the most advantages because the electrodes connection does not affect the piezofilm physical properties and the case can be easily shaped.

RESUMEN

Nueve transductores de membrana de polifluoruro de vinilideno (PVDF) fueron desarrollados para ser usados como receptores y transmisores en aplicaciones bajo el agua, tales como reflectometría acústica. Los requerimientos de diseño fueron orientados a satisfacer un ancho de banda de 10 a 160 kHz, minimizar el tamaño del transductor y generar técnicas de construcción que permitan a futuros investigadores modificar los transductores y adaptarlos a diferentes geometrías. Estos representan un concepto novedoso debido a su rango de frecuencia y su construcción física, fácilmente moldeable para aplicaciones personalizadas. Los nueve transductores fueron creados a través de la combinación de tres diferentes espesores de PVDF (28, 52 y 110 µm), y tres áreas activas circulares (con radios 2, 3 y 4 mm). Las sensitividades de recepción y transmisión fueron estudiadas a través de simulaciones computarizadas y pruebas experimentales, con respecto a tres parámetros: frecuencia, área activa y espesor de la lámina piezoeléctrica. La sensitividad de recepción aumentó como función del área activa, y no reveló una clara tendencia con respecto al espesor de la membrana o la frecuencia. La sensitividad de transmisión aumentó su magnitud al aumentar la frecuencia o el área activa, pero no dependió considerablemente del espesor. La técnica de construcción final seleccionada consistió en adherir el film de PVDF a una base conductiva pre-grabada, con un empaque moldeado en un material epóxico. Este ofrece las mayores ventajas ya que la conexión de los electrodos no afecta las propiedades físicas del piezofilm y el revestimiento puede ser fácilmente moldeado.

This work is dedicated first to God, for giving me the strength to finish it and the loving hands that raised me. To my parents, Luis and Francy, my sister Cristina, my big little brother Camilo, my soul sister Jeimmy and my friend Héctor. I know you were with me all the way. Thank you.

ACKNOWLEDGMENTS

This research was primarily supported by the National Institute of Health NIH, MBRS-SCORE program.

I want to thank the University of Puerto Rico for giving me the opportunity to come here and learn so many things, not only about engineering and science, but about such a wonderful people and culture.

Thanks to my advisor, Dr. Eduardo Juan for your help, guidance and support, for your trust making me a part of a great research team, but most of all, for being an unforgettable example of a professor, engineer and human being. I will never forget you and your beautiful family.

I would like to thank my professors, Dr. Raul Torres for his help and support, Dr. Gerson Beauchamp for his remarkable lessons, and Dr. Miguel Vélez-Reyes and Dr. Rafael Rodríguez-Solis for accepting being part of my graduate committee. It is an honor to have being your student.

Finally, I want to express my gratitude to Maria Elena Torres, Héctor Figueroa, Luis Quintero, Claudia Astudillo, Miguel Ángel Goenaga, Pablo Lozada, Víctor Marrero, Luis Giraldo, Carlos Giraldo, Alexander Pulliza and Andrés Bejarano.

TABLE OF CONTENTS

LIST OF TABLES

LIST OF FIGURES

1 INTRODUCTION

Cardiovascular disease is the first leading cause of mortality in the world for both men and women, accounting for more than 16.7 million deaths each year [1]. Just in the United States, it is the cause for almost 40% of deaths and more than one-fourth of the United States population lives with a cardiovascular disease [2]. Heart disease generates a serious social and economic impact, not only in patients, but in their families and the society, and statistics are not optimistic. Heart disease and stroke will cause death to more than 20 million people a year in 2020 and 24 million by 2030 [1]. Heart attacks and strokes are mainly caused by a condition in which fatty material is deposited along the inner walls of blood vessels, blocking the blood flow to the heart or the brain [3]. This fatty material thickens, hardens, and may eventually block the vessels. This disease is known as hardening of the arteries or atherosclerosis.

There are several methods used to detect, study and measure cardiovascular disease. One of them, still under research, is time-domain acoustic reflectometry, which has potential applications in the monitoring and guidance of intravascular catheters and the detection of atherosclerotic plaque via acoustic means.

1.1 TIME-DOMAIN ACOUSTIC REFLECTOMETRY

Time domain acoustic reflectometry is a non-invasive measurement technique that can be used to determine the internal profiles of tubes. The technique consists in transmitting an acoustic plane pulse through a tube. Acoustic reflections occur each time the pulse encounters a change in the characteristic impedance. By analyzing the reflections, it is possible to obtain the input impulse response of the system, from which the cross sectional area and compliance could be calculated as a function of distance [4].

Acoustic pulse reflectometry was developed as a seismological technique to observe stratifications in the earth's crust. In the seventies, a medical research team proposed to apply this technique to measure airway dimensions [5]. In 1977, Jackson et al. published a study in which the area-distance profiles of dog tracheas and airways were estimated using a pulse reflectometer [6]. A sound pulse created by a spark discharge was applied to the airway and the reflections were recorded by a microphone embedded in the wall of the source tube.

The first measurements on human patients were made in 1980. A sound pulse was applied to the airways through a source tube, filled with He/O_2 gas, in order to increase the speed of sound and thereby increase the bandwidth of the input pulse. This allowed researchers to obtain more information about the frequency range in which the airway wall behaves as rigid, simplifying the required analysis [7].

Since 1981, there have been many investigations about the use of acoustic pulse reflectometry for measuring the acoustical properties of musical wind instruments, such as bore reconstruction [8-11] and input impedance curve evaluations [12]. In the medical applications field, there have been new researches oriented to determine breathing tube placement in patients, both in adults [13-15] and children [16], as well to monitor the presence of fluid in the middle ear [17].

Recently, investigations on acoustic reflectometry have expanded to cardiovascular applications. As a first step to accomplish this, there have been two research projects at the University of Puerto Rico - Mayagüez about the guidance and monitoring of liquid-filled tubes and catheters [18], and the estimation of vessel wall compliance using acoustic reflectometry [19]. In the first, the sound wave propagation in rigid, liquid filled tubes was studied using an acoustic transmission line model. That research concluded that the acoustic pulse reflectometry could be used in a determined frequency range to study different liquid-filled tubes like the human body conduits, or as it was proposed, to monitor and guide intravascular catheters. The second project explored the use of pulse echo acoustic reflectometry to estimate the local wall compliance through computer simulation models, mechanical measurements, and in vitro acoustical measurements. This technique provides an innovative tool to measure local wall compliance, without touching, modifying or being near the tube walls.

1.2 CHALLENGES

The time-domain acoustic reflectometry technique requires that the generated pulse propagates only as a one-dimensional plane wave within the tube. To assure this, the pulse frequency must be smaller than the cut-off frequency of the lowest higher-order propagation mode, which is given by:

$$f_c = \frac{c}{1.707d} \tag{1.1}$$

where *c* is the sound velocity, and *d* is the diameter of the tube.

A rigid lossless tube model can only be used in vessels that behave acoustically as having rigid walls, which can be accomplished at a certain range of frequencies depending on the tube and the medium characteristics. In her research, Ordoñez [18] performed computer simulations based on an acoustic transmission line method, in order to determine the frequency range where the coronary arteries would behave as rigid tubes, but without exceeding the frequency at which only planar waves propagate. The recommended working frequency range for the coronary arteries was of 86 – 160 kHz.

The experiments performed in that research were limited by the restrictions imposed by the Reson TC4013 hydrophones that were employed. The main limitation was the hydrophone's sizes because they required to be placed on large diameter tubes, generating an incompatibility between the maximum frequency to avoid non planar waves, and the frequency range where the tubes behave as rigid conduits. In addition, because of their shape and required location, the hydrophones were obstructing the lumen of the pipe, causing sound losses and reflections.

1.2.1 DESIGN REQUIREMENTS

In order to continue with the research to apply time-domain acoustic reflectometry to liquid-filled tubes, it is essential to come across with acoustic transducers that can be used in different diameter pipes, specially in small tubes with higher cut-off frequencies. The transducer diameter must not exceed 1.27 cm, and it should be flush-mounting type or with a frontal sensing element, with the intention of being used by introducing it inside a tube of approximately 1.27 cm of diameter.

The transducers must be also designed to transmit and receive acoustic signals in a wide bandwidth, from 10 kHz to 160 kHz.

1.3 PVDF TRANSDUCERS DEVELOPMENT

The rapid advances on sensing technologies and their applications in different fields, including biomedical studies, has resulted in an increase in the demand for the miniaturization of devices, such as power supplies, actuators and sensors. Polyvinylidene Fluoride (PVDF) piezoelectric transducers are expected to offer a solution for those demands because they are inexpensive, space efficient, light weight, easily shaped, and can be bonded to a variety of surfaces.

PVDF is a ferroelectric polymer which offers advantages over alternative materials such as piezoceramics because of its much greater inherent sensitivity and good acoustic impedance match to water, producing less pronounced resonances. Its main disadvantage is its low relative permittivity, which means that small sensing elements will have low capacitance and suffer from signal loss through electrical loading. However, measures can be taken to improve the capacitance by lamination [20].

PVDF's strong piezoelectric properties were discovered by Kawaii in 1969. Since then, researchers have sough to apply this unique material to a wide range of industrial and medical applications. In the medical imaging field, the need to consider alternative materials emerged from the recognized limitations of conventional ceramics, such as lead zirconate titanate (PZT). PZT has high acoustical impedance and is difficult to form unto focused geometries because of its brittle nature. Because of its low acoustical impedance and rugged flexible constitution, PVDF appeared to solve both of these limitations. Indeed, early polymer transducers demonstrated spectacular bandwidths but the comparatively low coupling efficiencies of 0.15 to 0.2 compromised performances in the diagnostic frequency range [21].

PVDF is not commonly used in imaging systems that employ frequencies inferior to 15MHz, but it is essential for hydrophones construction and remains the standard for ultrasonic field calibration systems. PVDF and its copolymers have established a strong presence at frequencies above 15 MHz and have arguably produced the best images of tissue microstructures [21].

The unique features of PVDF, that include low acoustical impedance, moderate coupling coefficients and flexibility, enabled the initial development and utilization of low frequency transducers and, subsequently, the development of high performance high frequency transducers. PVDF has been used in several investigations for applications in different areas such as medical imaging transducers, ultrasound biomicroscopy [22], hydrophones, non-destructive testing (NDT) transducers, ultrasonic transducers calibration [23], surface acoustic waves (SAW) devices, measurement of shock waves [24, 25], energy storage [26], and industrial acoustic and vibration sensors.

High-frequency membrane hydrophones have been largely investigated. For example, Lum et al. [27] designed a membrane hydrophone with a 37 μm diameter spot poled electrode, on a polyvinylidene fluoride trifluoroethylene (PVDF-TrFE) film with 4 μm thickness. This hydrophone was designed for the characterization of high-frequency transducers such as intravascular ultrasound (IVUS) catheter transducers that operate from 10 to 40 MHz. It has a bandwidth of approximately 150 MHz.

Applications of PVDF membrane hydrophones also include the calibration of air-coupled ultrasonic transducers. Galbraith et al. [23] presented the design, fabrication and performance assessment of a PVDF hydrophone for the 100 kHz to 5 MHz frequency range, manufactured from a 28 μm thick film. Experimental validation was provided over the restricted range from 400 kHz to 1 MHz. It is used for calibration in air because the acoustic impedance of PVDF is an order of magnitude lower than piezoceramics devices, it has a wide uniform frequency response, provides good spatial resolution and a uniform sensitivity on water, and the receiving sensitivity behavior of the PVDF membrane is similar when operating in either air or water.

Lamination of PVDF has provided the opportunity of designing and producing hydrophones with enhanced performance, to be used as secondary standards by institutions such as the National Physical Laboratory (NPL) in the United Kingdom. GEC-Marconi has constructed two types of PVDF reference hydrophones, the bilaminar-shielded PVDF membrane hydrophone and PVDF sonar hydrophone [20].

The bilaminar-shielded PVDF membrane hydrophone consists of two layers of PVDF film with an electrode on one of the adjoining surfaces. The outside surfaces are almost completely covered with gold, forming the shield. In the case of the 25 μm thick film, this approach can achieve a sensitivity of the hydrophone plus an amplifier in the frequency range from 1 to 20 MHz.

The PVDF sonar hydrophone is made of a 6 layers lamination of 25 μm thick film, with the active electrode between the third and fourth layers. It has a 25 mm diameter and is mounted on a brass base. The frequency response is flat on the range from 200 kHz to 1 MHz, which is a range particularly difficult for piezoceramics hydrophones because they become too directional and can exhibit strong resonances.

As a different alternative to the membrane hydrophones, the needle type appeared [28]. It consists of a metal needle, rounded at its tip, coated with a thin layer of PVDF, as shown in Figure 1.1. The PVDF is polarized in a small zone around the needle point, which constitutes the sensitive area. The needle acts as the mechanical support for the PVDF layer, and as the active electrode. The other electrode is a conductive layer deposited on the external side, which additionally offers electrical shielding.

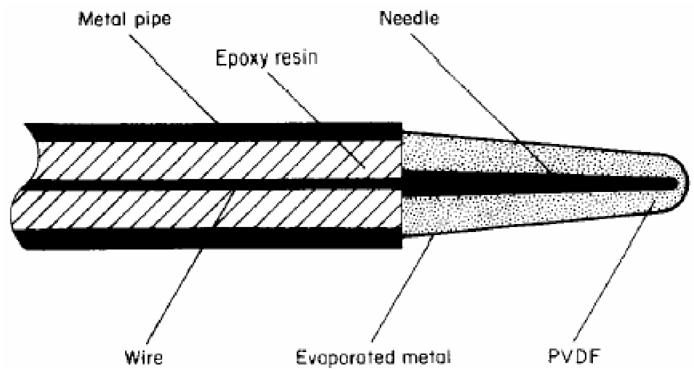

Figure 1.1. PVDF needle hydrophone structure example [28].

This type of construction offers an almost omnidirectional directivity and high spatial resolution of the ultrasonic sound field pattern. The hydrophone constructed by Platte [28], presented a flat frequency response between 1 MHz and 20 MHz.

PVDF hydrophones are usually designed to be used in frequencies greater that 1 MHz. However, Lewin et al. [29] published a study of the sensitivity versus frequency behavior of ultrasonic hydrophone probes below 1 MHz. The frequency responses of 13 different PVDF polymer hydrophone probes, including membrane and needle designs, were measured from 0.25 to 2.5 MHz. This information is important because there is evidence that probes with a deficient low-frequency response can introduce a considerable error in the estimation of Mechanical Index, which is widely accepted as one of the critical safety indicators for diagnostic ultrasound.

Although conventional PZT transducer sources are commercially available in the frequency range considered in that study, they are designed for non-destructive testing applications and are usually narrow-banded. Therefore, they constructed an acoustic source transducer using a piezoelectric PZT composite material as a flat piston of effective diameter of 20 mm.

The experimental data showed that a majority of the PVDF membrane hydrophones tested exhibit a relatively uniform response, within 2dB. In contrast to this, the needle probes showed less uniform behavior, with variations greater that 3dB in the frequency range considered. However, careful design improvements may result in a better behavior to comply with the current regulatory guidelines.

Although there are many investigations about high-frequency PVDF hydrophones, including theoretical and practical work, some hydrophones have been designed to offer a flat frequency response from 500 kHz to 15 MHz [30], but there are just a few reports of PVDF hydrophones used in the range below 500 kHz. Yiquan et al. [31] published a study of a multilayer planar PVDF standard hydrophone, capable of working in the range from 20 kHz to 4 MHz. The hydrophone consisted of a multilayer body, a PVDF film as one of the layers, a stainless steel tube and a DMOS integrated circuit. The PVDF film was 90 μm thick and 4mm diameter. The hydrophone presented a flat frequency response in the range from 100 kHz to 1 MHz.

A low-density extended acoustic sensor for low-frequency arrays was presented by Fox [32], based on a piezoelectric PVDF cable, which allows considerable design freedom because of its mechanical flexibility and high longitudinal piezoelectric coefficient. It can be made in lengths from 4 cm to more than 1 m, and in diameters from 8 mm to more than 40 mm. The device has a flat frequency response from less than 1 Hz to almost 8 kHz and is designed for applications in low-frequency sonar.

The transducers described previously are designed only as probe hydrophones and most of them are unusable as acoustic sources. In spite of all the PVDF advantages, its low electromechanical coupling factor, which reduces transmitting efficiency, has contributed to limit the interest in using it for transmitter applications. Lewin and Schafer [33] published a design of a wide-band acoustic source made of a 9 μm PVDF film, with 10 mm of diameter, glued directly to a polished backing material using a low viscosity epoxy. Figure 1.2 depicts the source schematic construction.

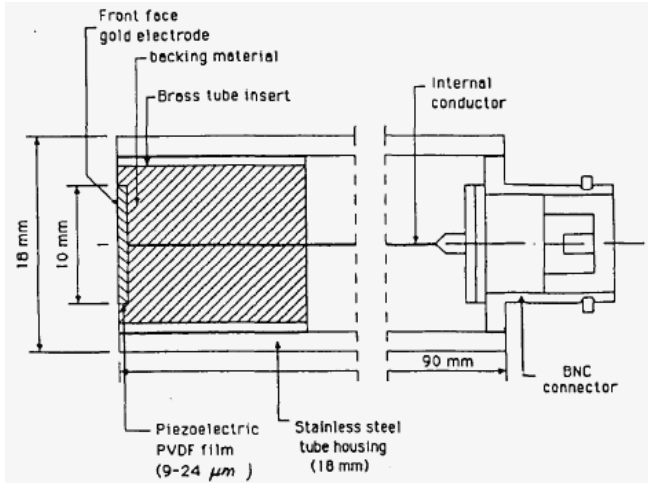

Figure 1.2. Schematic construction of a wide-band PVDF acoustic source [33].

These sources are intended to provide absolute calibration of ultrasound hydrophone probes since imaging transducers can hardly serve as acoustic sources over the full frequency range of interest, because their bandwidth is limited due to the matching layers and the resonant character of piezoceramics material, even for those described as broad-band. For the acoustic source designed, the experimental data demonstrated that the transmitting voltage response increases with frequency almost linearly, up to 40 MHz, which was the upper cutoff frequency of the spectrum analyzer used.

1.4 COMMERCIALLY AVAILABLE TRANSDUCERS

The Reson TC4013, employed in Ordoñez's research, is a broad band hydrophone that offers a usable frequency range from 1 Hz to 170 kHz [34]. It provides almost omnidirectional uniform directivity pattern in both horizontal and vertical axes. The manufacturer assures this hydrophone can be used to make absolute sound measurements, calibrations and as an omnidirectional reference projector. The hydrophone has a 9.5mm diameter tip, and the acoustic centre is at 10mm from the point. It is coated with Nitrile Butadiene Rubber (NBR). Figure 1.3 depicts the hydrophone dimensions in millimeters.

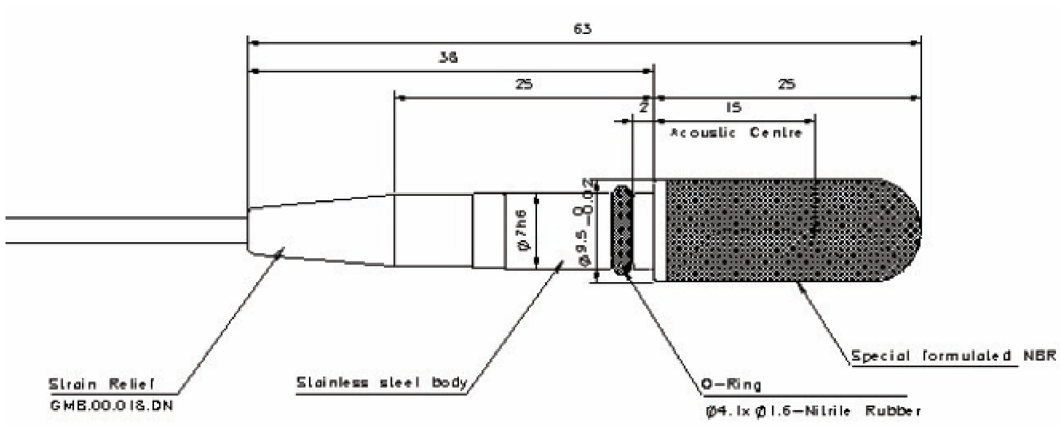

Figure 1.3. Reson TC4013 Outline dimensions [34].

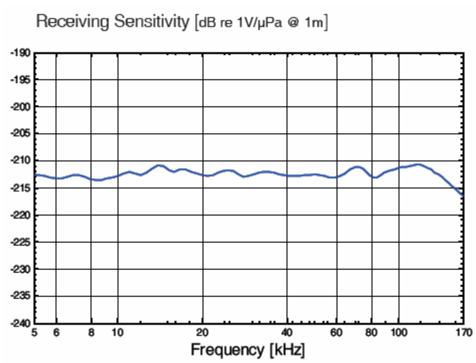

a)

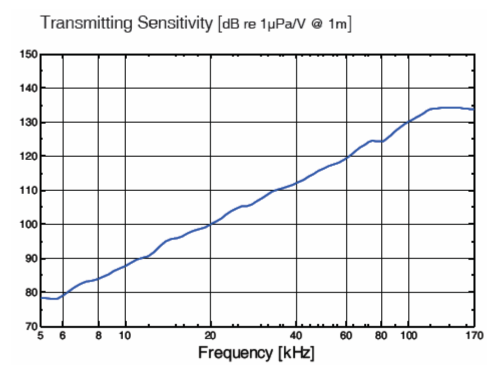

b)

Figure 1.4. Reson TC4013 a) Receiving Sensitivity (dB re 1V/μPa @ 1m). b) Transmitting Sensitivity (dB re 1 μPa/V @ 1m) [34].

As seen in Figure 1.4, the hydrophone exhibits a receiving linear frequency behavior from 5 kHz to 125 kHz, while the transmitting sensitivity increases with frequency until 170 kHz.

Reson has other hydrophones that could be used in acoustic underwater studies, such as the TC4050, a miniature flush-mounted probe hydrophone. It has a flat frequency response at low frequencies, from 0.3Hz to 40 kHz, and a usable frequency range from 0.3Hz to 100 kHz [34]. It also has an omnidirectional horizontal directivity pattern and a vertical directivity pattern of 270º. It is ideal for observing eddying and cavitations, and for measurements of pressure profiles of transient shock fronts. However, this hydrophone is not recommended as a transmitter.

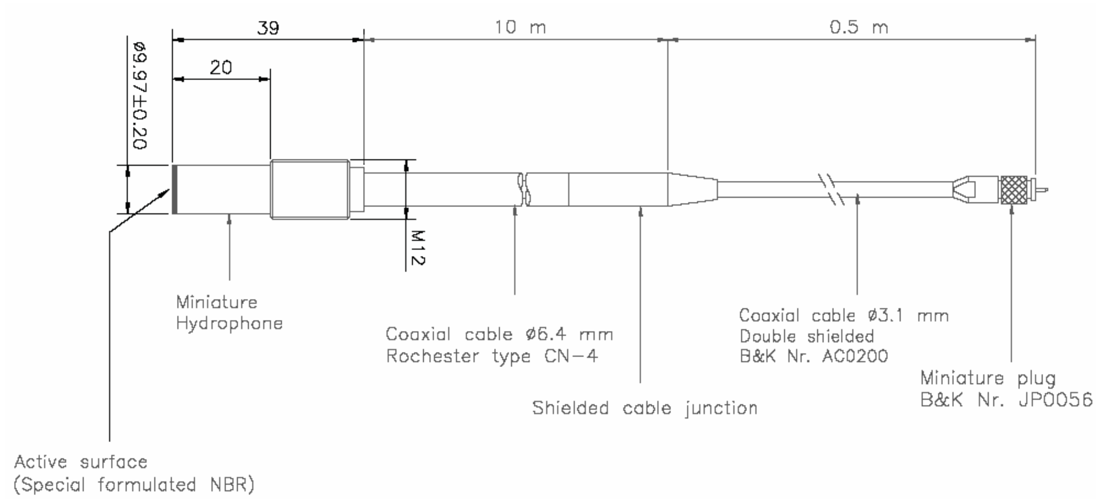

Figure 1.5. Reson TC4050 Outline dimensions [34].

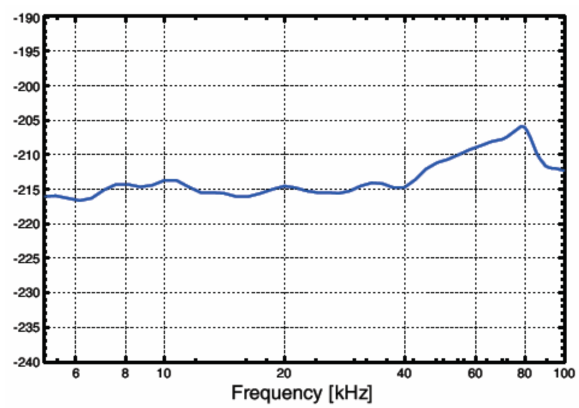

Figure 1.6. Reson TC4050 Receiving Sensitivity (dB re 1V/μPa @ 1m) [34].

Figure 1.5 shows the Reson TC4050 outline dimensions in millimeters, and Figure 1.6 describes its receiving sensitivity as a function of frequency.

In the area of broad band miniature hydrophones, Reson offers the TC4038 and TC4035. They exhibit almost the same acoustic characteristics, but the first one has a maximum operating depth of 20 m, while the second operates at a maximum of 300 m. They are designed as standard reference hydrophones for the 100 kHz to 500 kHz frequency range, where they provide a flat frequency response, omnidirectional horizontal directivity pattern, and 60º to 120º vertical directivity pattern. The usable frequency range is from 10 kHz to 800 kHz [34]. They are not recommended as transmitters.

Figure 1.7 display the Reson TC4038 outline dimensions in millimeters, and Figure 1.8 present its receiving sensitivity as a function of frequency.

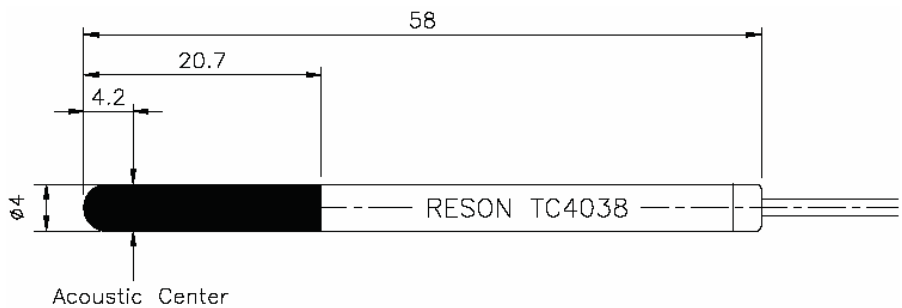

Figure 1.7. Reson TC4038 Outline dimensions [34].

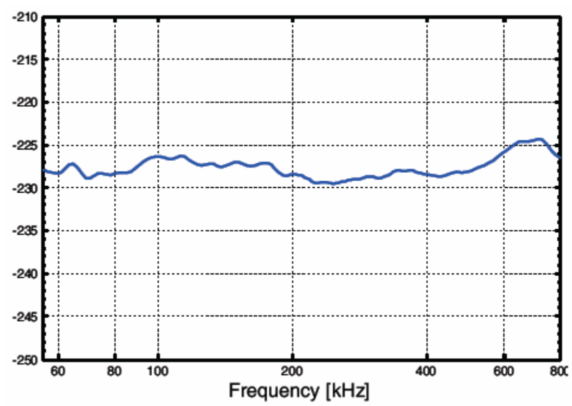

Figure 1.8. Reson TC4038 Receiving Sensitivity (dB re 1V/µPa @ 1m) [34].

There are many commercial transducers used to generate and receive underwater low frequency acoustic signals for applications such as navigation systems, sonar, leak detection, sensors, marine life studies, etc. Their usable frequency range varies from tenths of Hertz, to 20 kHz to 50 kHz [35-38]. Their sizes also vary considerably depending on the application and from one manufacturer to another. The hydrophones used for recording marine life sounds tend to be big and robust, used in navigation vessels, while some sensors can be small enough to fit in little spaces, such as the CTG099 from Chelsea Technology Group [38], with dimensions of 46 mm in length and of 17 mm in diameter. It works from 0.5 Hz to 20 kHz.

Advances in piezoelectric polymer materials and techniques have allowed the creation of PVDF hydrophones for the high frequency ultrasonic range, where it is common to find transducers of reduced physical dimensions. Companies such as Force Technologies are offering miniature ultrasonic hydrophones, for instance the MH28 and the MHA9-150 [39].

The MH28 is a PVDF needle-type miniature ultrasonic hydrophone with a usable bandwidth from 0.5 MHz to 20 MHz with a uniform response. The active element is a 28 μm PVDF film with nickel/silver electrodes. It has a 200 – 500 μm standard effective radius, identical with its physical dimension. It is calibrated from 1 to 20 MHz. The MHA9-150 is a similar hydrophone with an active element made of a 9 μm PVDF film with gold electrodes and an effective radius of 150 μm, identical with its physical dimensions. It has an enhanced bandwidth from 0.1 MHz to 80 MHz. It is calibrated continuous from 1 to 20 MHz, and with specific frequency values above 20MHz.

These needle-type miniature ultrasonic hydrophones were designed as a high quality tool for ultrasonic metrology applications, and because their physical dimensions are equal to their effective diameter, they are especially useful for applications in continuous wave acoustic fields where minimum disturbance measurements are required. The main application areas include acoustic output measurements, testing of medical and industrial equipment, transducer design, calibration reference standard and study of non-linear acoustic phenomena.

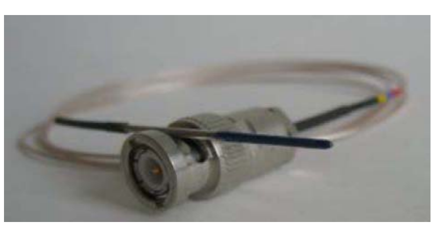

a)

b)

Figure 1.9. Force Technology Needle-Type Miniature Ultrasonic pictures. a) MH28. b) MHA9-150 [39].

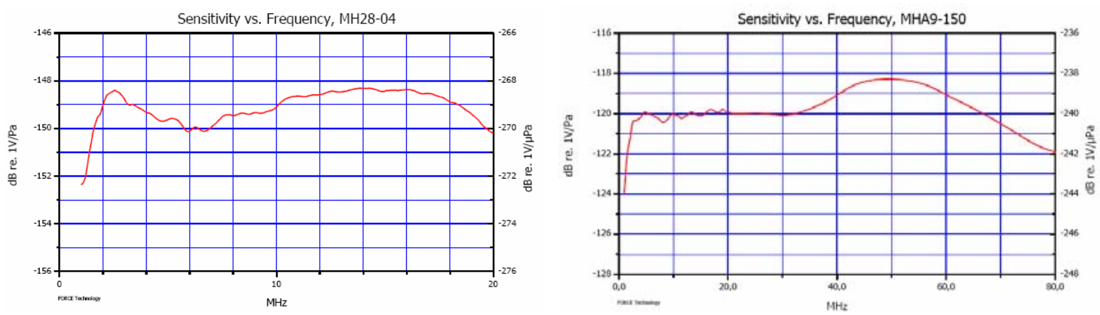

a) b)

Figure 1.10. Force Technology Needle-Type Miniature Ultrasonic Typical Sensitivity Frequency Response. a) MH28-04. b) MHA9-150 [39].

Figure 1.9 exhibits the pictures of the MH28 (a) and MHA9-150 (b) hydrophones, while Figure 1.10 represents the receiving sensitivity as function of frequency for both hydrophones, (a) MH28 and (b) MHA9-150.

Some PVDF miniature hydrophones are also available for broad band frequency applications. RP acoustics [40] offers two PVDF hydrophones, the Type *s*, with a sensitive area diameter of 1mm, and the Type I, with a sensitive area diameter of 3mm. They have a usable frequency range from 1 kHz to 3 MHz. The pressure sensitive element of the hydrophones is a PVDF foil attached and electrically contacted to the instrument tip. RP Acoustic hydrophones are calibrated using a reciprocity calibration sound source, controlled by a Fiber Optic Probe Hydrophone FOPH 2000, an instrument sold by the same company. These PVDF hydrophones are not suitable for transmitting applications. They are displayed in Figure 1.11

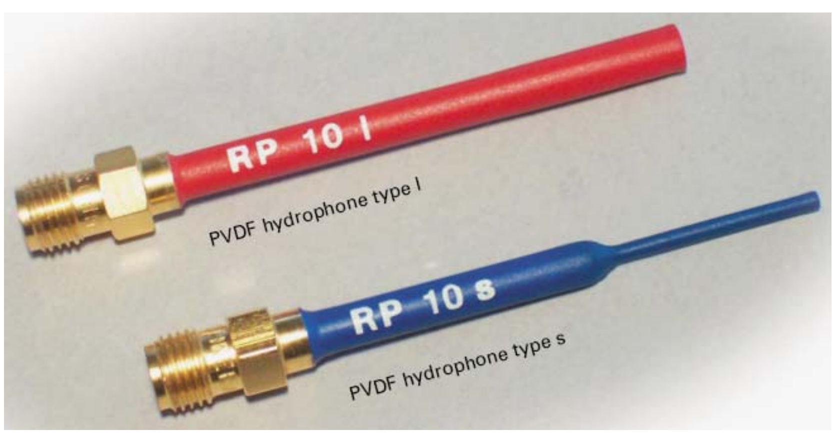

Figure 1.11. RP Acoustics PVDF Hydrophones type *l* and type *s* [40].

At the moment, the commercial available hydrophones, as the ones mentioned before, do not represent an appropriate solution for the application of time-domain acoustic reflectometry to study liquid-filled tubes, oriented to future work in blood vessels, because none of them complies with all the requirements established in previous investigations [18].

In this work, we designed and constructed nine custom-made PVDF transducers. The design requirements were oriented to comply with a bandwidth of approximately 10 kHz to at least 160 kHz, to minimize the transducer size and to generate construction techniques that will allow future researchers to modify the transducer and apply it to different geometries under study. The designed transducer will be useful to expand the acoustic reflectometry studies currently performed by our research group, as well as for other applications in liquid-filled conduits.

1.5 OBJECTIVES

The main goal of this project was to investigate the potential of designing and constructing a small-sized custom made polyvinylidene fluoride (PVDF) transducer that can be used to generate and receive signals for underwater acoustic pulse reflectometry studies. The specific objectives of this thesis are:

(a) Construct PVDF transducers with different areas and thickness, and evaluate the impact of these variables in the transducer's performance.

(b) Examine the transducers' frequency response as transmitters and receivers.

(c) Design and construct a water proof prototype case for the designed transducer.

(d) Document the construction techniques for future use in the laboratory.

1.6 THESIS OUTLINE

This thesis is divided into five chapters. This first chapter introduces the time-domain acoustic reflectometry, the transducers requirements and availability, and the research objectives. The second chapter contains the background theory of piezofilms and piezoelectricity, PVDF transducers models and properties, and an acoustic radiation model. The third chapter describes the methodology followed during the research with respect to the physical system setup and the experiments design, including the input signal design and the acquired signal processing methods. Besides, it explains the models used for the simulations and the transducers fabrication methods. Chapter four presents and discusses the results obtained from simulations and experiments, and analyzes the experimental results based on the models projections. Finally, the fifth chapter presents the conclusions for the transducers implemented and presents recommendations for future work.

2 THEORETICAL BACKGROUND

This chapter provides a theoretical background in piezo film transducers, its characteristics and circuit models. Besides, the polyvinylidene fluoride (PVDF) is presented as a convenient solution for the construction of piezo film membrane transducers. Four different models are presented, focusing in sensitivity analysis and directivity pattern. Finally, the PVDF material properties required to evaluate the models are listed.

2.1 PIEZO FILMS

Piezoelectricity, greek word for pressure electricity, was discovered by the Curie brothers in 1880. Up to 1910, the scientific community had defined the 20 natural crystal classes in which piezoelectric effects occurs, and defined 18 possible macroscopic piezoelectric coefficients. The first serious applications of piezoelectric devices took place during World War I, with an ultrasonic submarine detector.

Before World War II, researchers discovered that certain ceramic materials could be made piezoelectric when subjected to a high polarizing voltage, a process analogous to magnetizing a ferrous material. By the 1960's, researchers had discovered a weak piezoelectric effect in whale bone and tendon. This began an intense search for other organic materials that might exhibit piezoelectricity.

In 1969, Kawai found very high piezo-activity in the polarized fluoropolymer, polyvinylidene fluoride (PVDF) [21]. While other materials, like nylon and PVC exhibit the effect, none are as highly piezoelectric as PVDF and its copolymers. Since its discovery, PVDF has become increasingly attractive as a transducer material, combining mechanical ruggedness, flexibility, and chemical inertness with high piezoelectric response and useful acoustic properties [41].

One major advantage of piezo-film over piezo-ceramic is its low acoustic impedance, which is closer to that of water, human tissue and other organic materials. For example, the acoustic impedance of PVDF is only 2.6 times that of water, while piezo-ceramics are typically 11 times greater [42]. A close impedance match allows more efficient transduction of acoustic signals in water and tissue.

Piezo film does have some limitations for certain applications. It is a relatively weak electromechanical transmitter when compared to ceramics, particularly at resonance and in low frequency applications. Piezo films are required to work at low temperatures, below 100ºC, because of their fabrication process. Also, if the electrodes on the film are exposed, the sensor can be sensitive to electromagnetic radiation [42].

2.1.1 PIEZOELECTRICITY BASICS

2.1.1.1 Piezo Coefficients.

Among the properties of piezofilm materials are the tickness (t), piezo strain constant (d_{mn}), piezo stress constant (g_{mn}), electromechanical coupling factor (k_{mn}), capacitance (C), etc. The most widely used piezo coefficients, charge (d) and voltage (g), have two subscripts (m and n). The first refers to the electrical axis (m) and the second refers to the mechanical axis (n).

The convention values for the coefficients subscripts are presented in Figure 2.1. The length or stretch direction is represented by 1, the width or transverse direction is represented by 2, and the thickness direction is represented by 3. Considering that piezo films are thin, the electrodes are usually only applied to the top and bottom surfaces. For that reason, the electrical axis is always 3, since the charge or voltage is always transferred through the thickness of the film. The mechanical axis can be 1, 2, or 3, since the stress can be applied to any of these axes.

Piezoelectric materials are anisotropic; subsequently their electrical and mechanical responses differ depending on the axis where the electrical field or mechanical stress or strain is applied. Typically, piezo film is used in the mechanical 1 direction for low frequency transducers (below 100kHz) and in the mechanical 3 direction for high frequencies (above 100 kHz) [42].

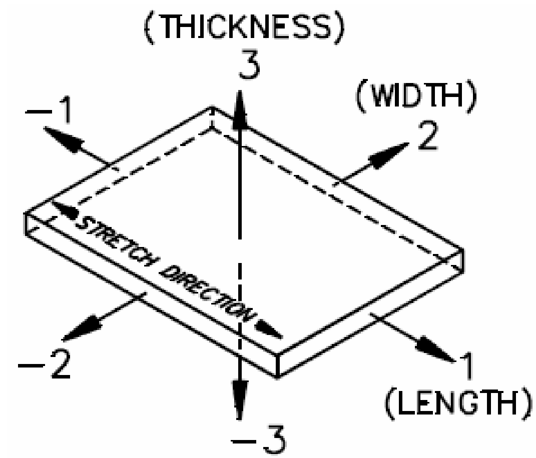

Figure 2.1. Numerical classification of axes [42].

2.1.1.2 Mechanical to Electrical Conversion.

The amplitude and frequency of the signal generated by a piezo material is directly proportional to its mechanical deformation. This deformation causes a change in the surface charge density of the material, generating a voltage between the electrode surfaces. When the force direction is opposite, the output voltage is of opposite polarity.

Piezoelectric materials are not suitable for static measurements because the electrical charges developed decay with a time constant determined by the dielectric constant and the internal resistance of the film, as well as the input impedance of the interface electronics connected to the film.

The open-circuit output voltage is given by:

$$V_o = g_{3n} X_n t \tag{2.1}$$

where n represents the mechanical axis of the applied stress (or strain), g is the appropriate piezoelectric coefficient for the axis of applied stress or strain, X_n is the applied stress in the relevant direction, and t is the film thickness.

Piezo films have strong pyro sensitivity that should be taken into account when designing mechanical sensors for very low frequency signals, below 1 Hz, because ambient temperature changes could modify the output with pyro-generated signal [42]. If a very long time constant is used, the film will generate a voltage corresponding to the change in temperature since switch-on. Since the output will be several volts per degree C, substantial offsets may be noticed.

2.1.1.3 Electrical to Mechanical Conversion.

Piezo films change dimensions when a voltage is applied to them, due to the attraction or repulsion of internal dipoles to the applied field. With one voltage polarity, the piezo film becomes thinner, longer and wider. The opposite polarity causes the film to become thicker and to contract in length and width. However, piezofilms are not suitable for devices requiring large displacements of forces. This consideration is especially important when designing loudspeaker elements, since low frequency performance (below 500Hz) tends to be limited. They can not create high amplitude pressure pulses at low audio frequencies, but they are still useful for the range in low to high ultrasound frequencies, as seen in current designs.

The deformation magnitude depends on the d_{3n} constant and it is given by the equations in Table 2.1.

Table 2.1. Equations of Electrical to Mechanical Conversion for Piezo Film Transducers [42], where *l* is the original film length (m) and *Δl* is its change, *w* is the original film width in meters and *Δw* is the change in film width, *t* is the original film thickness in meters and *Δt* is the change in film thickness, d_{3n} is the piezoelectric coefficient for the *n* direction change in meters per volt, and *V* is the applied voltage across the thickness *t*.

AXIS (n)	**EQUATION**
1 - Length	$\Delta l = l \cdot d_{31} \cdot \frac{V}{t}$
2 - Width	$\Delta w = w \cdot d_{32} \cdot \frac{V}{t}$
3 - Thickness	$\Delta t = t \cdot d_{33} \cdot \frac{V}{t} = d_{33} \cdot V$

2.1.2 MODELS

2.1.2.1 Simplified Receiving Equivalent Circuit.

Piezo films used as sensors can be modeled as a strain-dependent voltage source, in series with a capacitance, as represented in Figure 2.2. The voltage source amplitude is equal to the piezo film's open circuit voltage. The series capacitance is proportional to the film permittivity area and inversely proportional to film thickness [42]. This simplified equivalent circuit is appropriate for most applications except for very high frequencies (above 1 MHz).

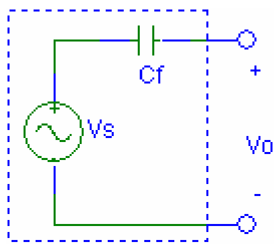

Figure 2.2. Piezo Film Voltage Source Equivalent Circuit.

The piezo film's capacitance can be calculated using:

$$C_f = \varepsilon \frac{A}{t} \tag{2.2}$$

where ε is the material permittivity, A is the active area of the film, which is defined by the area where the electrodes are overlapped, and t is the film thickness.

The piezo film impedance is regarded by the film capacitance, given by:

$$Z_f = \frac{1}{j2\pi f C_f} \tag{2.3}$$

Figure 2.3 describes an equivalent circuit where piezo film is represented by a charge generator, connected in parallel to a capacitance and an internal resistance. The induced charge Q is linearly proportional to the applied force. In low frequency applications, the internal film resistance R_f is very high and can be ignored. The open circuit output voltage can be found as $V=Q/C_f$.

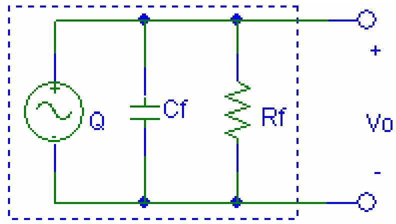

Figure 2.3. Piezo Film Charge Generator Equivalent Circuit.

2.1.2.2 Loading.

A properly designed interface circuit plays a key role in the optimization of piezo film sensors. The most critical part is the input resistance because it affects the low frequency measurement capability as well as the signal amplitude. Figure 2.4 depicts the potential divider formed by the series connection of the film capacitance and the circuit input resistance. As the ratio of input resistance to source impedance decreases, the output voltage decreases. Therefore, choosing a proper input resistance for the electronic interface is critical in minimizing the loading effect.

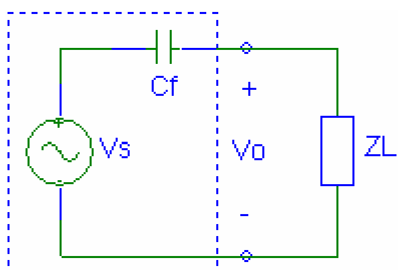

Figure 2.4. Piezo Film Equivalent Circuit with Load.

The output voltage will be given by:

$$V_o = V_s \frac{Z_i}{Z_f + Z_i} \tag{2.4}$$

If the load is completely resistive, the circuit will behave as a simple RC high-pass filter. The cut-off frequency will be given by:

$$f_c = \frac{1}{2\pi R_L C_f} \tag{2.5}$$

If the circuit is operated bellow the cut-off frequency, it behaves as a differentiator and the output will be proportional to the rate of change of the input parameter. Application of a constant stress will generate an initial level followed by an exponential decay, with a time constant $\tau = R_L C_f$. For low frequency measurements, the input resistance should be high enough so that the cut-off frequency is well below the desired operating frequency.

Although needle type transducers can be used, they require special consideration because of their small area, and therefore, small capacitance. The low frequency limit of operation will be defined by the greatest resistive load achievable, or by the largest capacitance load that still allows the signal to be easily detected.

The interface circuit could have an input capacitance which can also affect the output. In that case, the charge developed on the film due to an applied force decays with a time constant defined by $R_L(C_f + C_L)$. A capacitive load will increase the time constant but reduce the magnitude of the response because of the energy dissipated when transferring charge from one capacitor to another. Large capacitive loads are useful for attenuating the very large signals arising from powerful impacts.

The smaller the time constant, the quicker the signal decays. Because of this finite time constant, piezo film is suitable for dynamic measurements rather than static measurement. If a long time constant is desired, a high input resistance and film capacitance can be used. However this can also produce higher noise, requiring compensation through shielding [42].

2.1.2.3 KLM Resonator.

The KLM model is one of the most commonly used for piezoelectric transducers [43]. It was published by Krimholtz, Leedom and Mattaei as an alternative equivalent circuit to the Mason and Redwood models, in an effort to remove the circuit elements between the top of the transformer and the node of acoustic transmission [44]. It has been used extensively in medical imaging applications in an effort to design high frequency transducers, multilayers, and arrays.

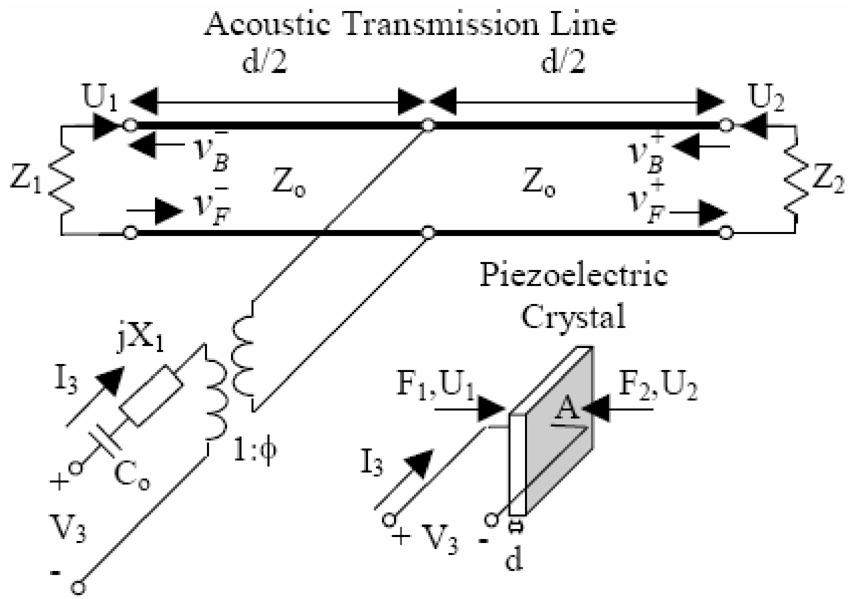

Figure 2.5. KLM Model for a piezoelectric crystal transducer [45].

The KLM equivalent model for a piezoelectric transducer is showed in Figure 2.5 [45]. In this model, V_3 and I_3 are the voltage and current applied to the piezoelectric crystal, which produce the resulting acoustic forces F and particle velocities U. In the graphic, the subscript F indicates forward traveling waves propagating towards interface 2, the subscript B indicates backward-traveling waves propagating towards interface 1, and the ± denote waves in the right and left half of the crystal, respectively.

The model parameters include the crystal thickness d, the crystal area A, and the characteristic impedance of the acoustic transmission line modeling the piezoelectric crystal Z_o. The impedances Z_1 and Z_2 are the radiation impedances of the mediums. The complete model includes a capacitor C_o, an impedance jX_1, and a transformer with ratio (1:Φ) that converts the electrical signal into the appropriate acoustical values. The values for these parameters are given by:

$$\begin{aligned}
Z_o &= \rho \cdot c \cdot A \\
C_o &= \frac{\varepsilon A}{d} \\
X_1 &= \frac{h^2}{\omega^2 Z_o} \sin\left(\frac{\omega \cdot d}{c}\right) \\
\phi &= \frac{\omega Z_o}{2h} \cos ec\left(\frac{\omega \cdot d}{2c}\right)
\end{aligned} \tag{2.6}$$

The input impedance of the piezoelectric transducer, seen looking into port 3, is:

$$Z_{in} = \frac{1}{j\omega C_o} + jX_1 + \frac{Z_a}{\phi^2} \tag{2.7}$$

where Z_a is the impedance seen looking into the acoustic transmission line, given by:

$$Z_a = \frac{Z_{L1} Z_{L2}}{Z_{L1} + Z_{L2}}; \qquad Z_{L1,2} = Z_o \frac{Z_{1,2} + jZ_o \tan\left(\frac{\omega \cdot d}{2c}\right)}{Z_o + jZ_{1,2} \tan\left(\frac{\omega \cdot d}{2c}\right)} \tag{2.8}$$

The pressure radiated by the transducer into each medium when it is excited by a voltage V_3 in the phasor domain, can be analyzed by summing the particle velocities at the center of the acoustical transmission line, because they are analogous to currents in an electrical transmission line. The pressure wave leaving the surface of a piezoelectric crystal will be given by:

$$P_2(\omega) = \frac{Z_2 V_3(\omega)}{\phi Z_{in}} \frac{\left(\Gamma_1 e^{-jkd/2} - e^{jkd/2}\right)}{e^{jkd} - \Gamma_1 \Gamma_2 e^{-jkd}} (1 + \Gamma_2) \tag{2.9}$$

$$P_1(\omega) = \frac{Z_1 V_3(\omega)}{\phi Z_{in}} \frac{\left(e^{jkd/2} - \Gamma_2 e^{-jkd/2}\right)}{e^{jkd} - \Gamma_1 \Gamma_2 e^{-jkd}} (1 + \Gamma_1) \tag{2.10}$$

where Γ_1 and Γ_1 are the transmission coefficients given by:

$$\Gamma_1 = \frac{Z_O - Z_1}{Z_O + Z_1}$$
$$\Gamma_2 = \frac{Z_O - Z_2}{Z_O + Z_2} \tag{2.11}$$

This expression can be used to calculate the pressure radiated by a piezoelectric crystal excited by a transient voltage pulse, by decomposing the pulse into the respective frequency components, determining the pressure radiated for each component in the Fourier domain, and then using the inverse Fourier transform to assemble the resulting pressure pulse.

2.2 POLYVINYLIDENE FLUORIDE (PVDF) TRANSDUCERS

2.2.1 MODELING

PVDF is commonly used to build hydrophones. The free-field sensitivity of these, commonly expressed in nV/Pa, is used to convert the measured voltage waveform to absolute acoustic pressure through a single calibration factor corresponding to the acoustic working frequency. This is appropriate for narrow-band systems, but not for measurements made on acoustic waveforms containing a broad spectrum of signals over a large frequency range.

The true acoustic pressure waveform could in principle be derived from the measured waveform through a process of deconvolution providing the impulse response of the hydrophone is known. This impulse response can be determined from knowledge of the magnitude and phase response of the hydrophone over the range of relevant frequencies. Therefore, it is necessary to have a model which accurately describes the transfer characteristics of the hydrophone and any instrumentation used in the measurements. This model will certainly depend not only in the PVDF characteristics, but in the hydrophone configuration and the instrumentation connected to it.

In order to solve this problem and improve measurement accuracy, there have been efforts to develop different methods to establish the relation between the voltage waveform and the acoustical waveform. The following subsections describe some models of special interest for this research.

2.2.1.1 Swartz and Plummer Model.

Yiquan et al. [31] presented in 1995 a new multilayer planar PVDF standard hydrophone and its applications, for use in the frequency range from 20 kHz to 4 MHz. They described the hydrophone performance properties and compared them with those of similar devices.

To calculate the sensitivity, the standard thin plate thickness mode Mason model equivalent circuit was used, which is a valid approach considering that the vibrator (PVDF film) has a very small ratio of thickness to diameter (90 µm / 4 mm). They used the model described by Swartz and Plummer [46]. The film is glued to a high impedance ceramic plate and the receiving side is low impedance water medium, thus the boundary conditions are of one fixed end and one free end. Therefore, the vibrator has a λ/4 vibration mode, λ being the wave length in the PVDF film.

The transducer's electrical port may be modeled in the ideal case as a Thevenin voltage source and series output impedance. The Thevenin voltage generator can be determined as a function of the input acoustic stress, by:

$$M_1 = \begin{cases} \dfrac{V_{out}}{T_{in}} = \left(\dfrac{2h}{j\omega C_0}\right)\left(\dfrac{1}{Z_M\left(1 - j\,{Z_0}\big/{Z_M}\right)\cot(k_0 l)}\right), k_0 < \dfrac{\pi}{2l} \\ \dfrac{l}{e_{33}}, k_0 = \dfrac{\pi}{2l} \end{cases} \tag{2.12}$$

where V_{out} is the equivalent output voltage, T_{in} is the acoustic input stress, h is the electric conversion coefficient, ω is the angular frequency (ω = 2πf; f: working frequency), C_0 is the static capacitance of the PVDF film, Z_M is the acoustic impedance of water medium, Z_0 is the film's acoustic impedance, l is the thickness of the vibrator, and k_0 is the wave number in the film (k_0 = 2π/λ).

The electric conversion coefficient h can be calculated from:

$$h = \frac{A}{l} e_{33} \tag{2.13}$$

where A is the area of the bottom electrode and e_{33} is the piezoelectric constant.

The resonance occurs when the following condition is true:

$$k_0 l = \frac{\pi}{2} \longrightarrow l = \frac{\lambda}{4} \tag{2.14}$$

The Thevenin series output impedance below resonance can be calculated from:

$$Z_{out} \cong \frac{\left(1 - k_T^2\right)}{j\omega C_0} \tag{2.15}$$

The electromechanical coupling coefficient k_T can be calculated in terms of the material stiffness (elastic) constant c^E_{33}, the piezoelectric stress constant e_{33}, and the dielectric constant ε^S_{33}. For the PVDF, k_T is much smaller than 1, therefore the equivalent output impedance is simply a capacitor of value C_0.

The sensitivity of the hydrophone, taking into account the glue layer, the protection layer and the gain of the DMOS integrated circuit used, is modified as:

$$M = KM_1 G \tag{2.16}$$

where K is the gain of the DMOS integrated circuit (about 10) and G is a correction coefficient between 0 and 1.

The value of G mainly depends on the thicknesses of the glue layer and the protection layer. If they are very thin, G is close to 1. The glue layer reduces the hydrophone's sensitivity because of three main reasons. First, since its impedance is different from those of the ceramic plate and the PVDF film, a vibration rate shunt is caused. Second, the glue layer increases the non-active portion of the PVDF film, decreasing the effective electromechanical coupling coefficient K_{eff} to a smaller value K^{*}_{eff}. And finally, the glue layer produces a coupling capacity C_B which causes a shunt of voltage and accordingly, the sensitivity decreases.

Considering the glue layer influence and the voltage shunt model [31], the total sensitivity will be given by:

$$M = K \cdot M_1 \cdot \frac{K^{*}_{eff}}{K_{eff}} \frac{C_0 C_B}{C_0 C_B + C_0 C_{gs} + C_B C_{gs}} K_d K_p \tag{2.17}$$

where K_d is the correction coefficient due to the vibration rate shunt, and K_p is the correction coefficient due to the protection layer.

For an epoxy layer, the effective electromechanical coupling coefficient will decrease approximately 10% (K^{*}_{eff} / $K_{eff} \approx 0.9$) when its thickness is 1/3 of the PVDF film. C_{gs} is very small (about 10 pF at 4 MHz) because a short cable (25 cm in length) is used to connect the grid of DMOS integrated circuit and the bottom electrode of the PVDF film. Consequently, the value of G is approximately 1.

To determine the hydrophone directional response, two physical models can be used, depending on the signal frequency. For 600 kHz, the wavelength is 2.5 mm, which is much less than the hydrophone's outer diameter (5 mm); in that case, the circular piston in a planar rigid baffle model is adequate. In the case of 200 kHz, the wavelength is 7.5 mm, which is greater than the hydrophone's outer diameter, so an un-baffled circular piston model should be used.

Table 2.2. Directional response physical models equations [31].

MODEL	EQUATION
1. Baffled circular piston	$R_1(\theta) = \frac{2J_1(ka\sin\theta_0)}{ka\sin\theta_0}$
2. Un-baffled circular piston	$R_1(\theta) = \frac{2J_1(ka\sin\theta_0)}{ka\sin\theta_0}\left(\frac{1+\cos\theta_0}{2}\right)$

The directional response to a plane wave incident at an angle θ_0 to the normal can be theoretically analyzed from equations in Table 2.2, where *k* is the wave number in water, *a* is the radius of the hydrophone and J_1 is the first order Bessel function.

Considering that the multilayer planar acoustic structure affects the hydrophone's directional response, a correction coefficient $K(\theta_0)$ is necessary. Then, the total hydrophone directional response will be expressed as:

$$R(\theta_0) = K(\theta_0) R_1(\theta_0) \tag{2.18}$$

Presuming that the protection layer, the aluminum electrode, the glue layer and the PVDF film of the hydrophone are all flexible; their thicknesses are small and can be neglected, and their acoustic impedances are approximately equal, the correction coefficient is given by:

$$K(\theta_0) = \frac{2\rho_2 c_2}{\rho_2 c_2 + \rho_0 c_0} = \frac{2}{1 + \dfrac{\rho_0}{\rho_2} \dfrac{\sqrt{n_{20}^2 - \sin^2\theta_0}}{\cos\theta_0}}; n_{20} = {}^{c_0}\!/_{c_2} \tag{2.19}$$

where ρ_0 is the density of water, ρ_2 is the density of the ceramic base, c_0 is the acoustic speed in water and c_2 is the acoustic speed in the ceramic base.

Substituting this formula, the complete hydrophone directional response can be calculated for both models, obtaining the following equations:

1. Baffled: $$R(\theta) = \frac{4J_1(ka\sin\theta_0)}{ka\sin\theta_0\left(1 + \dfrac{\rho_0}{\rho_2}\dfrac{\sqrt{n_{20}^2 - \sin^2\theta_0}}{\cos\theta_0}\right)} \tag{2.20}$$

2. Un-baffled: $$R_1(\theta) = \frac{2J_1(ka\sin\theta_0)(1 + \cos\theta_0)}{ka\sin\theta_0\left(1 + \dfrac{\rho_0}{\rho_2}\dfrac{\sqrt{n_{20}^2 - \sin^2\theta_0}}{\cos\theta_0}\right)} \tag{2.21}$$

2.2.1.2 Lum, Greenstein, Grossman and Szabo Model.

Lum et al. [27] developed a high-frequency membrane hydrophone with a 37 μm diameter spot poled electrode on a 4 μm thick film of the piezoelectric copolymer, polyvinylidene fluoride trifluoroethylene (PVDF-TrFE), for the frequency range from 10 to 150 MHz. The hydrophone acoustic properties were studied using an equivalent circuit model. The acoustic modeling program “PiezoCAD” was used to simulate the hydrophone.

The membrane’s structural thickness mode resonance frequency (f_0) is given by:

$$f_0 = \frac{c}{2t} \tag{2.22}$$

where c is the velocity and t is the thickness of the membrane.

The sensitivity of a membrane hydrophone is determined by the structural resonance of the membrane film, and the electrical and piezoelectric properties of the material, in this case, PVDF-TrFE. The open voltage sensitivity of a hydrophone with a spot poled electrode area and an interconnecting lead attached to the electrode is given by:

$$M_{OC} = \frac{V}{P} = \left(gtC_{spot}\right)\left(C_{spot} + C_s\right) \tag{2.23}$$

where g is the voltage sensitivity, t is the thickness, C_{spot} is the spot electrode capacitance, and C_s is the lead shunt capacitance.

It is important to design a hydrophone with the thickness resonance much larger than the frequency of interest, in order to maximize the sensitivity flat response. On the other hand, as the sensitivity is proportional to the thickness, if it decreases, the sensitivity will also drop. The final effect is that with decreasing thickness, the thickness resonance moves up in frequency but the peak sensitivity drops.

The directivity can be modeling using an ideal circularly symmetric uniform ultrasound transducer of radius b. The transmitted beam pattern will be given by:

$$T(\theta,z)=\left(\frac{j\pi b^2}{\lambda z}\right)\cdot\frac{2J_1\left(\frac{2\pi b\sin\theta}{\lambda}\right)}{\frac{2\pi b\sin\theta}{\lambda}}$$

$$T(r,z)\approx\left(\frac{j\pi b^2}{\lambda z}\right)\cdot\frac{2J_1\left(\frac{2\pi br}{z\lambda}\right)}{\frac{2\pi br}{z\lambda}} \tag{2.24}$$

where J_1 is the Bessel function of the first kind, λ is the acoustic wavelength in water, r is the radial distance, z is the axial distance from the transducer, and θ = arctan(r/z).

For reception, the hydrophone is modeled as an ideal stiff disc hydrophone of radius a, and its directivity will be given by:

$$D(\theta,z)=\left(\frac{j\pi a^2}{\pi z}\right)\cdot\frac{2J_1\left(\frac{2\pi a\sin\theta}{\lambda}\right)}{\frac{2\pi a\sin\theta}{\lambda}} \tag{2.25}$$

In reality, the construction of a practical hydrophone may cause its actual directivity to deviate from this ideal.

2.2.1.3 Galbraith and Hayward Model.

Galbraith and Hayward developed a PVDF membrane hydrophone for use in air-coupled ultrasonic transducer calibration [23]. They used a one-dimensional theoretical analysis to demonstrate the potential of PVDF as a hydrophone material for the frequency range from 100 kHz to 5 MHz, although experimental validation was made from 400 kHz to 1 MHz for a coplanar 28 μm thick membrane hydrophone.

The hydrophone was used in the thickness mode, as displayed in Figure 2.6. The device is assumed to be sensing a normally incident plane wave, where F_1 denotes the force incident on the front face of the transducer and V_o is the voltage generated across the electrodes. Z_E represents the lumped impedance of any electrical loading such as signal conditioning electronics, cables and electrode lead capacitance.

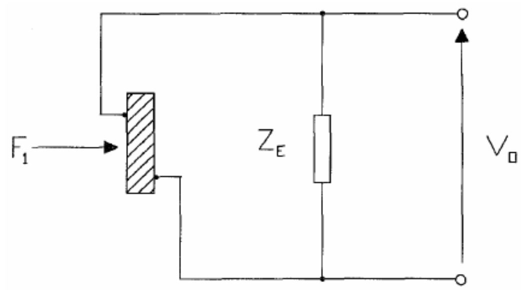

Figure 2.6. Membrane transducer receiver configuration [23].

The sensitivity is calculated as a Laplace transfer function, as follows:

$$\frac{V_o(s)}{F_1(s)} = \frac{\dfrac{-h_{33}T_F K_F(s)U(s)}{sZ_C}}{1-\dfrac{k_t^2 Z_F(s)}{sT}\left(\dfrac{K_F(s)T_F}{2}+\dfrac{K_B(s)T_B}{2}\right)} \tag{2.26}$$

where: h_{33} is the piezoelectric charge constant in the thickness direction, Z_C is the transducer material characteristic acoustic impedance, and T is the transit time for mechanical waves to cross the device thickness. K_F and K_B are the reverberation factors which characterize the mechanical wave energy that propagates within the transducer in response to an external force. T_F and T_B are the transmission coefficients which describe the fraction of incident force transmitted into the transducer at the front and back faces respectively.

The forward-loop voltage attenuation factor U represents the influence on primary piezoelectric activity of the external electrical load connected to the transducer. The electrical load impedance Z_E will depend on the signal conditioning preamplifier input resistance R_E, appearing in parallel with the cable as input capacitance. If R_E is large, the forward voltage transfer function U is approximated by:

$$U \approx \frac{C_0}{C_0 + C_1} \tag{2.27}$$

where C_0 is the hydrophone static capacitance, and C_1 is the cable capacitances.

To simplify the model, it is assumed that the relatively low electromechanical coupling coefficient k_t of the PVDF enables to approximate k_t^2 to cero; the mechanical loading on both faces is the same and the hydrophone works far below resonance, therefore sT is small and ωT tends to zero. This produces the following expression:

$$\frac{V_O}{F_1} = \frac{-h_{33}T}{Z_C}U \tag{2.28}$$

If C_0 is much lesser than C_1, which is normally the case, the force-voltage relationship will be given by the next expression:

$$\frac{V_O}{F_1} = \frac{-h_{33}T}{Z_C}\left(\frac{C_0}{C_1}\right) \tag{2.29}$$

This equation proposes that the output voltage is independent of frequency and mechanical loading conditions, depending only on the transducer material parameters and the ratio between the static and load capacitance. This is why a standard membrane hydrophone calibrated for use in water may be applied to the air medium.

2.2.1.4 Koch and Molkenstruck Model.

At high frequencies, above 1MHz, there are some additional effects that should be considered in a piezoelectric transducer model, such as dielectric losses and shunt capacities. Besides, when a long distance between the hydrophone and the amplifier can not be avoided, cable effects play an important role at high frequencies. Koch and Molkenstruck developed a model including those issues as part of their study on primary calibration of hydrophones with extended frequency range from 1 to 70 MHz, using optical interferometry [47].

The model developed included three main parts: calculation of the pressure in the membrane, the electrical properties of the hydrophone, and the cable transformation. It presumes an acoustic plane wave perpendicular to the membrane hydrophone, as shown in Figure 2.7. The wave penetrates into the electrodes and the membrane, and is partly reflected from each interface. This results in resonance effects leads at certain frequencies.

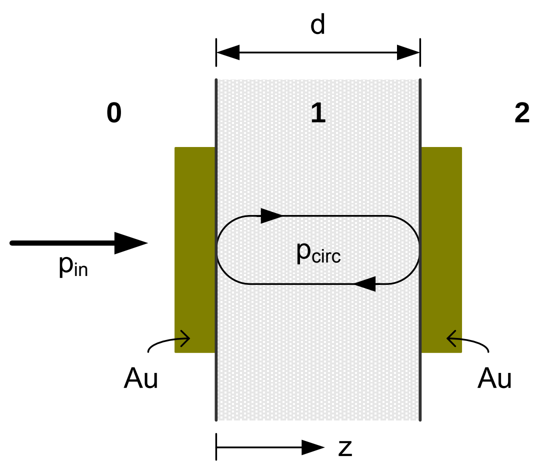

Figure 2.7. Sound propagation inside and outside a membrane of thickness *d* and gold electrodes. p_{in} is the input acoustic field and p_{circ} is the circulating field [47].

The electrodes are characterized by reflection and transmission factors, and the membrane is represented as a single acoustic resonator of length *d*. Then, a Fabry-Perot resonator was applied to calculate the circulating pressure p_{circ} as:

$$p_{circ} = \frac{T_{p,01} p_{in}}{1 - R_{p,12} R_{p,10} e^{(iK2d - \alpha 2d)}} \tag{2.30}$$

where p_{in} is the input acoustic field, *d* is the membrane thickness, $T_{p,01}$ is the complex transmission of the gold electrode from water to membrane, $R_{p,10}$ is the reflection coefficient of the gold electrode from membrane side, $R_{p,12}$ is the reflection coefficient of the gold electrode from water side, *K* is the acoustic wave vector in the membrane, and α is the acoustic absorption.

The pressure at a position 0 ≤ z ≤ d is obtained by superposition of the two waves traveling in the membrane, in opposite directions:

$$p(z) = p_{circ} e^{(iKz - \alpha z)} + p_{circ} e^{(iK(2d - z) - \alpha(2d - z))} R_{p,12} \tag{2.31}$$

Assuming the polarization of the PVDF to be uniform, the spatially average pressure is calculated by:

$$\bar{p} = \sqrt{\left(\frac{1}{d}\int_0^{d-d_{pol}} \mathrm{Re}[p(z)]dz\right)^2 + \left(\frac{1}{d}\int_0^{d-d_{pol}} \mathrm{Im}[p(z)]dz\right)^2} \tag{2.32}$$

The voltage resultant from the charge generated at the electrodes of the active hydrophone spot was calculated using the piezoelectric constant d_{33} = 15^{x}10^{-12} m/V. For simplicity, only the longitudinal part of the membrane deformation was considered. The generated voltage U_E can be found by:

$$U_E = \frac{d_{33}\bar{p}}{\varepsilon_r \varepsilon_0} \tag{2.33}$$

where ε_r is the relative dielectric constant and ε_0 is the dielectric permeability of free space.

The hydrophone electric properties can be modeled by an equivalent network containing an ideal source with open-circuit voltage U_E. The spot is represented by a capacitor with losses (C_{spot}) and an admittance (Y_{spot}). The lead electrodes and the shielding deposited on the membrane, being immersed in the water form a capacitor to ground that bypasses the spot and, therefore, reduces the sensitivity. These losses are represented by C_{H2O} and Y_{H2O}. Figure 2.8 illustrates the equivalent circuit.

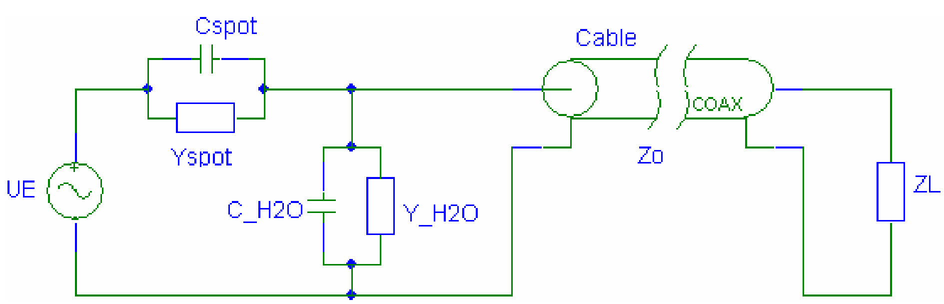

Figure 2.8. Equivalent circuit of a membrane hydrophone with electrode losses.

C_{spot} is mainly given by the geometry, while Y_{spot} is mainly determined by the dielectric losses of PVDF. They can be found using next equations.

$$C_{spot} = \frac{\varepsilon'_{PVDF}\varepsilon_0 \pi R^2}{d}; \qquad Y_{spot} = 2\pi f C_{spot} \tan(\delta_{PVDF}) \tag{2.34}$$

where ε'_{PVDF} is the real part of the relative dielectric constant of PVDF, R is the radius of the active spot area, and Tan(δ_{PVDF}) is the loss factor of PVDF

The relative dielectric constant ε_{PVDF}, the loss factor $tan(\delta_{PVDF})$ and the acoustic absorption α depend on the frequency. They were fitted by linear and quadratic polynomials, as presented in the following equations. The frequency values are in MHz.

$$\begin{aligned}
&\varepsilon'_{PVDF} = 8.04 - 2.31\log(f) \\
&\tan(\delta_{PVDF}) = 0.22 + 0.07\log(f) - 0.055(\log(f))^2 \\
&\alpha = (0.15 + 0.099 f)1/mm
\end{aligned} \tag{2.35}$$

The capacitance C_{H2O} was found as 52 pF through graphical representations for a stripline in a homogeneous medium. The admittance Y_{H2O} mainly depends on the dielectric losses of water. The loss factor $tan(\delta_{H2O})$ is extremely sensitive to dissolved particles and because the chemical composition of the tank fluid was unknown, it was determined through experimental results fitting.

The hydrophone impedance Z_h is given by:

$$\frac{1}{Z_h} = j2\pi f\left(C_{spot} + C_{H2O}\right) + 2\pi f\left(\tan(\delta_{PVDF})C_{spot} + \tan(\delta_{H2O})C_{H2O}\right) \tag{2.36}$$

The end-of-cable impedance Z'_h is found through an impedance transformation:

$$Z'_h = Z_0 \frac{Z_h - jZ_0 \tan(\beta l)}{Z_0 - jZ_h \tan(\beta l)}; \qquad \beta = \frac{2\pi f}{c_{cable}} \tag{2.37}$$

where β is the propagation constant of the cable, with c_{cable} = 2x10^8 m/s

The piezoelectric coefficients were assumed to be constant. The most critical parameter was the sound velocity in PVDF, and the experimental data obtained verified the value of 2200 m/s.

The interaction between the cable and the capacitive input of the spot generates a resonance-like behavior at 40 MHz. In this frequency range, the end-of-cable hydrophone impedance mainly depends on the admittance Y_{H2O}, which is caused by dielectric losses in the water and it strongly depends on the tank water quality. Then, the measurements obtained at this frequency depend very much on the measurement conditions. To avoid this effect, the losses should be minimized by a bilaminar structure or with matched protecting layers on the rear side. Additionally, a short cable length is recommended for high frequency applications.

The theoretical model shows a small increase in the sensitivity with decreasing frequencies below 1 MHz, but it was not confirmed with the experimental data. In the model, this increase is caused by the decreasing dielectric constant ε_r at low frequencies, which is not, however, supported by a sufficient number of experimental data.

2.2.2 PVDF PROPERTIES

The models described in previous section can be a powerful engineering tool; however, the benefit of a model is only as accurate as the material properties used in it. This led the efforts to perform other investigations whose objectives were to measure and/or calculate the elastic, dielectric and piezoelectric properties of PVDF. Some of these studies considered the properties values as constants [26, 48, 49], while other considered their frequency dependency [41, 50, 51].

There are different factors which made PVDF properties measurements very difficult. One of them is the nature of the process of turning the PVDF from an inert polymer to a poled piezo-electric film, which is complicated and involves several changes with inherent randomness and can result in considerable variation in the material properties of the final film. Besides, poled material is available only as thin films, and not all parameters can be measured in that form. Consequently, the material properties provided in the literature are mostly for specific PVDF configurations, and they are provided as an indication of typical values.

Table 2.3 lists the typical properties of PVDF film with 9, 28, 52 and 110 μm thickness, fabricated by Measurements Specialties, Inc, with silver ink printed electrodes. Table 2.4 documents the piezoelectric, pyroelectric and other constants of a PVDF film at room temperature and frequency 1 kHz [31]. The PVDF film was manufactured at Shanghai Institute of Organic Chemistry, Academia Sinica. Table 2.5 details the model input parameters used by Gélat et al. [52] in their theoretical model for a 25 μm PVDF film and 0.5 mm diameter membrane hydrophone.

Table 2.3. Typical properties of PVDF film by MSI [42].

Parameter	Symbol	Value	Units
Thickness	t	9, 28, 52, 110	μm
Piezo Strain constant	d_{31} d_{33}	23 -3.3	10^{-12} $\frac{m/m}{V/m}$ or $\frac{C/m^2}{N/m^2}$
Piezo Stress constant	g_{31} g_{33}	216 -330	10^{-3} $\frac{V/m}{N/m^2}$ or $\frac{m/m}{C/m^2}$
Electromechanical Coupling Factor	k_{31} k_t	12% 14%	
Capacitance	C	380 for 28μm	pF/cm^2, @ 1 kHz
Young's Modulus	Y	[2;4]	10^9 N/m^2
Speed of Sound Stretch direction Thickness direction	V_0	 1500 2200	m/s
Pyroelectric Coefficient	p	30	10^{-6} C/m^2 ºK
Permittivity	ε	[106;113]	10^{-12} F/m
Relative Permittivity	$\varepsilon/\varepsilon_0$	[12;13]	
Mass Density	ρ_m	1.78	10^3 kg/m^3
Volume Resistivity	ρ_e	$>10^{13}$	Ohm/m^3
Surface Metallization Resistivity	R_{oe}	0.1	$Ohms/m^2$ for Ag Ink
Loss Tangent	$\tan \delta_e$	0.02	@ 1 kHz
Yield Strength		[45;55]	10^6 N/m^2 (stretch axis)
Temperature Range		-40 to 100	ºC
Water Absorption		<0.02	% H_2O
Maximum Operating Voltage		750 (30)	V/μm, DC, @ 25ºC
Breakdown Voltage		2000 (80)	V/μm, DC, @ 25ºC

Table 2.4. PVDF constants at 1 kHz, by Yiquan et al. [31].

Parameter	Symbol	Value	Units
Thickness	*l*	90	µm
Piezo Strain constant	d_{31}	26	pC/N
Piezo Stress constant	g_{31}	250	10^{-3} Vm/N
Electromechanical Coupling Factor	*K*	18%	
Stiffness Constant (Young's Modulus)	*Y*	3.0	10^{9} N/m^{2}
Pyroelectric Coefficient	*p*	30	10^{-6} C/m^{2} ºK
Dielectric constant (relative permittivity)	$\varepsilon/\varepsilon_0$	14	
Mass Density	ρ	1.78	10^{3} kg/m
Unpolarizing Temperature		135	ºC

Table 2.5. Membrane hydrophone theoretical model parameters, by Gélat et al. [52].

Parameter	Symbol	Value	Units
Thickness Gold Chromium PVDF Glue	*t*	 0.1 0.05 25 0.5	µm
Piezo Strain constant	d_{33}	14	10^{-12} C/N
Speed of Sound Water Gold Chromium PVDF Glue Cable	*c*	 1482.36 3240 6608 2300 1600 2 x 10^{8}	m/s
Dielectric constant	ε_0	8.85	10^{-12} F/m
Modulus of Relative Permittivity PVDF	$\lvert\varepsilon_r\rvert = \lvert\varepsilon/\varepsilon_0\rvert$	$-3.1\log_{10}(f)+29$, for *f* ≤ 25 MHz	With *f* in Hz
Material Density Water Gold Chromium PVDF Glue	ρ	 0.9982 19.281 7.194 1.780 1.000	10^{3} kg/m^{3}
Loss Tangent of relative permittivity PVDF	tan δ	$0.22+0.07\log_{10}(f)$ $-0.055\log_{10}(f^{2})$	With *f* in MHz
Attenuation coefficient PVDF Glue	α	 111 104	neper / (m MHz)

2.3 ACOUSTIC RADIATION

The rigid circular piston mounted flush with the surface on an infinite baffle is a useful model applicable to several related problems, such as organ pipes and loudspeakers [53, 54]. In this section, the radiation from a plane circular disk will be explained. Although the problem will be solved for a piston as a transmitter, the far field directional characteristics of a given piston are the same as transmitter or receiver [54].

The physical system consists on a circular piston of radius *a*, mounted on a flat rigid baffle of infinite extent. The radiating surface of the piston moves uniformly with speed u_p, normal to the baffle, where:

$$u_p = u_0 e^{j\omega t} \tag{2.38}$$

At near field ($r<<a$), the acoustic axial pressure displays strong interference effects because the acoustic field close to the piston is complicated. One way to demark the minimum distance required to speak about far field is r_1, given by next equation. However, this quantity is useful only if the ratio a/λ is large enough to make r_1 positive.

$$r_1 = \frac{a^2}{\lambda} - \frac{\lambda}{4} \tag{2.39}$$

For far field conditions ($r>>a$), the acoustic pressure will be given by [53, 54]:

$$p(r,\theta,t) = j\frac{a^2 \rho_0 c_0 u_0 k}{2r} e^{j(\omega t - kr)} \left[\frac{2J_1(ka\sin\theta)}{ka\sin\theta} \right] \tag{2.40}$$

where *r* is the distance from the disk, *θ* is the angle from the disk axis, *a* is the disk radius, *k* is the wave number, J_1 is the Bessel function of order 1.

The piston directivity function is defined by the bracketed term. It determines the angular dependence of *p* and it approximates to 1 as θ goes to 0. The directivity is given by:

$$D(\theta) = \frac{2J_1(ka\sin\theta)}{ka\sin\theta} \tag{2.41}$$

2.4 SUMMARY

In this section the fundamental concepts of piezoelectric films were presented, including their characteristics of conversion from mechanical to electrical, and vice versa. Different models were presented, starting with simple equivalent circuits for piezoelectric transducers, and continuing with more complex models, some of them developed specifically for PVDF membrane transducers, taking into consideration other factors such as physical configuration, wave reflections, attenuations, etc. The PVDF constants are presented from three different sources to allow a comparison of the parameters, and finally an acoustic radiation model for a circular piston is presented in order to analyze the far field radiation.

3 MATERIALS AND METHODOLOGY

This chapter describes the materials and methods used in the research. First, the PVDF transducers design considerations are explained and the used construction techniques are documented. The second part of the chapter presents the transducers models used for computer simulations. After this, the experiments strategy is explained, as well as the techniques used to analyze the simulated and experimentally obtained data. Finally, the experimental setup used in the underwater acoustical measurements is depicted.

3.1 TRANSDUCERS CONSTRUCTION TECHNIQUES

PVDF piezo film sheets were used in this research to construct several transducers. The PVDF films used were fabricated by Measurement Specialties, Inc. The thicknesses available were 9, 28, 52 and 110 µm, and the last three were selected for the tests. The films were printed with silver ink electrodes on both surfaces at fabrication. PVDF constants provided by the manufacturer can be found in Table 2.3.

3.1.1 CONSTRUCTION TECHNIQUES EVOLUTION

Initially, a very simple PVDF transducer was created only to verify the material capabilities in water. It consisted of a PVDF film with one electrode on each side. The cable was connected to the electrodes by soldering it to a copper conductive tape attached to each piezo film electrode, as it can be seen in Figure 3.1. Although this simple device was verified to work both, in air and water, its acoustic response varied with the film movement, as it flexed and bend in different directions. The performance of a device like this is marginal and unpredictable, then it is advisable to control the shape of the film and the support structure [42].

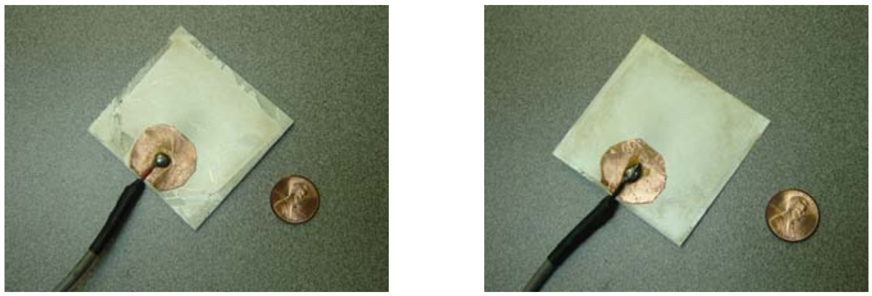

Figure 3.1. Initial unbounded – unshielded PVDF transducer.

The positive and negative electrodes were isolated by taking off the silver paint from the film borders on the positive electrode side. To remove the paint, different materials were tested, having the best results with lacquer thinner. The active area was calculated measuring only the region were both piezofilm surfaces have conductive paint. Figure 3.2 presents an example of a PVDF film prepared. The positive electrode has been peel off on one side to isolate it from the negative electrode, which covers the complete surface from the other side. As it can be seen from the figure, the piezofilm total area is x_1y_1, but the active area is x_2y_2.

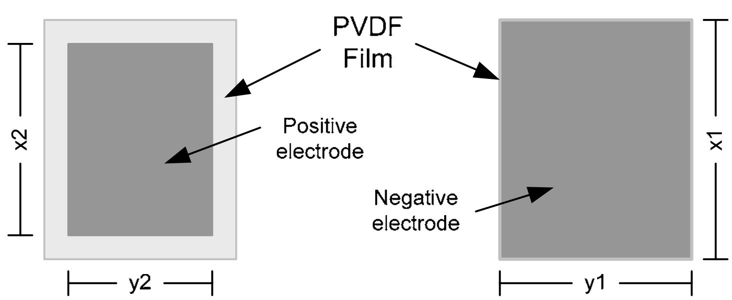

Figure 3.2. Positive and negative electrodes silver conductive paint.

Afterwards, a framed transducer was constructed and it is presented in Figure 3.3. The same principle was used for the PVDF film preparation, but since it was designed to be submergible, the positive electrode was isolated from the water using a coating layer. The electrodes were bounded to the film using a copper conductive tape, soldered to a cable. This part was isolated using plastic silicon. Although the design pretended to maintain the film tense through the acrylic frame, it was not effective for this particular characteristic. However, this design can be considered a membrane transducer, working in the thickness mode.

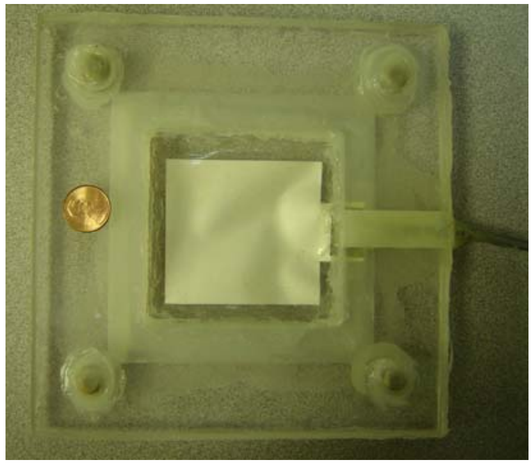

Figure 3.3. First thickness mode PVDF membrane transducer framed and unshielded.

Later, a framed transducer was created, decreasing its size and improving the tensile characteristics, using an adjustable frame made of acrylic, as shown in Figure 3.4. This transducer was constructed using a single PVDF film, bent over its self, to create the shielded configuration. The electrodes were connected using eyelets soldered to a shielded cable.

Figure 3.4. Framed and shielded PVDF 2-layers membrane transducer, without backing material.

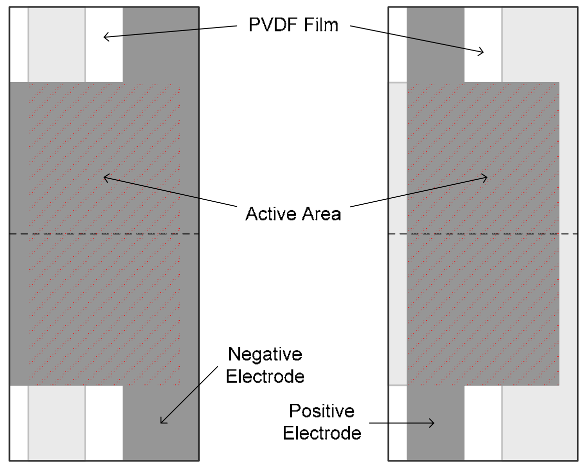

Figure 3.5. PVDF electrode pattern for the framed and shielded PVDF 2-layers membrane transducer without backing material.

This structure had the advantage of being, not only smaller, but shielded, which made it better to reject noise and did not need an additional coating layer, since the positive electrode was already isolated from the outside. The PVDF film was prepared following the patter described in Figure 3.5, in order to outline the conductive ink electrodes. Then, the PVDF film was bent over the positive electrode, in a way that it remains inside the construction, and two circular holes were opened to fix the connectors with a screw, as presented in Figure 3.6.

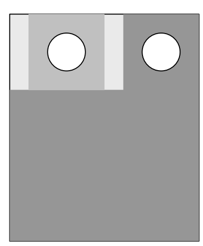

Figure 3.6. Framed and shielded PVDF 2-layers membrane transducer diagram.

Once the concept was developed, several transducers were designed in order to satisfy the physical constraints required by sensing acoustical signals, not only in open field, but in liquid filled tubes too. Therefore, the construction techniques learned to that moment were applied to develop smaller circular transducers, until attaining the final structure, described in next section.

3.1.2 FINAL TRANSDUCERS CONSTRUCTION

The final design selected, as shown in Figure 3.7, consisted on a circular PVDF single membrane, attached to a copper clad printed circuit board FR4, which serves at the same time as backing material and electrode connector. The negative electrode is external, and therefore it is in direct contact with the water when the transducer is in use. The positive electrode is internal, in direct contact with the copper board, and isolated from the water by the PVDF film itself.

Figure 3.7. PVDF transducer final design.

Different PVDF transducers were designed in order to evaluate the influence of area and thickness in the sensitivity response. The areas were modified by changing the active area radius, from 2, 3 and 4 mm. The thicknesses used were 28, 52 and 110 μm. The combination of three areas and three thicknesses gave a total of nine different transducers. The construction procedure for all nine transducers was the same, and it is described afterward.

First, the copper clad board is created for the three different sizes. The board consists of an internal active area circle of radius r, which possible values are 2, 3 and 4 mm, as seen in Figure 3.8. The external radius r_2 is equal to r + 1.5 mm, approximately. Two holes are opened to connect the cable to the electrodes.

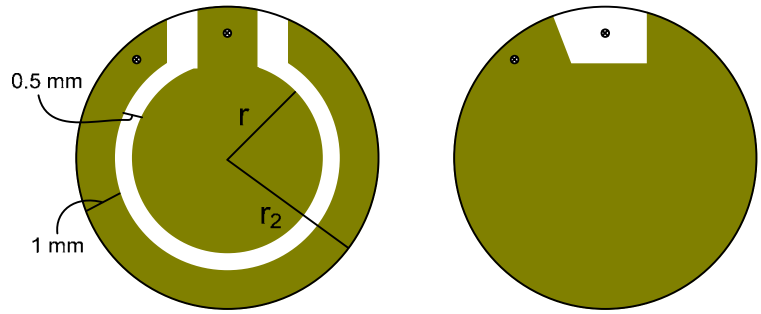

Figure 3.8. Copper coated board schematic.

The internal circle acts as the positive electrode, in contact with the active area silver ink electrode painted on the PVDF film, while the external circle and the backing copper act as the negative electrode. This design provides the advantages of a shielded configuration, without the necessity of using two PVDF layers.

The copper surface is smooth out with sandpaper in order to eliminate little imperfections and adhered material as oxide and dirt. Figure 3.9 shows a picture of the finished copper coated board. If a double sided copper clad board is not available, the backing electrode can be created using a self adhesive electrical copper tape, like the 3M-1181N-ND.

Figure 3.9. Copper board picture.

Since the PVDF does not support high temperatures, it is important to weld the cable to the electrodes, before bonding the PVDF film. The positive electrode cable is welded to the leg connected to the internal circle, while the negative electrode cable is welded to the external circle and the backing copper, at both sides of the board. The cable used for the connections was a two meters (2 m) microphone shielded cable with one conductor, General Cable Carol Brand C1300.

Figure 3.10. Copper coated board welded to the cable.

The welding points were sleeked with a drilling machine, in order to leave them as flat as possible to allow the PVDF film to make contact with the copper board without being considerably deformed by the welding. Care must be taken because if the point is excessively reduced, the connection could fail. The connectivity was verified using a meter. Figure 3.10 shows one of the copper coated boards welded to the shielded cable.

The second stage of the construction consists on preparing the PVDF film. For this part, a rectangular PVDF film is cut, from a size enough to cover the complete copper board at least two times. The active area is determined by the positive electrode size, since the negative electrode will be all over the other surface. Then, a circular protective tape template is cut and adhered to the positive electrode side. This tape will cover the active area, allowing peeling off the silver paint from the rest of the surface. The other side (negative electrode) is completely covered by protective tape. The 3M Scotch gloss finish transparent tape was used as protective tape, since it does not peel the silver ink when it is took off. This stage can be seen in Figure 3.11. Next, the silver conductive paint from the internal side is removed with lacquer thinner, except by the part protected with the tape, creating the active area positive electrode.

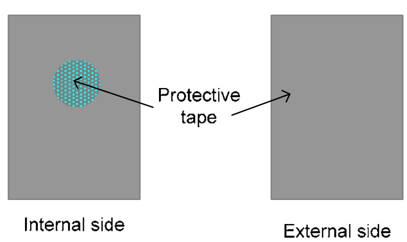

Figure 3.11. Piezofilm electrodes protective tape.

A conductive adhesive tape was used to attach the PVDF film to the copper board. The tape 3M-970312 conducts only in the vertical axis, but not in the horizontal axes, allowing it to be used all over the board without generating a conductive path between the two electrodes, despite being attached to both of them. A square piece of conductive tape was attached to the copper board, without removing the protective layer from the other side. Since the tape is squared and the board is circular, there is a remaining piece of tape that must be cut using the board as a mold. This was made being careful of not wrinkle the tape.

Before attaching the board to the PVDF film, it was necessary to draw marks to the film in order to facilitate the correct board placement. This is essential, since the positive electrode on the board is separated by just 0.5 mm from the negative electrode. Then, the protective tape was removed from the PVDF film positive electrode and from the conductive tape on attached to the board, and they were stuck together using the marks to align the board borders, as seen in Figure 3.12.

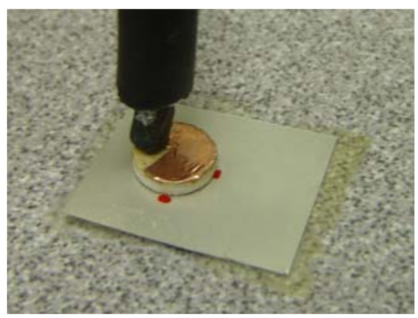

Figure 3.12. PVDF film attached to the copper coated board.

Then, the PVDF film, along with the negative electrode protective tape, was cut using the board as a mold, but leaving a piece of PVDF in order to bend it over the board to make contact with the negative electrode, as seen in Figure 3.13.

Figure 3.13. Final cut of PVDF film attached to the copper coated board.

To secure the PVDF free piece bent over the board, it was glued to the board's cross sectional area using an epoxy. This is especially critical for the transducers constructed with thicker films (i.e. 110 μm). Next, the protective tape was detached from the bent part, but not from the frontal electrode. The film was connected to the backing negative electrode using an adhesive copper tape, and the connections were verified using a meter. At this point, the transducer is ready, but without the case, as it can be seen in Figure 3.14.

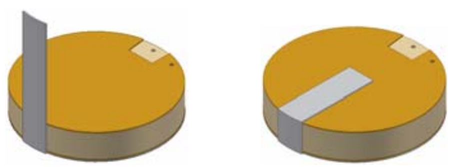

(a)

(b)

Figure 3.14. PVDF transducer core ready, without a case. (a) Schematic. (b) Picture.

In order to use these transducers inside a liquid medium, it was necessary to create a case for them, which isolates the positive electrode from the medium, at the same time that protects the connections. The transducers' case was formed using plastic epoxy. This design offers the advantage of being adaptable to different geometries requirements, without changing the transducer construction.

(a)

(b)

(c)

Figure 3.15. PVDF transducers' case process.

The epoxy was applied to cover the transducer's perimeter, as seen in Figure 3.15 (a). Once the epoxy was completely dry and cured, it was shaped with a polishing machine, giving it the desired aspect, as shown in Figure 3.15 (b). Finally, a thin layer of aquarium sealant silicone was used to seal the PVDF film borders, and heat shrink tubing was used to cover the epoxy borders on the transducer's cable, as shown in Figure 3.15 (c).

3.1.2.1 Constructed transducers' specifications

Figure 3.16 presents the final transducers schematic. The diameters dimensions depend on the active area radius, as listed in Table 3.1. The minimum total diameter obtained was approximately of 1.1 cm, and the maximum was 1.5 cm. These diameters are not exactly the same for all transducers due to the manual case fabrication process, and they are similar to the maximum size established in the design requirements (diameter 1.27 cm).

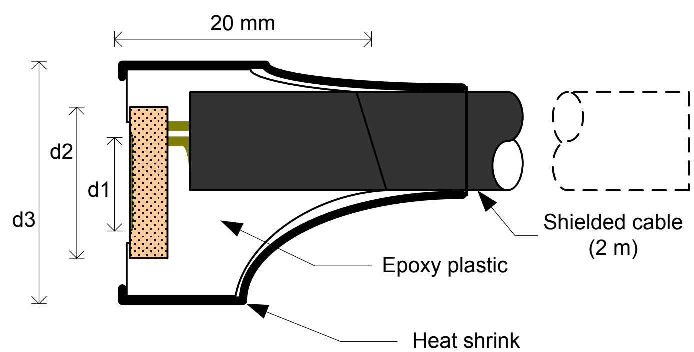

Figure 3.16. PVDF Transducers outline dimensions schematic

Table 3.1. PVDF Transducers dimensions

ACTIVE AREA RADIUS	d_1	d_2	d_3
2 mm	4 mm	7 mm	11 mm
3 mm	6 mm	9 mm	13 mm
4 mm	8 mm	11 mm	15 mm

Since the sensing element is on the tip, the transducers can be used as flush-mounting type, or can be introduced into a tube to transmit or receive frontal waves.

3.2 TRANSDUCERS MODELING

The constructed transducers were modeled in order to clarify their experimental behavior. The sensitivity was estimated for a single membrane transducer as a function of frequency, active area and thickness with the purpose of identify the influence of these factors in the transducer's response. It was calculated for the conversion from mechanical to electrical (receiving), and from electrical to mechanical (transmitting). The directivity effect was not of interest and therefore it was not considered for the calculations; besides, all the tests were realized with angle zero.

3.2.1 RECEIVING SENSITIVITY

Since the designed transducers consisted of a single piezofilm bonded to a copper plate, which has high acoustic impedance, and the receiving side is low impedance water medium, the Swartz and Plummer [46] model was applied (explained in section 2.2.1.1, page 27). The resonance frequency is given by:

$$f_r = \frac{c_{PVDF}}{4t} \tag{3.1}$$

where c_{PVDF} is the speed of sound in PVDF and t is the membrane thickness.

The PVDF transducer must be used in a frequency range well below the resonance frequency, in order to maintain the linear response. From the previous equation, it can be seen that this frequency depends only on the film thickness and is not affected by the active area. Table 3.2 lists the calculated resonance frequencies for all the different PVDF film thicknesses used. As it can be seen, the minimum resonance frequency (5 MHz) is much greater that the maximum frequency of interest (160 kHz), therefore, the selected thicknesses are appropriate for the desired frequency range.

Table 3.2. PVDF transducers receiving resonance frequencies.

THICKNESS (μm)	f_r (MHz)
28	19.64
52	10.58
110	5.00

The PVDF film was modeled with a Thevenin equivalent circuit, where the voltage source depends on the open circuit sensitivity, and the impedance is given by the capacitance of the film. The static capacitance of the film C_o depends on the film physical area, while the electric conversion coefficient h depends on the transducer active area. The stiffened acoustic impedances of the three mediums (copper, water and PVDF) were calculated multiplying density by speed of sound in the respective medium.

The PVDF equivalent voltage source is given by:

$$V_{PVDF} = P_{in}\left(\frac{2h}{j\omega C_0}\right)\left(\frac{1}{Z_M\left(1 - j\,{}^{Z_0}\!/_{Z_M}\right)\cot(k_0 l)}\right) \tag{3.2}$$

The piezofilm static capacitance is given by:

$$C_{PVDF} = \varepsilon\frac{A}{t} \tag{3.3}$$

Although some authors consider the permittivity as frequency dependant [47, 52], it was supposed constant, since for the frequency range from 10 to 160 kHz, it does not vary considerably. Table 3.3 lists the capacitances corresponding to the nine transducers built.

Table 3.3. PVDF transducers capacitance.

THICKNESS (μm)	ACTIVE AREA RADIUS (mm)	PHYSICAL RADIUS (mm)	CAPACITANCE (pF)
28	2	3.5	155.3125
	3	4.5	256.7410
	4	5.5	383.5268
52	2	3.5	83.6298
	3	4.5	138.2452
	4	5.5	206.5144
110	2	3.5	39.5341
	3	4.5	65.3523
	4	5.5	97.6250

The transducer is connected to the pre-amplifier circuit using a cable. These elements are modeled as impedances through a simplified electrical circuit, shown in Figure 3.17, where Vs is the voltage generated by the piezo film, Z_{PVDF} is the piezo film impedance, Z_{Cb} is the cable impedance, and Z_L is the pre-amplifier input impedance.

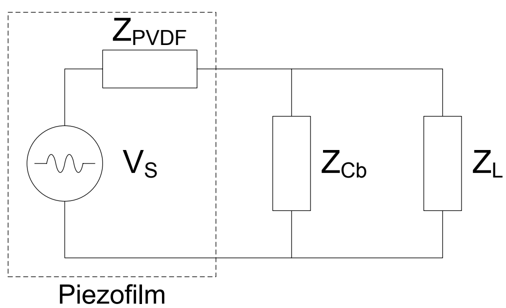

Figure 3.17. PVDF hydrophone equivalent closed circuit.

The cable was represented as a capacitance connected from the positive to the negative node, and it was calculated using the capacitance per feet parameter given by the manufacturer (42 pF/ft) and the cable length (2m), resulting in a total of 275 pF. The electrical load impedance is composed of a capacitor connected in parallel with a resistor. The capacitor is given by the input capacitance specified for the instrumentation amplifier (6pF). The resistance is set by the amplifier and an additional resistor of 1 MΩ connected in parallel with the electrical input. This resistor is used in order to control de high pass filter effect of the piezo film capacitance.

The relation between the output voltage and the voltage generated by the piezo film can be calculated through the potential divider as:

$$M_2 = \frac{V_{out}}{V_s} = \frac{Z_T}{Z_T + Z_{PVDF}} \tag{3.4}$$

where Z_T is the total output impedance, given by:

$$Z_T = Z_{Cb} \| Z_L = \frac{1}{j\omega(C_{Cb} + C_L) + \frac{1}{R_{Cb}} + \frac{1}{R_L}} \tag{3.5}$$

The receiving sensitivity M is defined as the relation between the input pressure and the output voltage generated by the system, and is given by the product of M_1 and M_2, as:

$$M = \frac{V_{out}}{P_{in}} = M_1 \cdot M_2 \tag{3.6}$$

3.2.2 TRANSMITTING SENSITIVITY

The transmitting sensitivity indicates the ability of the PVDF film to convert the electrical input into an acoustic pressure. The KLM resonator model, explained in section 2.1.2.3 (page 23) was used to model the PVDF transducers transmitting behavior.

The resonator is connected to two mediums. The copper plate was taken as medium 1, and the water as medium 2. The acoustic impedances of the three mediums (copper, water and PVDF) were calculated multiplying the mass density by the speed of sound in the respective medium, and the contact area. The piezo film capacitance is calculated with the same values used for the receiving sensitivity, included in Table 3.3.

The complete model parameters include a conversion coefficient *h*, which relates the voltage applied to the transducer, with the displacement generated, given by the inverse of the piezo strain constant d_{33}.

The pressure radiated by the transducer into medium two (water) when it is excited by a voltage V_3 in the phasor domain, is given by:

$$P_2(\omega) = \frac{Z_2 V_3(\omega)}{\phi Z_{in}} \frac{\left(\Gamma_1 e^{-jkd/2} - e^{jkd/2}\right)}{e^{jkd} - \Gamma_1 \Gamma_2 e^{-jkd}} (1 + \Gamma_2) \tag{3.7}$$

3.3 PHYSICAL SYSTEM SETUP

The physical system was designed in order to generate and record acoustic pulses under the water. Figure 3.18 displays a block diagram of the different parts that compose the system configuration.

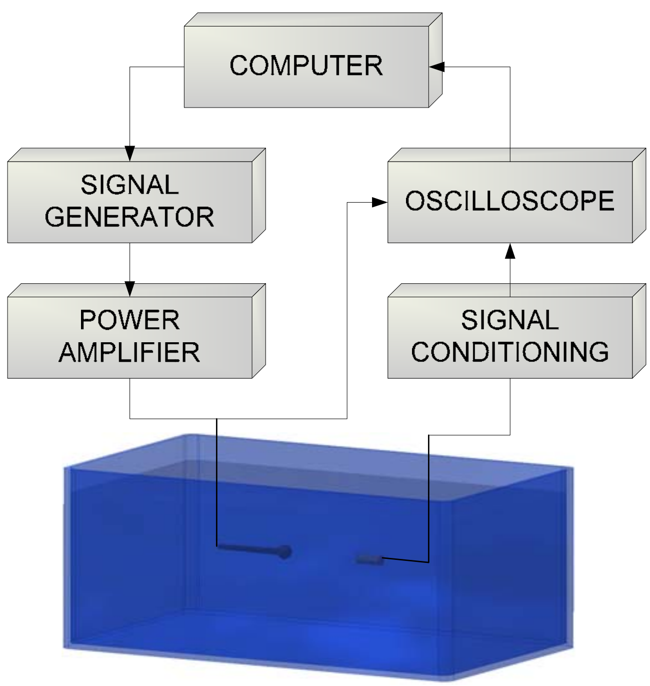

Figure 3.18. Physical system setup block diagram.

As depicted in the diagram, a computer was used to generate the system input, an electrical sequence containing an amplitude modulated Hanning pulse, which is sent through the serial driver directly to the function arbitrary waveform generator. It converts the electrical sequence into an electrical signal, that is amplified by a sound power amplifier and finally it is connected to the transmitter. The resulting acoustic signal is sensed by the receiver and processed through a conditioning electronic circuit, in order to eliminate unwanted noise and amplify the signal. Then, this signal is acquired by an oscilloscope and sent to the computer by a serial driver, where the data is analyzed. The parts that compose the system are explained with more details in the next sections.

3.3.1 COMPUTER

A personal computer with Windows XP, MATLAB 7.01 – R14 and LabView 7.1 was used. Two independent virtual instruments were developed in LabView to communicate with the signal generator and the oscilloscope, and to make some simple analysis. MATLAB was used to perform more complex analysis of the signals.

3.3.2 SERIAL DRIVERS

Considering that the acoustic signal was generated and recorded by external devices, the communication of the computer with the signal generator and the oscilloscope was achieved by developing a Virtual Instrument in LabView, based on the driver's basic functions provided by the equipment manufacturer (Agilent).

The drivers allow the computer to control the devices using the special commands programmed in LabView. The signal generator and oscilloscope used have the capability of communicate through serial protocol, however, the computer used did not have a RS232 serial port, therefore, an USB to serial adapter cable was used.

3.3.3 SIGNAL GENERATOR

The electric pulse sequence to be sent through the transmitter is initially generated in the computer using a VI in LabView. It is connected to the Agilent 33120A 15MHz Function Arbitrary Waveform Generator through a serial driver. This device has the capability of saving four arbitrary waveforms in the non volatile memory. This feature is exploited to save the different pulses used to characterize the transducers.

Each pulse is composed of a sequence of 4096 samples, which is the maximum allowed by the signal generator. The signal amplitude oscillates between ±2047, allowing just integer numbers. The VI creates and stores groups of four pulses in the signal generator, changing the carrier frequency of each one by increments specified by the user. This programming cycle can be made several times, depending on the initial and final frequencies. The pulse duration is also specified by the user.

The signal generator can be configured to supply an arbitrary waveform stored in the memory. The signal frequency and amplitude can be modified through the computer interface, or directly using the selectors in the device panel. To generate a pulse, the burst option is selected with a rate of 50 Hz.

3.3.4 POWER AMPLIFIER

In some cases, the signal generator could not provide enough power to the acoustic transmitter, so a TASCAM PA-30B power amplifier was used. Although this is a sound amplifier and therefore it is designed to work at sonic frequencies, its frequency response was measured in the range of interest, from 10 to 160 kHz, and is shown in Figure 3.19.

As expected, the amplifier output amplitude decreased when the frequency increased. However, for the frequency range of interest, the output variation range is 1.26 dB, which is less than -3dB and can be considered an acceptable flat response

[55, 56]. Considering that the signal phase will not be analyzed in the experiments, the phase response of the amplifier is of no interest and therefore was not analyzed.

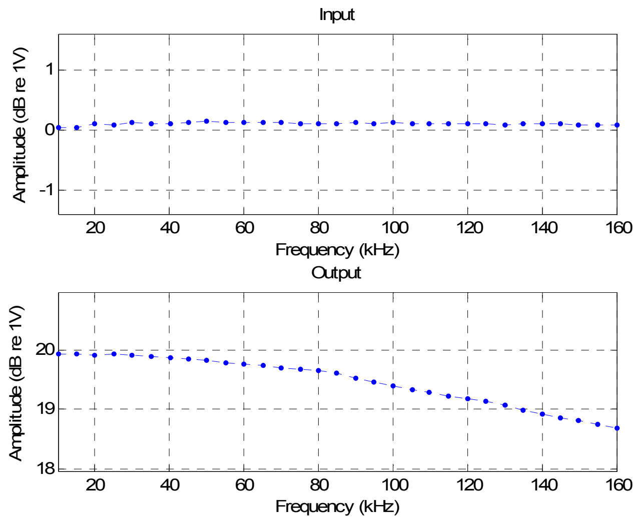

Figure 3.19. Tascam PA-30B measured frequency response.

The amplitude transfer function is illustrated in Figure 3.20. The initial gain configured was approximately 20 dB (G=10V/V), and it decreases as the frequency increases. The maximum variation is of -1.32 dB, which corresponds to an error of ±3.41% with respect to the media (19.37 dB). In this document, the unit dB is used to reference the description of voltages ratios, considering equal impedances in the two points of measurement.

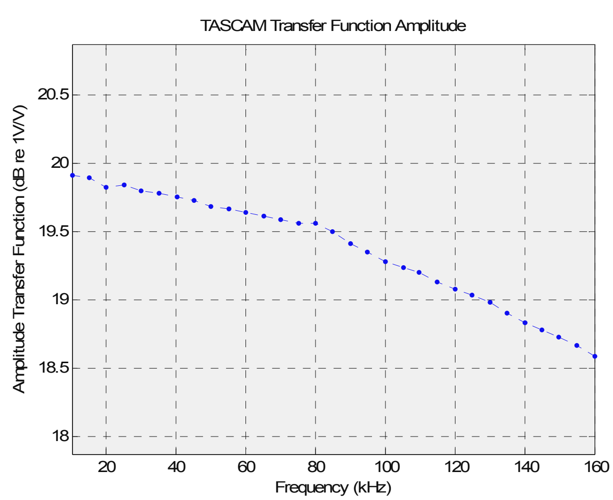

Figure 3.20. Tascam PA-30B Amplitude FFT Transfer Function.

3.3.5 SIGNAL CONDITIONING

The signal conditioning stage is composed by a pre-amplifier, filters and an amplifier, as seen in Figure 3.21. A low pass filter is needed to eliminate aliasing and high frequency noise. A high pass filter is needed to eliminate 60 Hz noise and DC offsets. The amplifier should provide enough amplitude to allow the oscilloscope to read the signal, but it should not exceed the saturation levels. The total gain of the circuit in the pass band is 1000 V/V (60 dB).

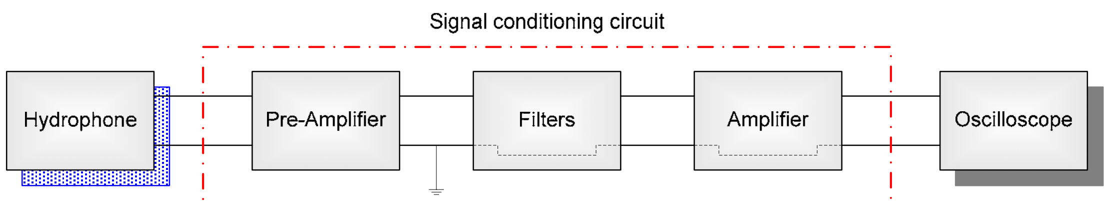

Figure 3.21. Signal conditioning circuit modules.

3.3.5.1 Pre-Amplifier

The interface circuit connected to the hydrophone was designed considering the dynamic response and load impedance requirements. The dynamic response for the frequency range and signal amplitude requirements include a gain bandwidth of at least 1.6 MHz, enough to allow a minimum gain of 10 V/V (20dB) at 160 kHz. Another important parameter that determines the speed of the operational amplifier is the slew rate (SR). For adequate full power response, the slew rate must be greater than [57]:

$$SR = \pi V_{pp} f_C \tag{3.8}$$

The required Slew Rate is 12.06 V/µs, given by a maximum output of 24 V_{pp} at 160 kHz.

Since the piezo film hydrophone frequency response is affected by the load impedance connected to it, the pre-amplifier input resistance should be large enough to guarantee that the cut-off frequency will be well bellow 10 kHz. Additionally, since the input capacitance extends the time constant but attenuates the magnitude of the response [42], it should be as small as possible. Additionally, since the signal level is small, a low leakage high impedance buffer amplifier is recommended.

The pre-amplifier was implemented with an INA110, which is a fast-settling FET-input instrumentation amplifier [58]. It has a small signal band width of 2.5 MHz for a gain of 10. With full power, the band width is 270 kHz for a gain between 2 to 100. The typical slew rate is 17 V/μs. Therefore, the amplifier's dynamic response is more than adequate. Its impedance is given by a resistor of $5\text{x}10^{12}$ Ω, in parallel with a capacitance of 6 pF. The INA110 has a low bias current of typically 20 pA and maximum 50 pA.

The gain in this circuit can be configured to fixed internal values of 10, 100, 200 and 500 connecting pin 3 with pins 13, 12, 16 and 11, respectively. If pin 3 is not connected, the gain is 1. Other gain values can be set by adding an external resistor, R_G, between pin 3 and pins 11, 12 and 16. The pre-amplifier implemented has a fixed gain of 10 V/V and supply voltages of ±15 V_{DC}. The schematic is sketched in Figure 3.22.

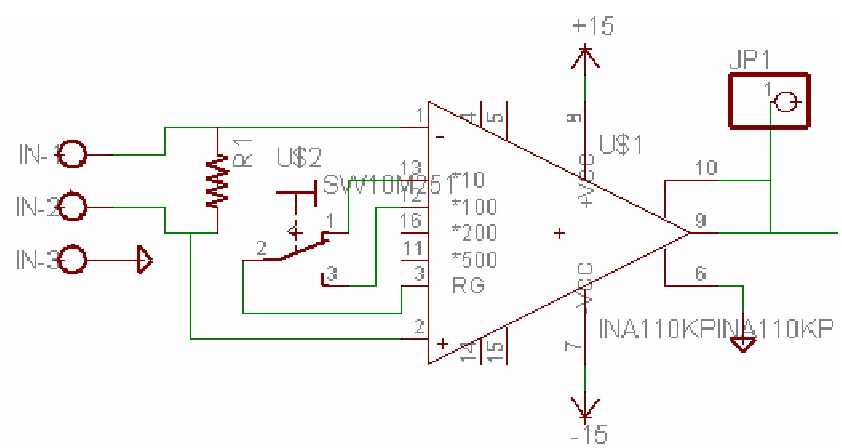

Figure 3.22. Pre-amplifier circuit schematic (INA110).

The preamplifier response was experimentally verified with sinusoidal waves of a determined frequency, from 10 to 160 kHz, at increments of 5 kHz. The magnitude of the signal acquired FFT was calculated, as shown in Figure 3.23 (a). The real frequency response of the system has a good agreement with the expected one, exhibiting an almost constant gain of approximately 20.19 dB in the frequency range of interest, as seen in Figure 3.23 (b), with a maximum variation of 0.08 dB. In this document, the unit dB is used to reference the description of voltages ratios, considering equal impedances in the two points of measurement.

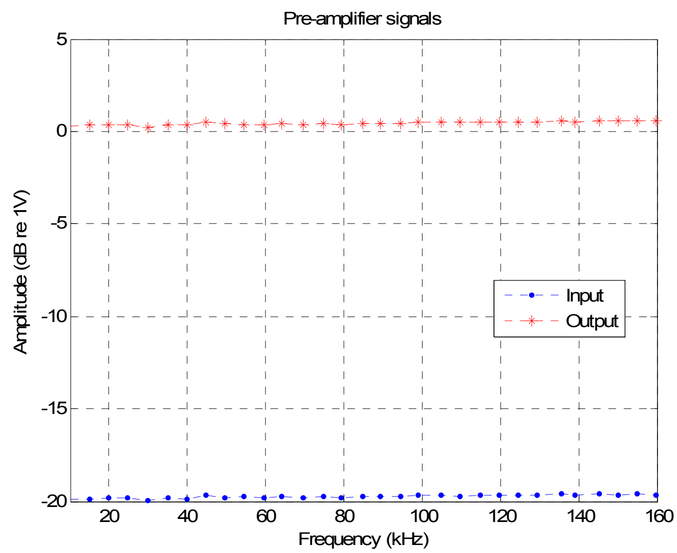

(a)

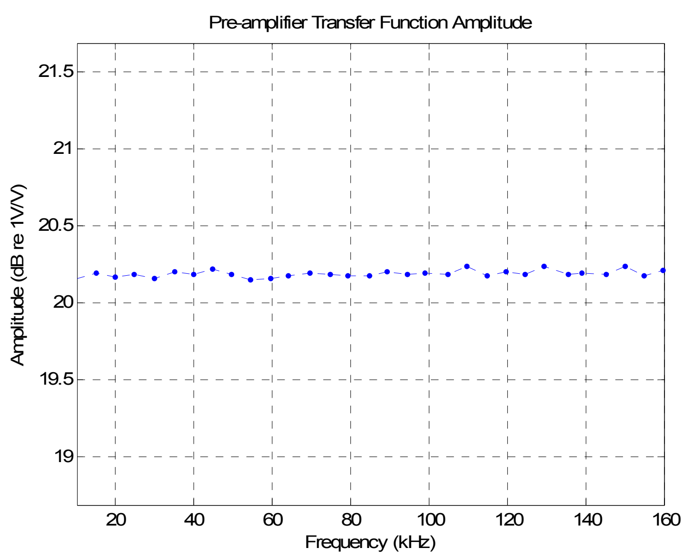

(b)

Figure 3.23. Preamplifier measured frequency response. (a) Input and output signals FFT. (b) Amplitude transfer function FFT.

3.3.5.2 Filters

The filters stage is composed by a fourth order high pass filter, in series with a second order low pass filter. The high pass has a cut-off frequency of 4 kHz, selected to eliminate 60 Hz noise and some undesired signals generated by acoustic noise. The low pass has a cut-off frequency of 200 kHz, to eliminate possible aliasing. Both filters were implemented using the Sallen-Key topology, with unitary gain and Butterworth coefficients, in order to obtain a flat amplitude response in the pass band.

The components were selected considering the guidelines suggested by Texas Instruments [57]. For high performance filters, ceramic capacitors were used to minimize the variations of f_C and Q. Besides, the capacitor values are in the range from 1 nF to several μF. The lower limit avoids coming too close to parasitic capacitances. If the capacitor used is close to 400 times the common-mode input capacitance of the operational amplifier used in a Sallen-Key filter, it must be considered for accurate filter response. The resistor values should be within the range of 1 kΩ to 100 kΩ. The lower limit avoids excessive current flow from the operational amplifier output, while the upper limit is to avoid excessive resistor noise.

The operational amplifier was selected considering its dynamic response of gain bandwidth and slew rate. The slew rate consideration is the same used for the pre amplifier; however, the gain bandwidth is different for each filter because it is affected by the filter quality factor Q. In general, the open-loop gain should be 100 times (40 dB above) the peak gain (Q) of a filter section to allow a maximum gain error of 1%.

The ideal unity gain bandwidth of an operational amplifier for an individual second order filter section i can be calculated by:

$$\text{Q<1, then} \qquad f_T = 100 \cdot G \cdot f_C \cdot \frac{f_{Ci}}{f_C} \tag{3.9}$$

$$\text{Q>1, then} \qquad f_T = 100 \cdot G \cdot \frac{f_C}{a_i} \sqrt{\frac{Q_i^2 - 0.5}{Q_i^2 - 0.25}} \tag{3.10}$$

where G is the gain, f_C is the total filter cut-off frequency, f_{Ci} is the filter section cut-off frequency, a_i is a filter coefficient and Q_i is the quality factor of the partial filter.

Table 3.4 exhibits the minimum and recommended frequency bandwidth calculated for the high pass (f_C = 4 kHz) and low pass (f_C = 200 kHz) filters.

Table 3.4. Operational amplifiers minimum and recommended bandwidth for the filters stage.

FILTER	MINIMUM BANDWIDTH	RECOMMENDED BANDWIDTH
High pass		
First stage	2.9 kHz	287.6 kHz
Second stage	4.8 kHz	475.7 kHz
Low pass	237.8 kHz	23.8 MHz

The operational amplifier selected was the LF356 which has in input resistance of 10^{12} Ω, input capacitance of 3 pF, gain bandwidth product of 5 MHz, and a slew rate of 12 V/μs [59]. Although this operational amplifier does not satisfy the recommended bandwidth for the low pass filter, it covers all the required conditions and offers a good balance between performance and cost.

The filters schematic is sketched in Figure 3.24. The fourth order high pass filter frequency response is illustrated in Figure 3.25, while Figure 3.26 demonstrates the second order low pass filter response.

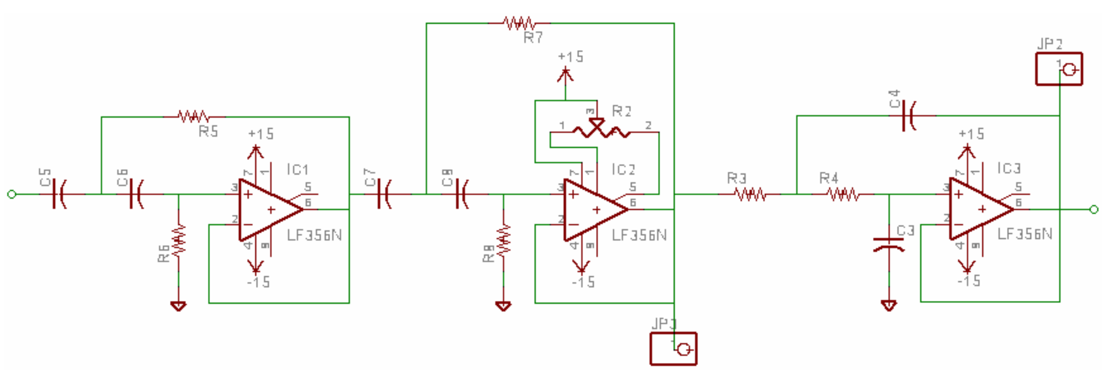

Figure 3.24. Filter circuit schematic.

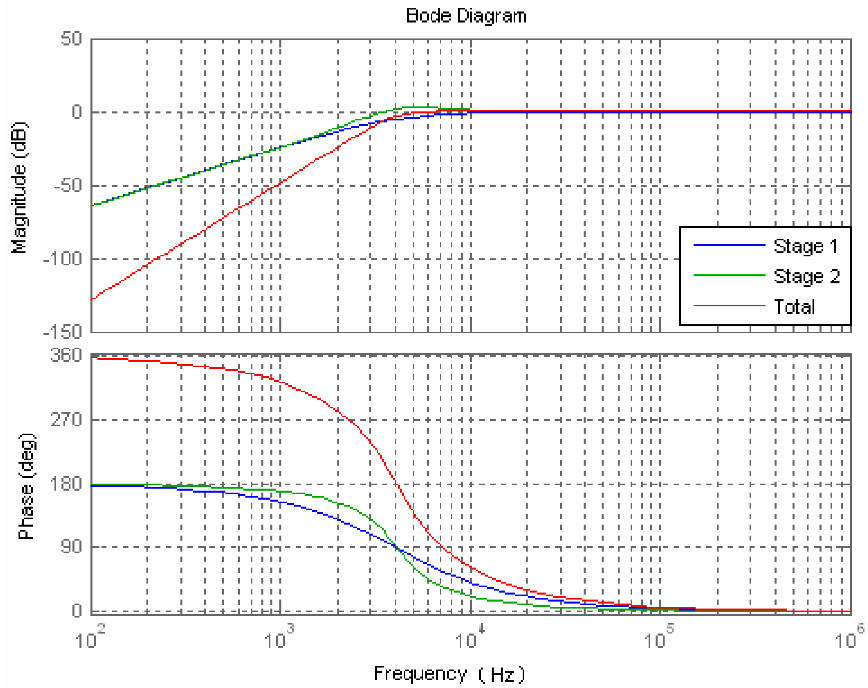

Figure 3.25. Bode diagram 4th order High Pass filter

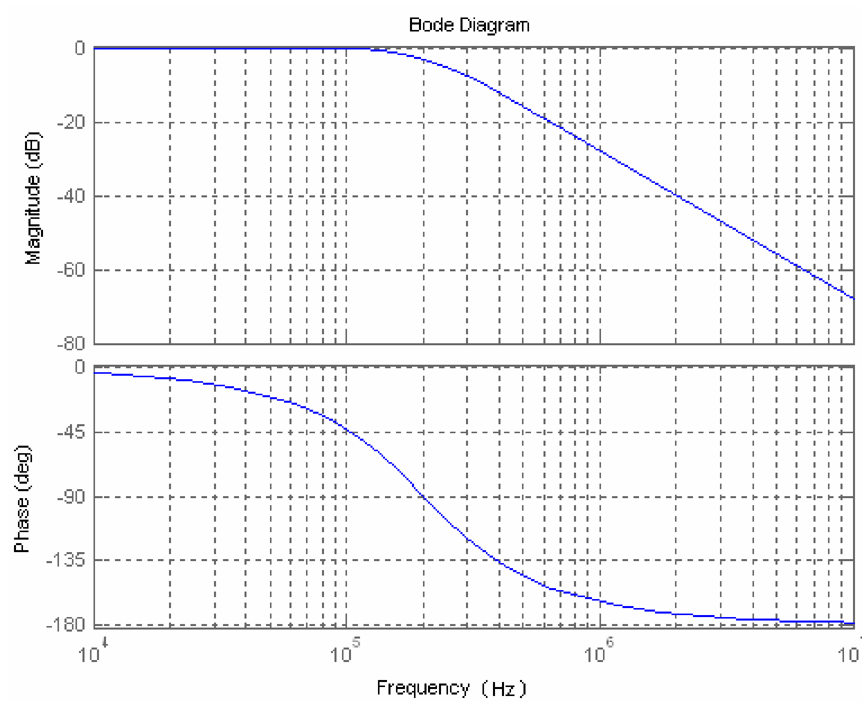

Figure 3.26. Bode diagram 2nd order Low Pass filter.

3.3.5.3 Amplifier

After being pre-amplified and filtered, the signal is amplified by a total gain of 100 V/V (40dB). This was executed in two stages, each one with a gain of 10 V/V (20 dB). The reason for using two stages, instead of a single one, was to diminish the operational amplifier gain bandwidth requirements, since this was a critical parameter for selecting the component. Additionally, an offset control was employed for both stages. The circuit was implemented using the LF356 op amp, as shown in Figure 3.27.

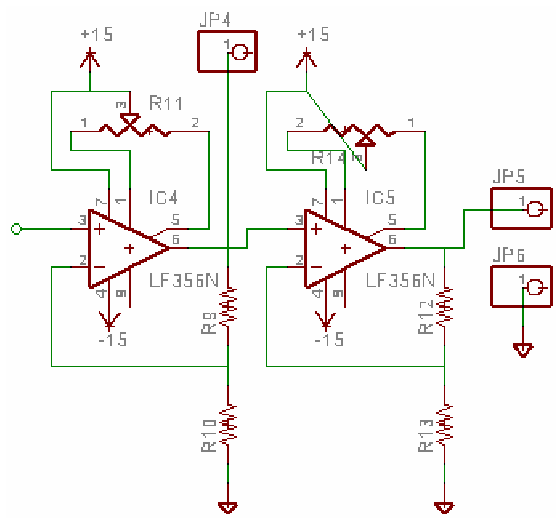

Figure 3.27. Amplifier circuit schematic.

3.3.5.4 Complete circuit frequency response

The behavior of the complete conditioning circuit was experimentally verified with sinusoidal waves of a determined frequency, from 10 to 160 kHz, with increments of 5 kHz. The amplitude transfer function was calculated and it is displayed in Figure 3.28. Although the circuit was designed to have a flat frequency response in the frequency range of interest, the transfer function gain noticeably decreases as the frequency increases, presenting a variation of 2.78 dB. This variation is caused by the low pass filter, added to the bandwidth effect of the operational amplifiers, but since it is lesser than 3 dB, the response can be considered fairly flat.

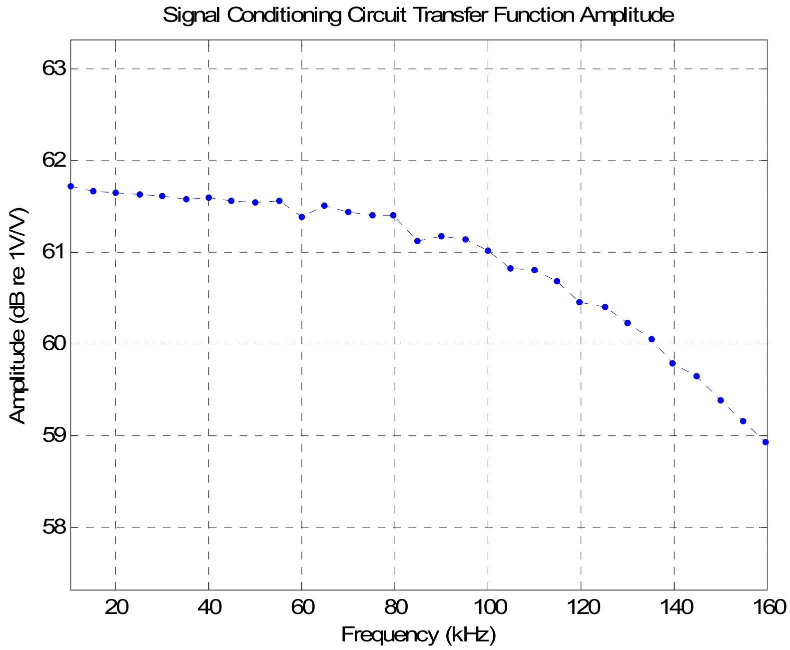

Figure 3.28. Signal conditioning circuit amplitude frequency response.

3.3.6 DATA ACQUISITION

The data acquisition module is in charge of sampling the analog signals, convert them to digital and send the samples to the Virtual Instrument in LabView. The data acquisition module must have a sample frequency greater that 1.6 MHZ, in order to consider the signals acquired as continuous. The oscilloscope Agilent 54621A was used with this purpose. It acquires the signal and sends the samples to the PC through the serial port.

The oscilloscope is able to acquire a maximum of 2000 samples in a time window fixed by the user in the VI. The minimum time window accepted by the oscilloscope is 50 μs, which determines a maximum sample frequency of 40 MHz. The maximum time window accepted is 500 s, producing a minimum sample frequency of 4 Hz.

Considering that the sample frequency must be greater than 1.6 MHz, the maximum time window acceptable for this system is 1.25 ms. This imposes a restriction for the pulse duration, since the total time acquired by the oscilloscope must be in the range from 50 μs to 1.25 ms.

3.3.7 TRANSDUCERS

The PVDF transducers developed were tested both, as receivers and as transmitters. In order to execute the experiments, a Reson TC4033 robust spherical reference hydrophone was employed. For the first experiments configuration, the Reson TC4033 was used as transmitter while the PVDF hydrophones were used as receivers. For the second configuration, the TC4033 acted as receiver, while the PVDF transducers were operated as transmitters.

The TC4033 provides uniform omnidirectional characteristics in the frequency range from 1 Hz to 140 kHz, and a linear frequency range from 1 Hz to 80 kHz. It has an operating depth of 900 m and it is encapsulated in a special formulated NBR. Because of its excellent signal to noise ratio, acoustic characteristics and durability, it is ideal for a wide range of applications, including calibration purposes. Figure 3.29 depicts the hydrophone dimensions in millimeters.

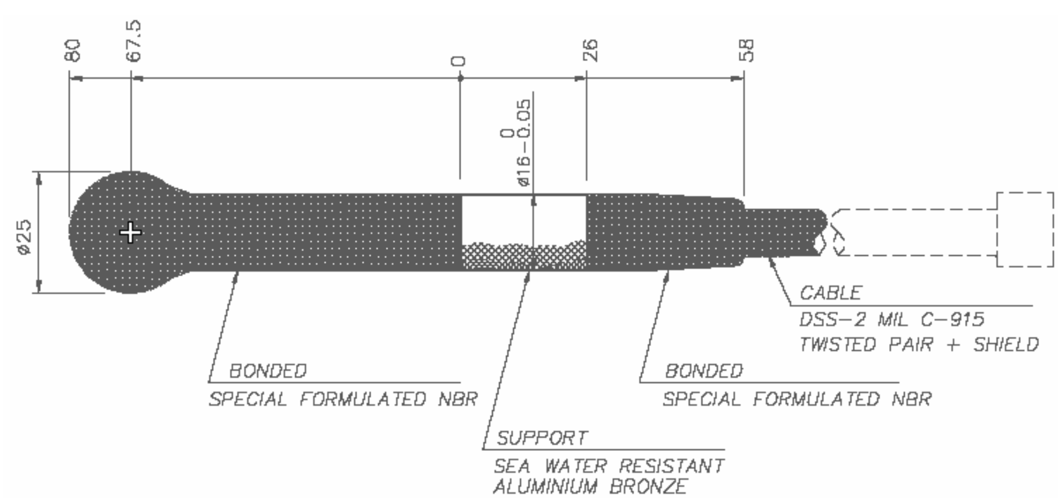

Figure 3.29. Reson TC4033 Outline Dimensions [34].

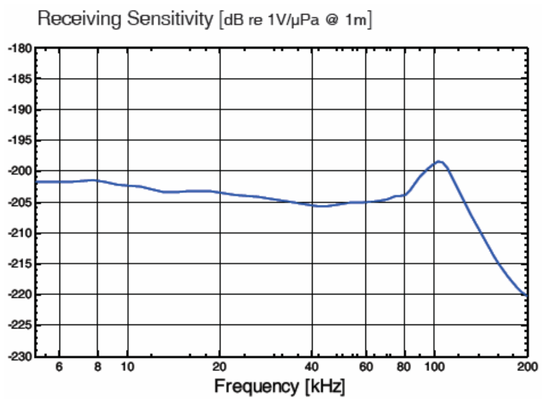

a)

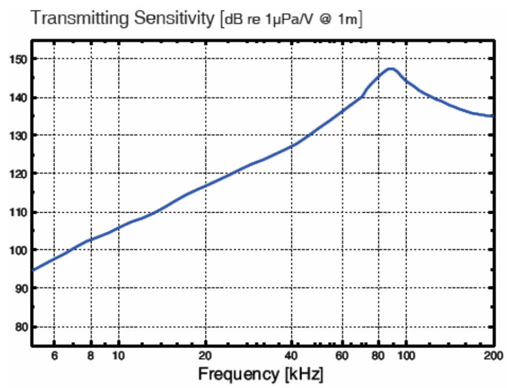

b)

Figure 3.30. Reson TC4033 a) Receiving Sensitivity (dB re 1V/μPa @ 1m). b) Transmitting Sensitivity (dB re 1 μPa @ 1m) [34]

As seen in Figure 3.30, the hydrophone exhibits a receiving linear frequency behavior from 5 kHz to 80 kHz, while the transmitting sensitivity increases with frequency until reach its maximum at 90 kHz approximately, and starts decreasing after that. This resonance tendency is consistent with the hydrophone impedance behavior, showed in Figure 3.31.

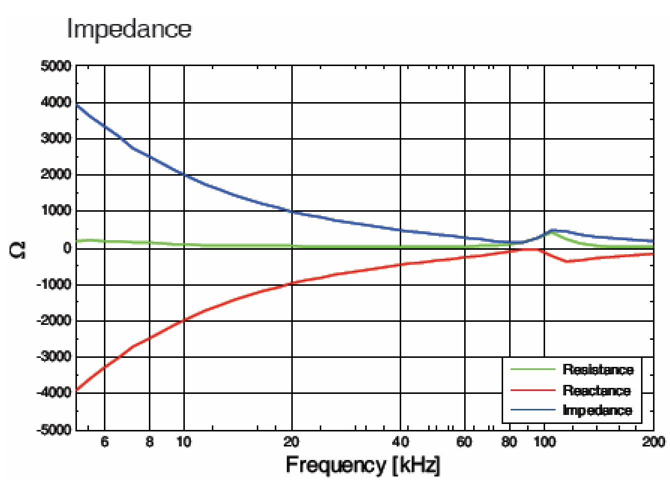

Figure 3.31. Reson TC4033 Impedance vs. Frequency [34].

3.3.8 WATER TANK

As seen in Figure 3.32, both transducers, transmitter and receiver, are submerged in a tank filled with fresh water. The tank dimensions are approximately 88 cm in length, 52 cm in width and 36 cm in depth. The transducers are placed in a frame designed to keep them in a fixed position and to facilitate their appropriate location in the tank.

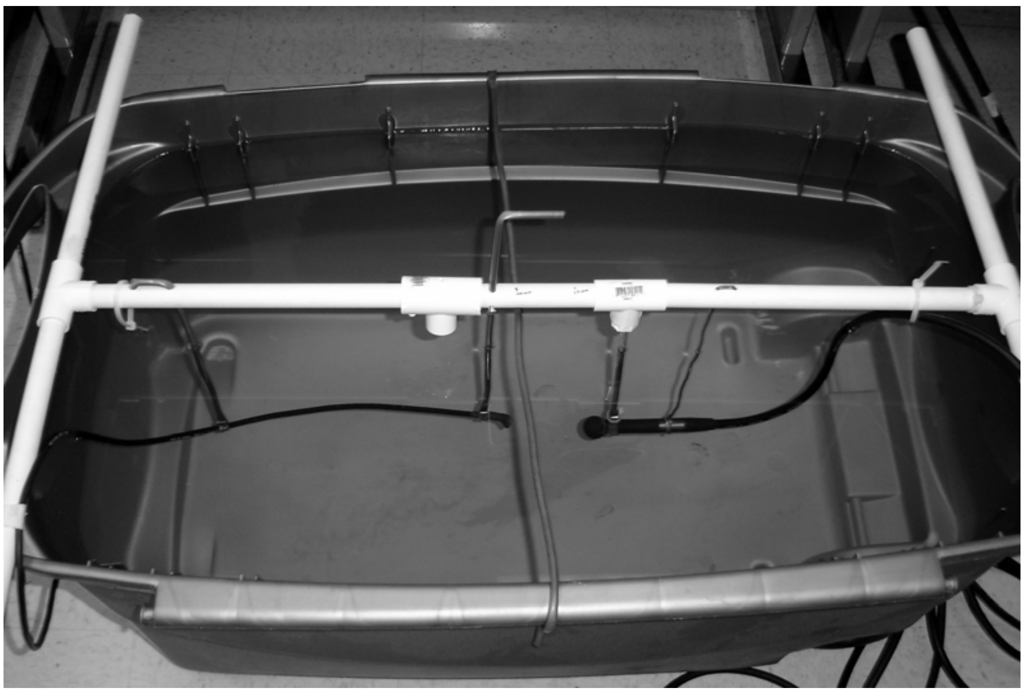

Figure 3.32. Transducers holding frame submerged in the water tank.

The Reson TC4033 is attached by the bronze support and the PVDF transducers are attached to other adjustable support in front of it, in order to place all the PVDF transducers in the same distance and angle from the Reson, for all the different tests. The frame is designed to situate the transducers at the middle of the tank, in order to maximize the distance between them and the tank walls. This distance determines the maximum pulse duration permitted in order to differentiate the incident pulse from its reflections on the tank walls and the water surface.

3.4 EXPERIMENTAL DESIGN

There are several methods that are adequate to measure a transducer's bandwidth, including a comparison against known standard hydrophones, reciprocity technique [31], time delay spectrometry (TDS) [33], optical interferometry [47], and shock wave method [27]. In most of these methods, a sine swept continuous signal is used to drive the transducer. The continuous wave approach requires to be performed in an anechoic water tank with free field properties which is a difficult requisite to satisfy because anechoic water tanks are complicated and expensive to build. However, this can be solved in some cases by sending burst tones instead of continuous signals [47]. On the other hand, the frequency sweep approach requires using a linear wide bandwidth source, which is very difficult to find. For this reason, it is common to measure the transducers bandwidth, covering the desired frequency range with discrete frequency points separated by a fixed delta [20, 23, 47].

In this research, the approach of several burst signals of discrete frequencies was used. The PVDF transducers' frequency responses were measured using modulated acoustic pulses, with central frequencies varying from 10 kHz to 160 kHz, spaced by 5 kHz. To study the receiving sensitivity behavior, the acoustic pulses were sent with a Reson TC4033, and the response was recorded from the PVDF hydrophone. Likewise, to study the transmitting sensitivity behavior, the acoustic pulses were generated with the PVDF transducer, and the response was recorded from the Reson TC4033.

3.4.1 GENERATION OF ACOUSTIC PULSES

The pulses used in this research to evaluate the system response at different frequencies were designed considering the frequency range of interest and the maximum pulse duration. The frequency ranges from 10 kHz to 160 kHz, with variations of 5 kHz, resulting in 31 different pulses. The pulses duration was calculated considering the tank's dimensions, in order to avoid superposition with reflected signals. The pulse duration is the same for all frequencies.

The tank's smallest dimension is depth (36 cm). Placing the transducers in the three dimensional tank's center, the minimum distance between the transducers and a reflecting surface (the tank's bottom and the water surface) is 18 cm. The total distance traveled by the first reflected signal will be the sum of the distance between the source and the reflecting surface, plus the distance between the reflecting surface and the hydrophone, which in this case are approximately the same because the source and the receiver were located closed to each other. Considering the speed of sound in water, the first reflected signal will arrive to the receiver approximately 243.24 μs, after the pulse start. To avoid superposition, the pulse duration was selected as 200 μs.

The amplitude modulated Hanning pulses were generated, using 31 different carrier frequencies, and some of them are shown in Figure 3.33. Since the pulses were to be stored in the Agilent signal generator, the sequence $x_0[n]$ was generated using a LabView Virtual Instrument and a MATLAB subroutine. The sample frequency used for the sequence was given by the maximum samples number allowed by the signal generator (4096), divided by the pulse duration (200 μs), resulting in 20.48 MHz. The amplitude oscillated between ±2047, in integer numbers, as required by the signal generator. The electrical output amplitude is modified with the signal generator control panel.

Figure 3.33 presents five representative examples of the pulses created, starting with the lowest carrier frequency (10 kHz) and finishing with the highest carrier frequency (160 kHz). It can be seen from the figure that all the pulses maintain constant their duration in time, bandwidth in frequency and FFT amplitude, but varying the central frequency. In order to do a frequency sweep, the FFT maximum amplitude, which occurs at the central frequency, can be selected and plotted for all the pulses, as presented in Figure 3.34. It can be seen that the 31 pulses set constitute a constant function in frequency, and therefore this set can be used as a completely frequency flat excitation input for the system to characterize.

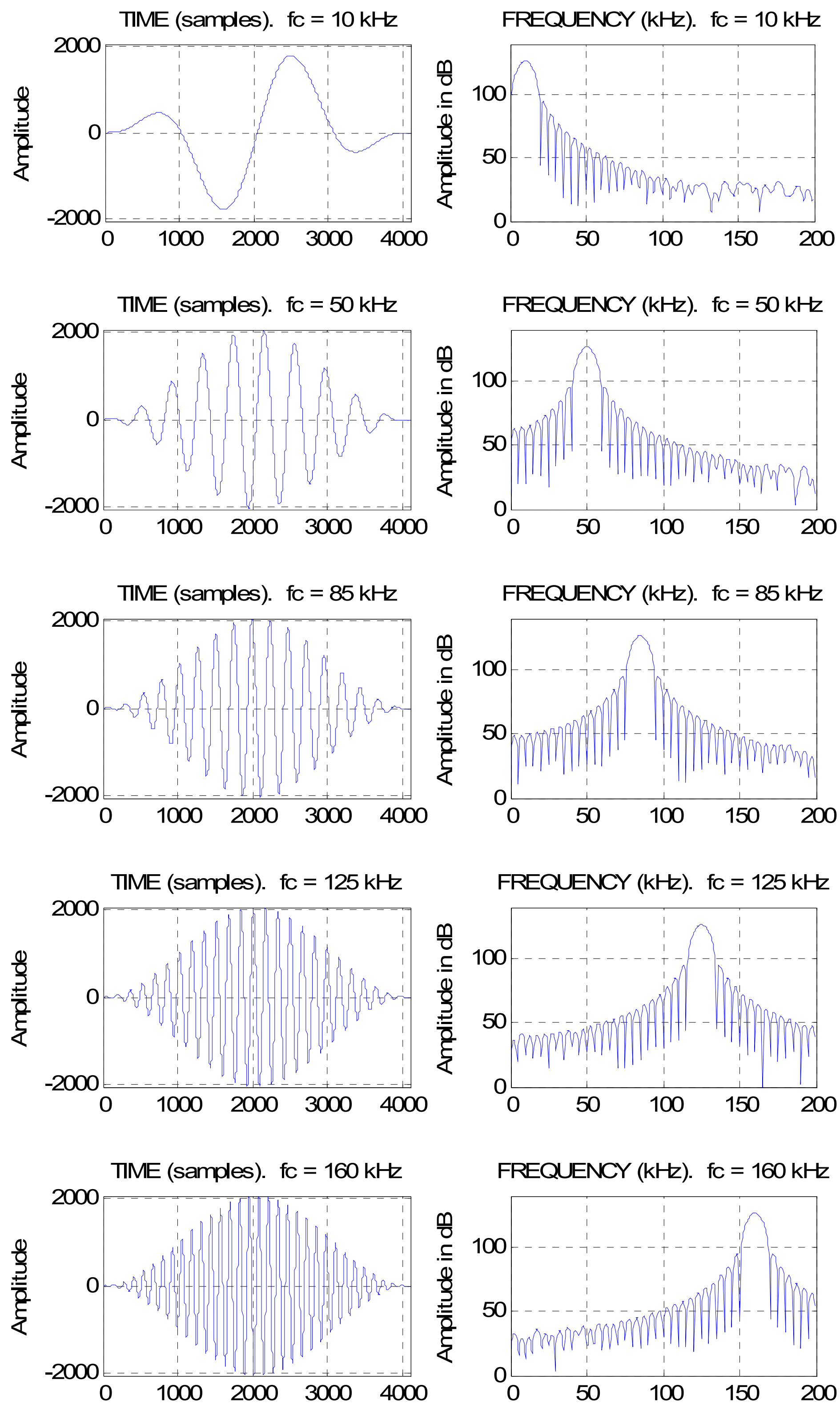

Figure 3.33. Amplitude modulated Hanning pulses $x_0[n]$ in time (left) and frequency (right).

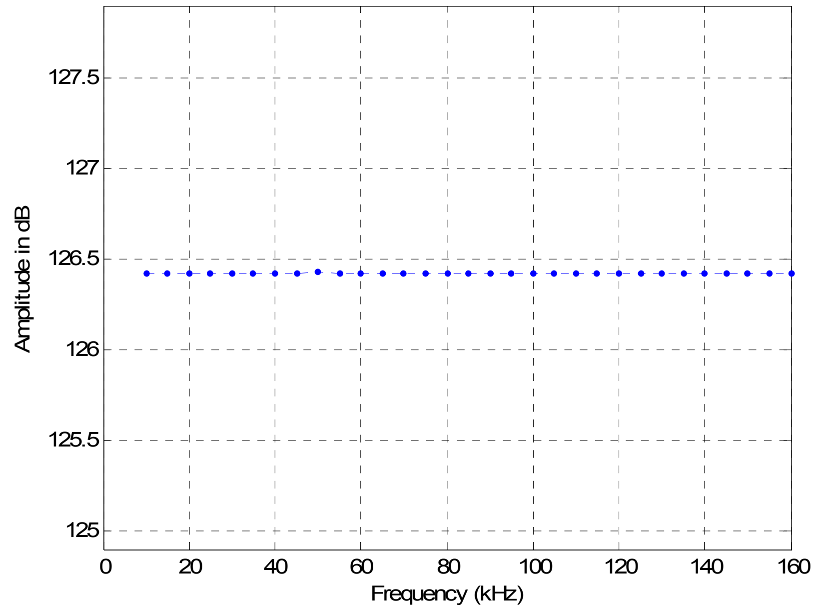

Figure 3.34. Frequency sweep of total set containing the 31 amplitude modulated pulses. Each point correspond to the FFT amplitude of one pulse, at its carrier frequency.

To comply with the far field requirements, the transducers (transmitter and receiver) must be separated by a distance *x* that satisfies the following conditions [53, 57]:

$$x >> r \quad \text{and} \quad x >> kr^2 \tag{3.11}$$

where *r* is the transducer radius and *k* is the wave number.

Since all the transducers must be tested at the same distance, the worst case scenario was considered, meaning the biggest transducer (*r*=4mm) and the biggest *k* (for *f*=160 kHz). It was obtained from the first condition that *x* >> 4 mm and from the second, *x* >> 10.86 mm. Then, a distance of 120 mm was used.

3.4.2 DATA ANALYSIS

Once the input pulse is sent and the output pulse is recorded, the signals are compared in order to evaluate the system response and identify behavior patterns. Figure 3.35 presents the different signals obtainable from the system.

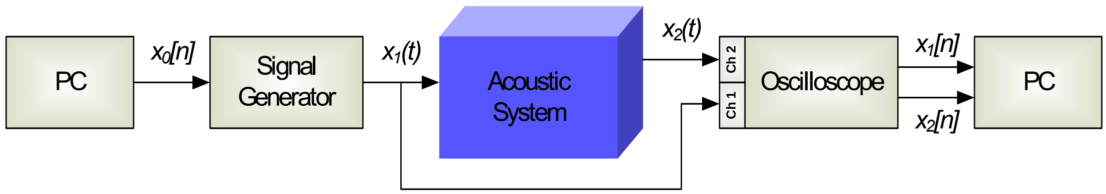

Figure 3.35. Experimental setup signals.

Signals x_0, x_1 and x_2 have different time windows. Sequence $x_0[n]$ is the initial pulse, contains 4096 samples and a time window of 200 µs. Based on this sequence, the signal generator creates $x_1(t)$ which is a continuous signal, with a burst rate of 50 Hz. The total period of the signal $x_1(t)$ is 20 ms, where the first 200 µs correspond to the pulse x_0, and the rest is zero volts. Signal $x_2(t)$ is the electrical response generated by the receiver because of acoustic excitation, including the sent pulse and its reflections. It is a continuous signal and it should be periodical, as the excitation x_1.

The oscilloscope samples the signals $x_1(t)$ and $x_2(t)$ and sends them to the PC as the sequences $x_1[n]$ and $x_2[n]$, respectively. These sequences have 2000 points each one, which is the maximum allowed by the oscilloscope. Considering that the pulse of interest has duration of 200 µs, the acquisition time window selected was 400 µs, enough time to acquired the initial pulse delayed by the distance between the transducers. Given the time window and the samples number, the sample frequency used was 5 MHz, which is more than 31 times the maximum frequency to be tested (160 kHz), allowing considering the sequences $x_1[n]$ and $x_2[n]$ as continuous signals in the analysis.

The analysis procedure consists in several steps. First, the pulses x_1 and x_2 are compared with the theoretical pulse x_0 in order to identify the start point. This is executed using a cross correlation function. The sent pulse x_1 is delayed with respect to x_0 because of the acquisition procedure with the oscilloscope. The received signal x_2 is delayed with respect to x_1 because of the time taken by the signal to travel from the transmitter to the receiver. These delays are eliminated and the signals' beginnings are cropped in order to facilitate the comparison.

On the other hand, the received signal x_2 contains, besides of the sent pulse reading, the reflected signals. To eliminate these undesired components, both signals (x_1 and x_2) are cropped to contain only a time window equivalent to the sent pulse duration (200 µs) plus a security factor (10 µs).

Afterwards, the Fast Fourier Transform (FFT) is calculated for the sent pulse x_1 and the received pulse x_2. The maximum amplitude in frequency will be given in the central frequency range, as seen in Figure 3.33. This magnitude is recorded in a new array ($Y_1[m]$ and $Y_2[m]$), and the procedure is repeated for all the frequencies, resulting in arrays of 31 points each one.

Figure 3.36 presents the transfer functions existent in the acoustic system, and how they are related. The total acoustic system transfer function, $H(\omega)$ is equal to the multiplication in frequency of the three stages transfer functions, $H_1(\omega)$ for the transmitter, $H_2(\omega)$ for the receiver and $H_3(\omega)$ for the signal conditioning circuit.

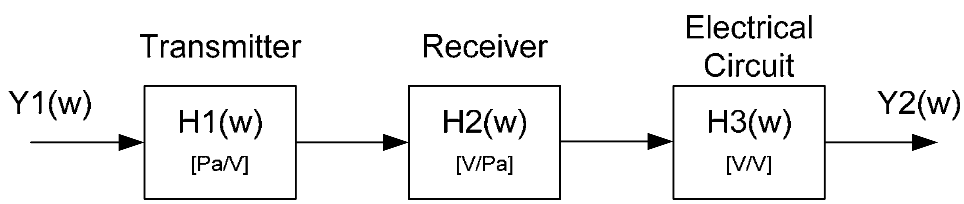

Figure 3.36. Acoustic system transfer functions in frequency.

In order to determine the total acoustic system transfer function in frequency, the amplitude transfer function $H(\omega)$ is calculated dividing the output $Y_2(\omega)$ by the input $Y_1(\omega)$. To determine the PVDF transducer frequency behavior, it is necessary to compensate for the Reson and electrical circuit effects. Therefore, the PVDF experimental sensitivity can be calculated by:

$$H_{PVDF}[m] = \frac{Y_2[m]}{Y_1[m] \bullet H_{\mathrm{Re}son}[m] \bullet H_{ElctCrt}[m]} \tag{3.12}$$

The Reson transducer has two different transfer functions, one for the transmitting sensitivity and other for the receiving sensitivity, as seen in Figure 3.30. These functions were approximated by a polynomial fitting, in order to evaluate them in the exact frequency values required, corresponding to the carrier frequencies. The same procedure was executed for the electrical circuit.

4 RESULTS AND DISCUSSION

The purpose of this chapter is to present and discuss the experimental results obtained from the different tests performed, as well as the results obtained from the transducers models computer simulations. The chapter is divided in three parts. The first part discloses the experimental results for the receiving and transmitting configurations of the nine designed transducers. The second part shows the simulated results for the nine transducers implemented, for the receiving and transmitting sensitivity and presents the sensitivity dependence on the transducers radius, film thickness and electrical load. In the third part, the trends observed for the experimental results are analyzed based on the results obtained from the theoretical model simulations.

4.1 EXPERIMENTAL RESULTS AND DISCUSSION

This section presents and discusses the results obtained from the different experiments performed to investigate the PVDF transducers frequency behavior. The transducers were excited with 31 amplitude modulated Hanning acoustic pulses, with carrier frequencies varying from 10 to 160 kHz, spaced by 5 kHz. To study the receiving behavior, the acoustic pulses were sent with the Reson TC4033, and the response was recorded from the PVDF hydrophone. Likewise, to study the transmitting behavior, the acoustic pulses were sent with the PVDF transducer, and the response was recorded from the Reson. Finally, a compensation function was included to eliminate the effects of the Reson and the signal conditioning circuit, in order to set apart the PVDF sensitivity behavior.

The transducers were located inside the water tank, attached to a holding frame. They were at approximately 18 cm from the tank's bottom, 18 cm from the water surface, and 26 cm from the closest tank wall. The transmitter and receiver were separated by a constant distance of 12 cm, for all tests. Additionally, they were attached to the holding frame, placed one in front of the other, maintaining a constant angle of zero degrees among their acoustical axes. This was made with the intention of avoid directivity effects.

The first part of this section describes the data acquired from each test and an example of how it was processed to obtain the results. The second part shows the plots describing the receiving behavior obtained from the nine transducers evaluated, including the whole system. Next, the compensation transfer function is applied and the results are presented for the PVDF receiving sensitivity. Finally, the transmitting behavior is presented in the same way as the receiving behavior, first for the whole system, and then compensated for the PVDF transmitting sensitivity. The results are discussed in each subsection.

4.1.1 ACQUIRED SIGNALS PROCESSING

The nine transducers were examined under two different configurations: as receivers and as transmitters, conforming a group of 18 experiments. Each experiment consists of a set of 31 different tests, where a 200 μs pulse with a specific carrier frequency was sent and received through the acoustical system. The signals acquired from each test were saved in an independent .mat file, generating a total of 558 files, 62 for each transducer. These files were processed and analyzed afterwards with the help of several programs developed in MATLAB, in order to obtain a single transfer function curve for the transducer in its respective configuration, transmitting or receiving.

The original files were saved using a Virtual Instrument created in LabView. Since all of them are equal in structure, the files' names are coded to identify the information about the experiment configuration transmitter-receiver (Reson-PVDF, or PVDF-Reson), the transducer radius, the film thickness and the central frequency under test. The files contain the signals acquired by the oscilloscope through channels 1 and 2, corresponding to the electrical input to transmitter $x_1(t)$ and the electrical signal received $x_2(t)$, among other information necessary to the analysis, such as sample time and vectors length.

The sent and received signals are supposed to be similar in time and frequency, but x_2 has a delay with respect to x_1 due to the time taken by the signal to travel from the transmitter to the receiver. Besides, x_2 contains not only the initial pulse sent, but its reflections on the tank walls and water surface. Their frequency content is similar, but these reflections can introduce deviations in the received signal FFT. As an example, Figure 4.1 presents the signals saved in the file "\Reson-PVDF\r3_t052\f085.mat". They correspond to a test made with the Reson as transmitter and the PVDF as receiver, for a transducer with radius 3 mm, thickness 52 µm, receiving a pulse with central frequency 85 kHz. Note the good agreement in the frequency content between both signals.

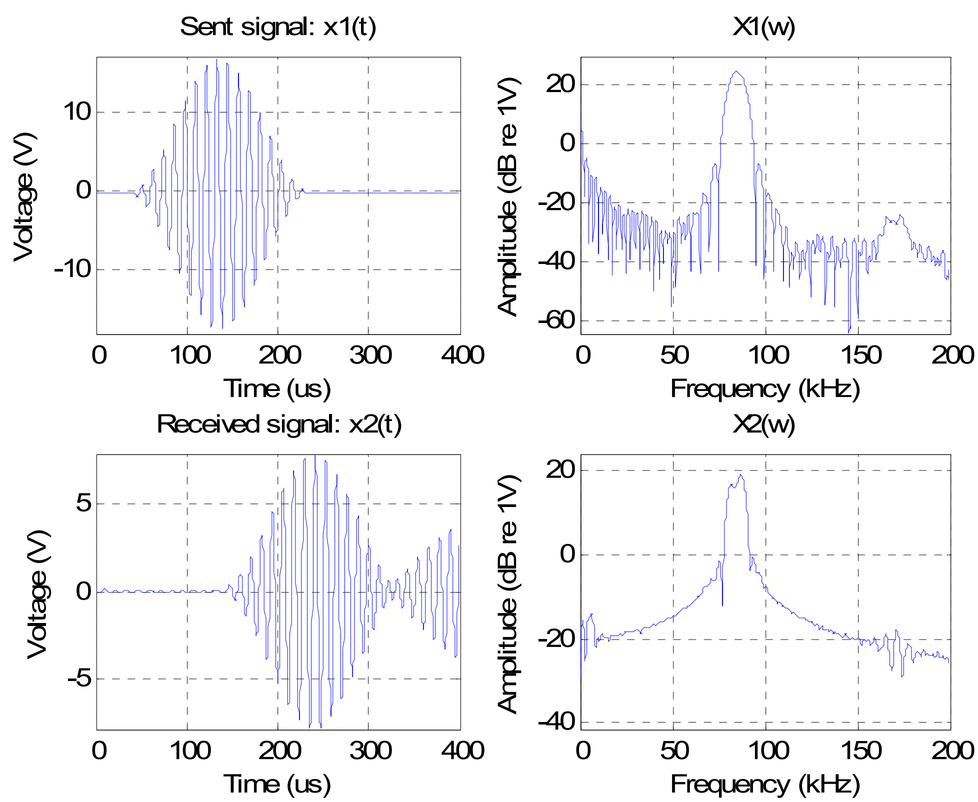

Figure 4.1. Experimental signals example for a PVDF hydrophone of radius 3 mm, thickness 52 µm, receiving at central frequency 85 kHz. Complete signals acquired by the oscilloscope, in time (left) and frequency (right).

Afterwards, the signals are cropped in order to get only the initial pulse. To identify a pulses' starting point, the acquired signals, x_1 and x_2, are compared to the theoretical pulse x_0 using a cross correlation function in MATLAB. Since the pulse duration is known, the pulses end can be identified too. The resulting signals, x_1_cut and x_2_cut, are saved in a file with the same name of the original one, adding an identifier "_cut". Continuing with the previous example, Figure 4.2 shows the pulses obtained from cutting the acquired signals, and saved in the file "\Reson-PVDF\r3_t052\f085_cut.mat".

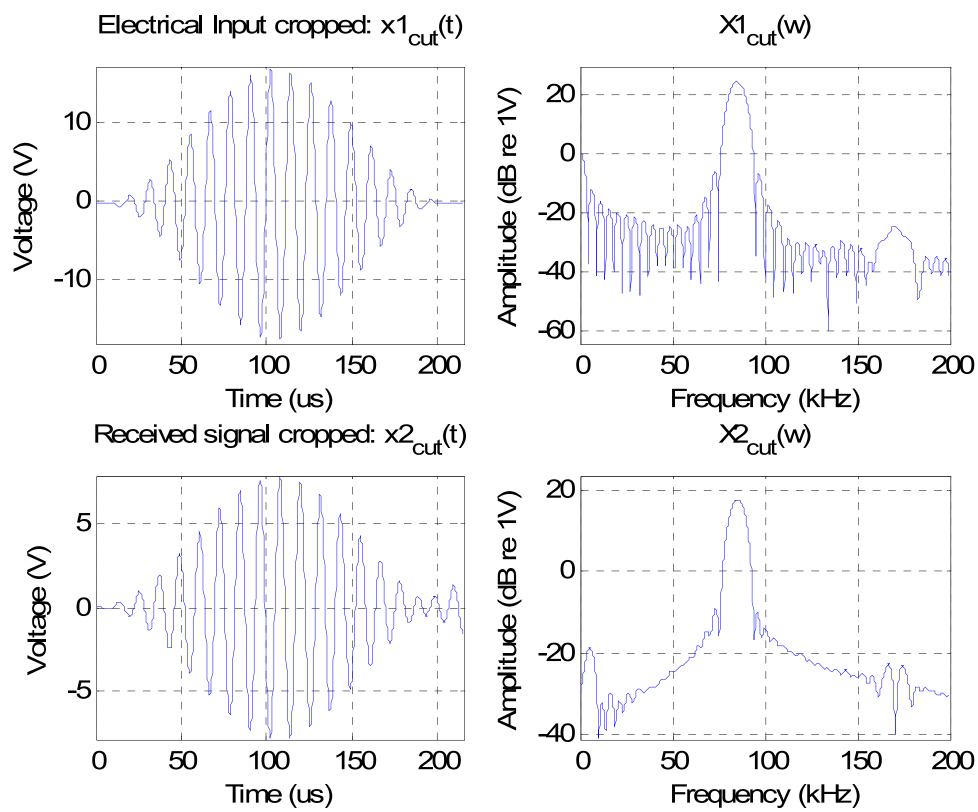

Figure 4.2. Pulses resulting from cutting the acquired signals from a PVDF transducer with radius 3 mm and thickness 52 μm, receiving at central frequency 85 kHz, in time (left) and frequency (right).

It can be clearly noticed from Figure 4.2 that the received pulse corresponds almost exactly to the electrical input sent to the transmitter. This can be observed for the waveform in time, and the frequency content, differing only in the amplitudes.

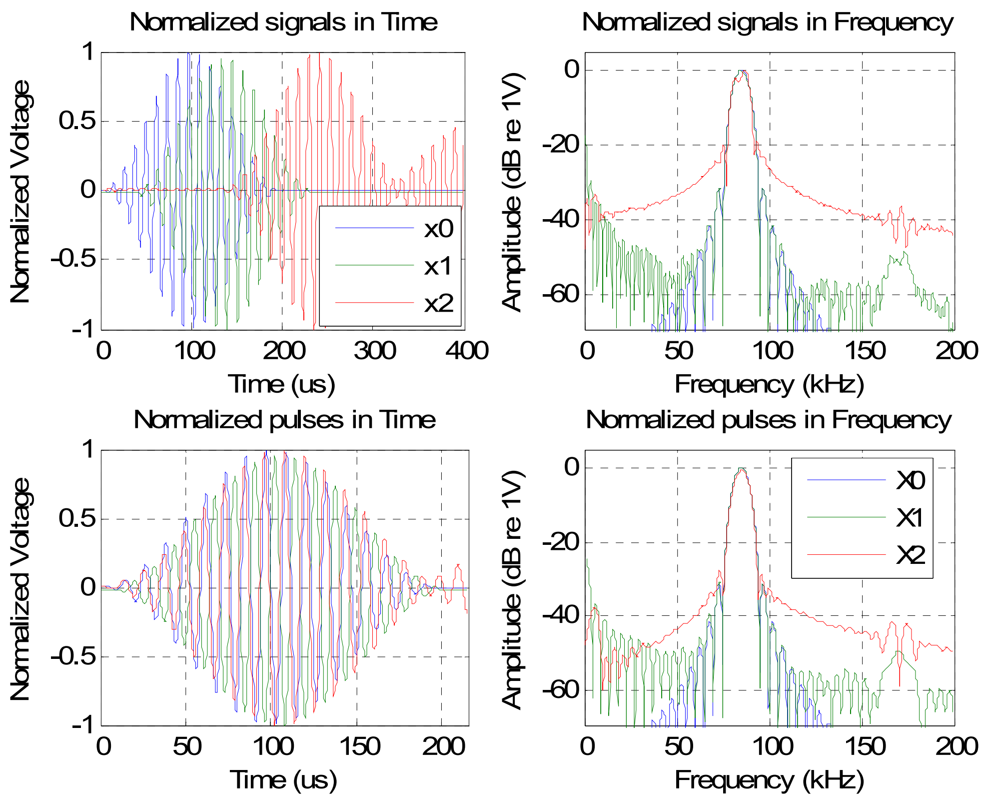

Figure 4.3. Comparison of normalized signals and pulses x_0 (theoretical), x_1 (electrical input sent to transmitter) and x_2 (electrical received), in time (left) and frequency (right), for a PVDF transducer with radius 3 mm and thickness 52 μm, receiving at central frequency 85 kHz.

Figure 4.3 illustrates in the same graph, the normalized signals (acquired originally) and pulses (signals after being cut) under consideration, for the theoretical x_0, electrical input sent to transmitter x_1, and received signal x_2. As shown in Figure 4.2 and Figure 4.3, the received signals presents all the characteristics expected, including the reflected signals, the time delay due to the distance between the transmitter and the receiver, and, extremely important, the frequency content is the same as the one from the transmitted signal.

From the 558 set tests, a representative sample of three has been included in this section. The first one, described on the previous pages, presented the response of a PVDF transducer with radius 3mm, thickness 52 μm, at 85 kHz. Figure 4.4 reveals the response of a PVDF transducer with radius 4 mm, thickness 110 μm, at 25 kHz.

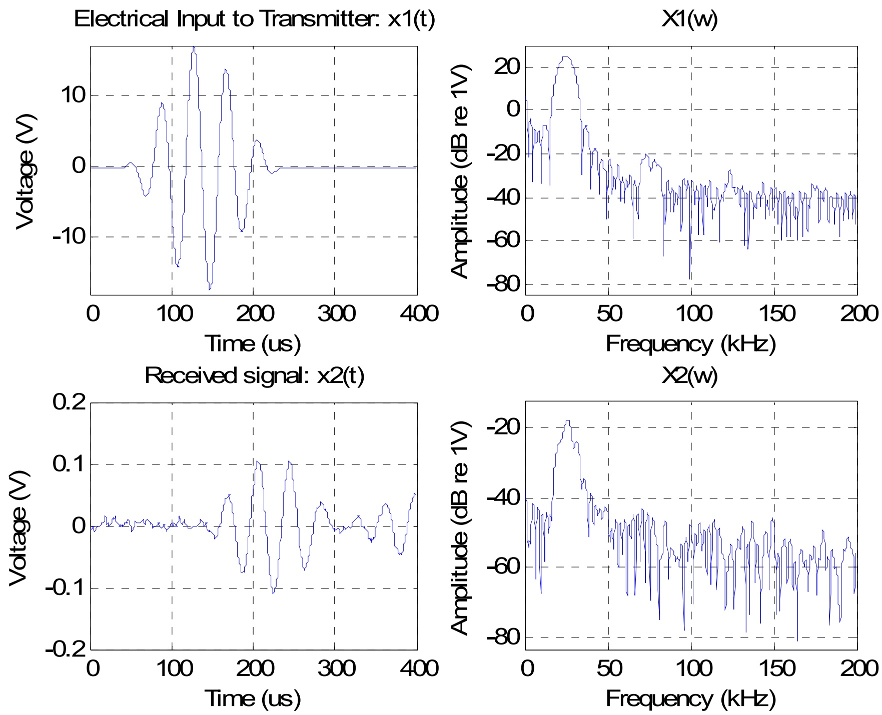
Electrical Input to Transmitter: x1(t)
Voltage (V)
Time (us)
X1(w)
Amplitude (dB re 1V)
Frequency (kHz)
Received signal: x2(t)
Voltage (V)
Time (us)
X2(w)
Amplitude (dB re 1V)
Frequency (kHz)

(a)

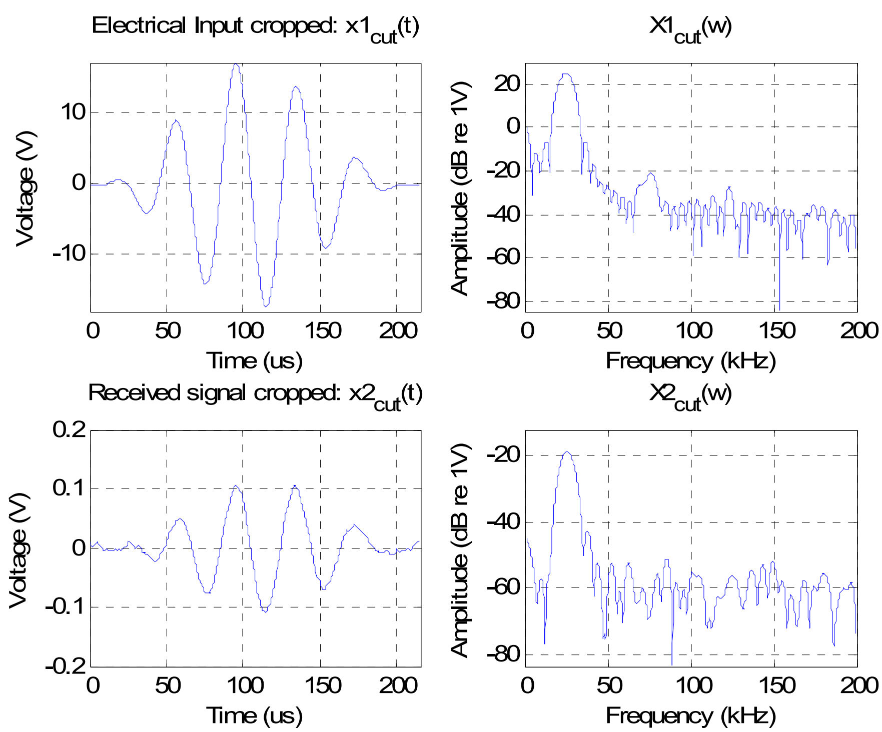
Electrical Input cropped: $x1_{cut}(t)$
Voltage (V)
Time (us)
$X1_{cut}(w)$
Amplitude (dB re 1V)
Frequency (kHz)
Received signal cropped: $x2_{cut}(t)$
Voltage (V)
Time (us)
$X2_{cut}(w)$
Amplitude (dB re 1V)
Frequency (kHz)

(b)

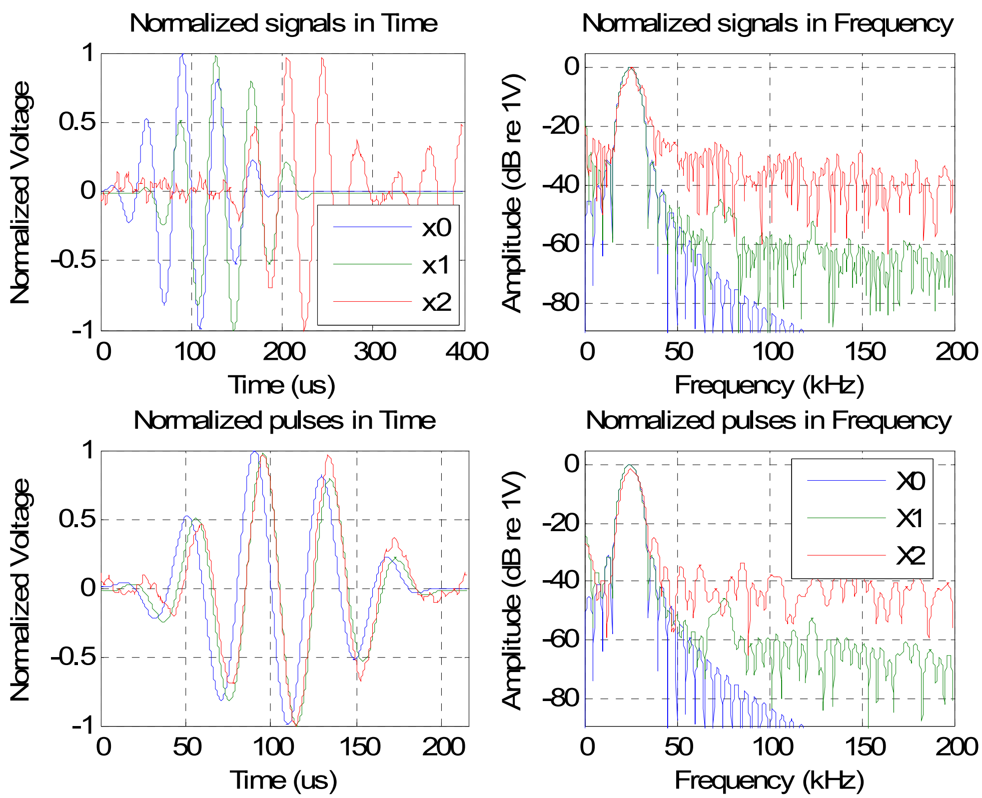

(c)

Figure 4.4. Signal processing example for a PVDF transducer with radius 4 mm, thickness 110 µm, receiving at central frequency 25 kHz. (a) Complete signals acquired by the oscilloscope. (b) Pulses obtained from cutting the original signals. (c) Comparison of normalized signals and pulses x_0 (theorical), x_1 (electrical input sent to transmitter) and x_2 (electrical received), in time (left) and frequency (right).

As in the previous case, note the excellent agreement between the three signals (x_0, x_1 and x_2), in time wave form and frequency content, although the received signal amplitude is much smaller than for the previous case.

Figure 4.5 demonstrates the response of a PVDF transducer with radius 2 mm, thickness 28 µm, at 150 kHz.

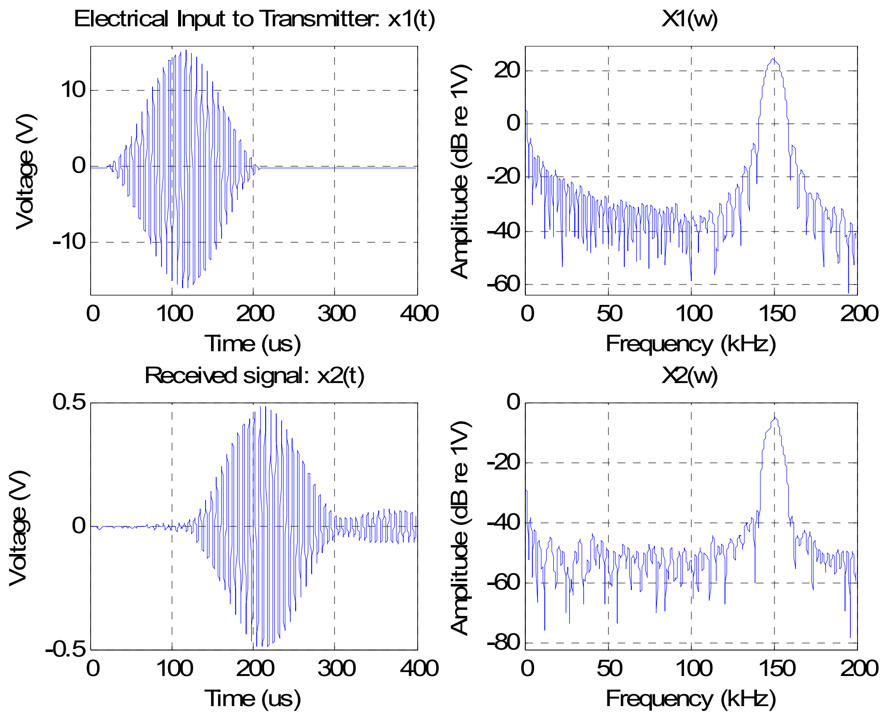
Electrical Input to Transmitter: x1(t)
X1(w)
Voltage (V)
Time (us)
Amplitude (dB re 1V)
Frequency (kHz)
Received signal: x2(t)
X2(w)
Voltage (V)
Time (us)
Amplitude (dB re 1V)
Frequency (kHz)

(a)

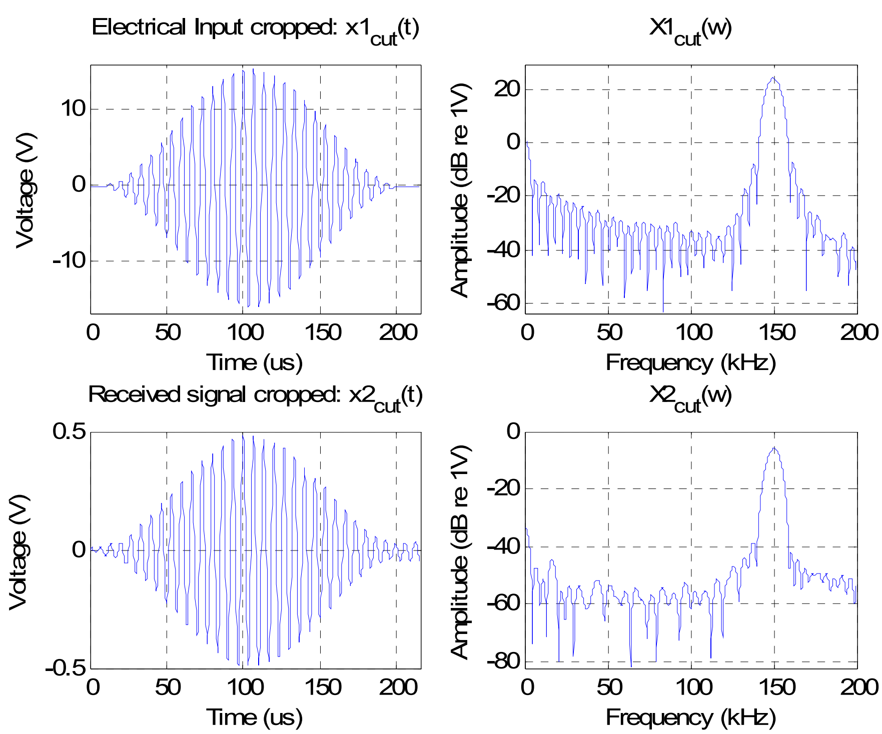
Electrical Input cropped: $x1_{cut}(t)$
$X1_{cut}(w)$
Voltage (V)
Time (us)
Amplitude (dB re 1V)
Frequency (kHz)
Received signal cropped: $x2_{cut}(t)$
$X2_{cut}(w)$
Voltage (V)
Time (us)
Amplitude (dB re 1V)
Frequency (kHz)

(b)

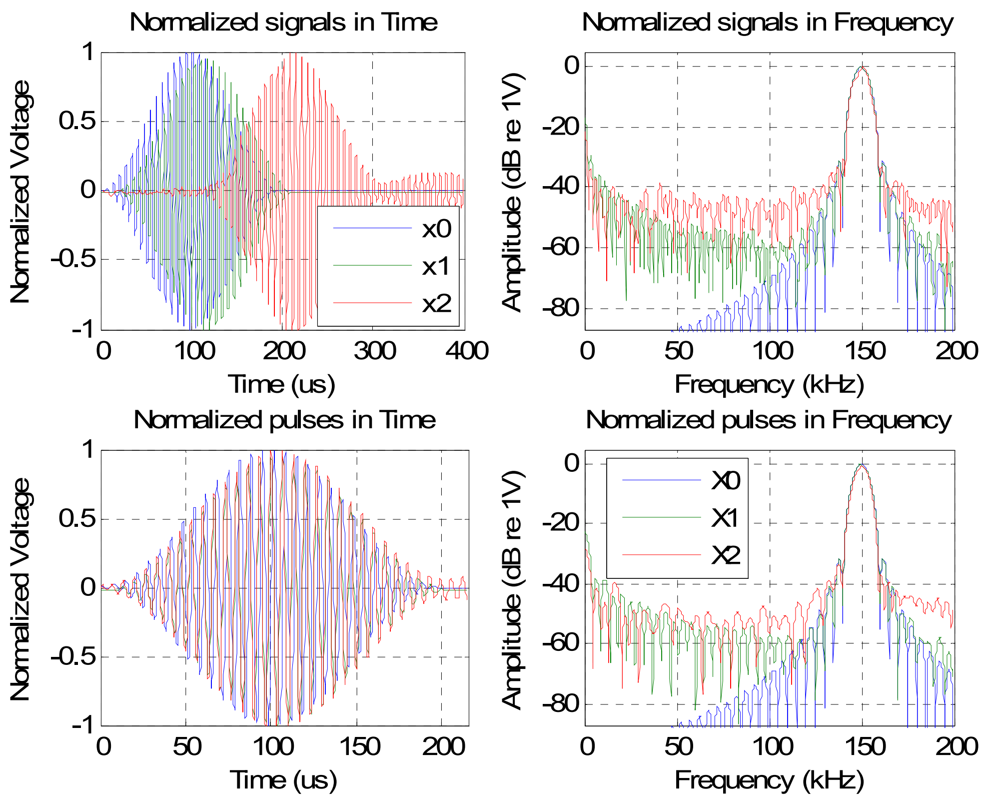

(c)

Figure 4.5. Signal processing example for PVDF transducer with radius 2 mm, thickness 28 µm, receiving at central frequency 150 kHz. (a) Complete signals acquired by the oscilloscope. (b) Pulses obtained from cutting the original signals. (c) Comparison of normalized signals and pulses x_0 (theorical), x_1 (electrical input sent to transmitter) and x_2 (electrical received), in time (left) and frequency (right).

After the pulses are extracted from the complete signals and saved in new files, a program developed in MATLAB executes the equivalent of a frequency sweep for each transducer experiment. The program opens each frequency correspondent file, calculates the pulses FFT ($X_1(f)$ and $X_2(f)$), and searches the maximum amplitude in the electrical input pulse FFT $X_1(f)$. This point corresponds to the central frequency f_c; for that reason, the $X_1(f_c)$ and $X_2(f_c)$ amplitudes at this specific frequency are stored in a new array.

After sweeping the 31 files, corresponding to 31 central frequencies, a vector with the signal amplitude in the frequency range from 10 kHz to 160 kHz is obtained for the system input (electrical input sent to the transmitter) and output (electrical pulse received). From these vectors, an amplitude transfer function can be calculated by means of dividing the output over the input. This procedure is repeated for the 18 experiments developed.

4.1.2 PVDF RECEIVING - TOTAL SYSTEM TRANSFER FUNCTION

The nine transducers were examined as receivers, applying the same voltage input to the Reson TC4033, and recording the output voltage from the signal conditioning circuit. The following subsections present the results obtained for the response of the entire system, including the power amplifier, Reson as transmitter, PVDF as receiver, signal conditioning circuit and acquisition system. The results are presented in two different ways, to facilitate the analysis and identification of each variable influence.

4.1.2.1 Receiving transfer function vs. radius, with fixed thickness

This section shows the experimental receiving behavior of the nine transducers, divided in three groups. Each group has the same film thickness, while the radius varies. The carrier frequency range for all the tests is from 10 kHz to 160 kHz.

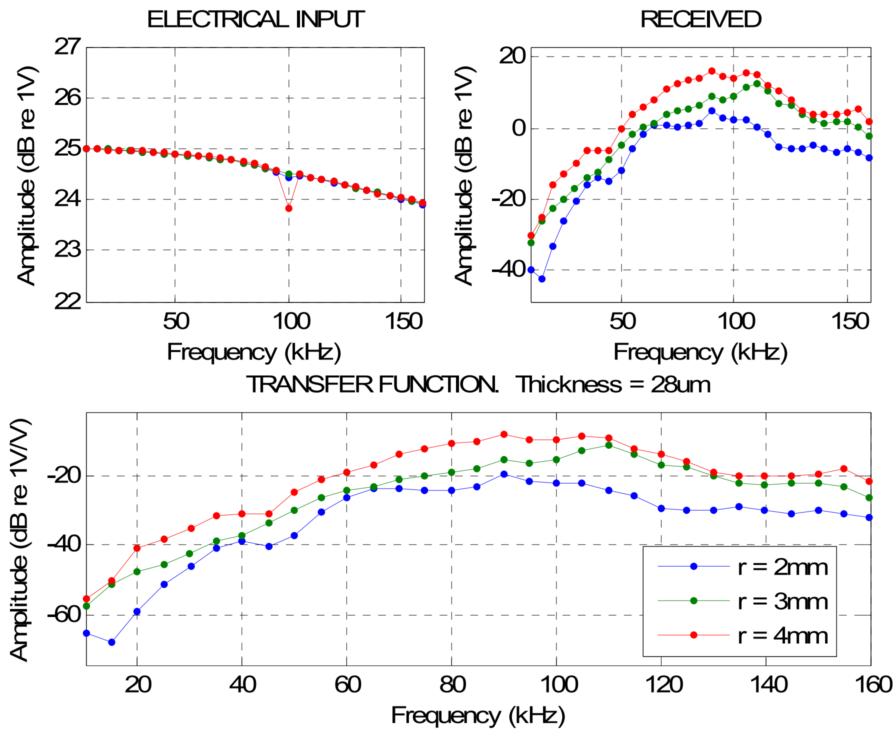
ELECTRICAL INPUT
Amplitude (dB re 1V)
Frequency (kHz)
RECEIVED
Amplitude (dB re 1V)
Frequency (kHz)
TRANSFER FUNCTION. Thickness = 28um
Amplitude (dB re 1V/V)
Frequency (kHz)
r = 2mm
r = 3mm
r = 4mm

(a)

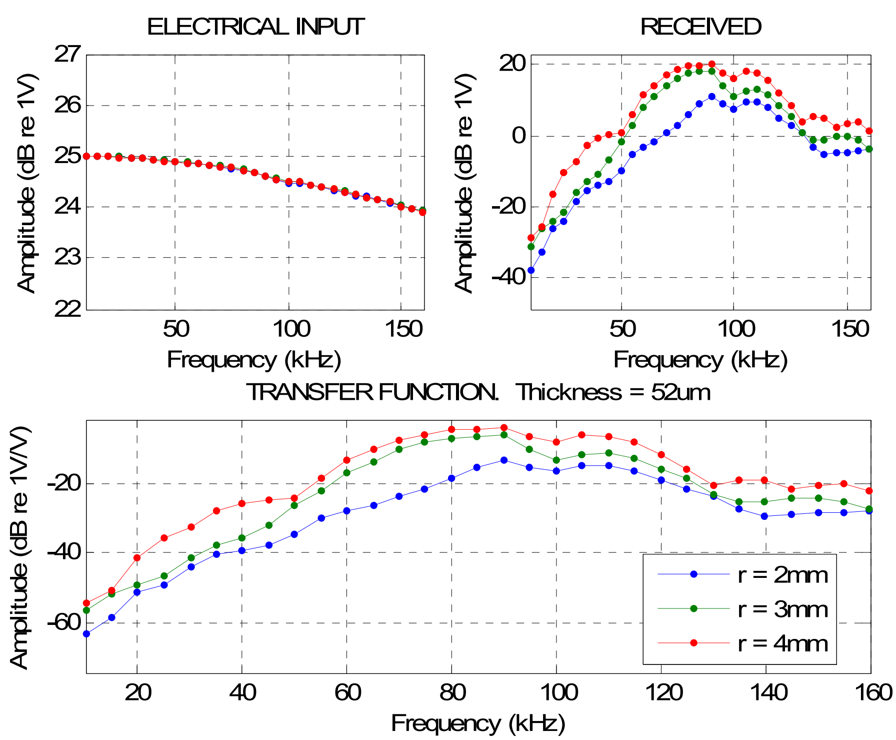
ELECTRICAL INPUT
Amplitude (dB re 1V)
Frequency (kHz)
RECEIVED
Amplitude (dB re 1V)
Frequency (kHz)
TRANSFER FUNCTION. Thickness = 52um
Amplitude (dB re 1V/V)
Frequency (kHz)
r = 2mm
r = 3mm
r = 4mm

(b)

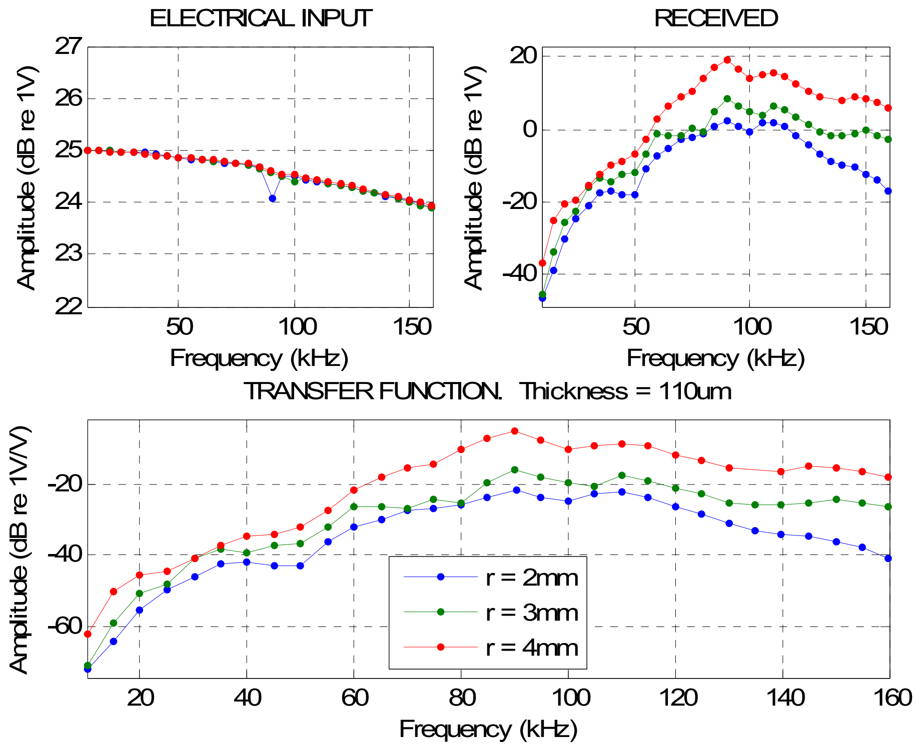

(c)

Figure 4.6. Experimental receiving transfer functions vs. frequency, for different radiuses (2, 3 and 4 mm). (a) Thickness = 28 μm, (b) Thickness = 52 μm, and (c) Thickness = 110 μm. Amplitude in dB (re 1 V/V). Frequency range: 10 kHz to 160 kHz.

4.1.2.2 Receiving transfer function vs. thickness, with fixed radius

Similar to the previous section, this section shows the experimental receiving behavior of the nine transducers, divided in three groups. Each group has the same active area radius, while the piezofilm thickness varies. The frequency range for all the tests is from 10 kHz to 160 kHz.

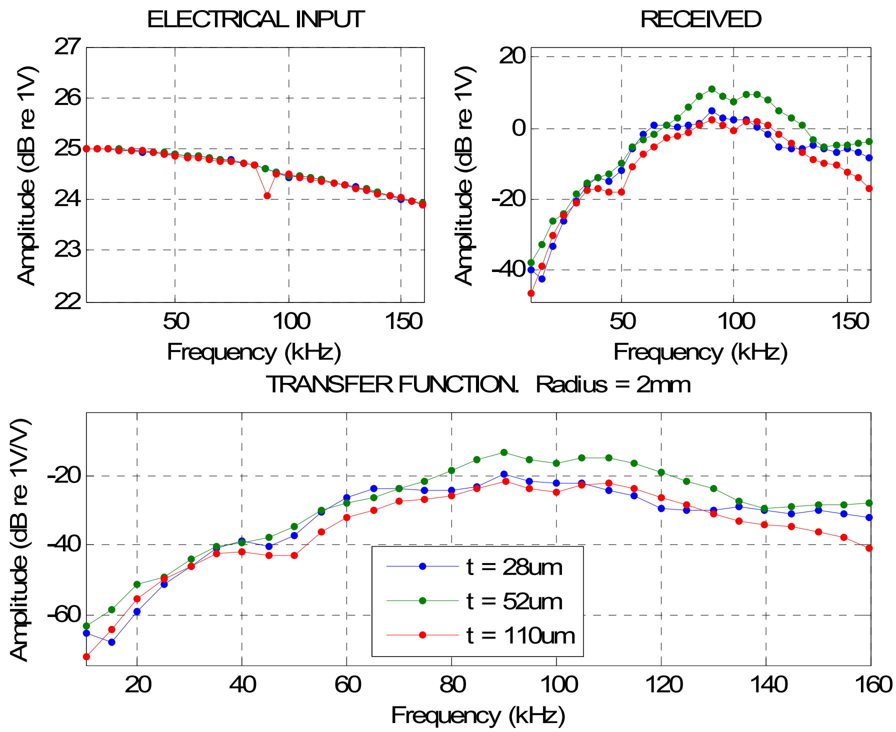

ELECTRICAL INPUT
Amplitude (dB re 1V)
Frequency (kHz)
RECEIVED
Amplitude (dB re 1V)
Frequency (kHz)
TRANSFER FUNCTION. Radius = 2mm
Amplitude (dB re 1V/V)
Frequency (kHz)
t = 28um
t = 52um
t = 110um

(a)

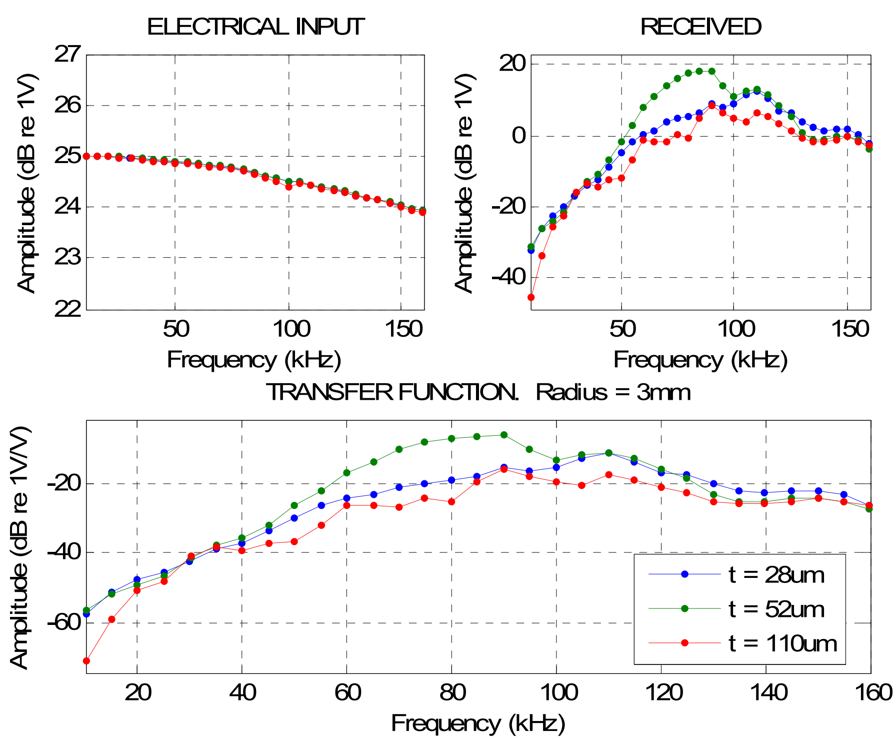

ELECTRICAL INPUT
Amplitude (dB re 1V)
Frequency (kHz)
RECEIVED
Amplitude (dB re 1V)
Frequency (kHz)
TRANSFER FUNCTION. Radius = 3mm
Amplitude (dB re 1V/V)
Frequency (kHz)
t = 28um
t = 52um
t = 110um

(b)

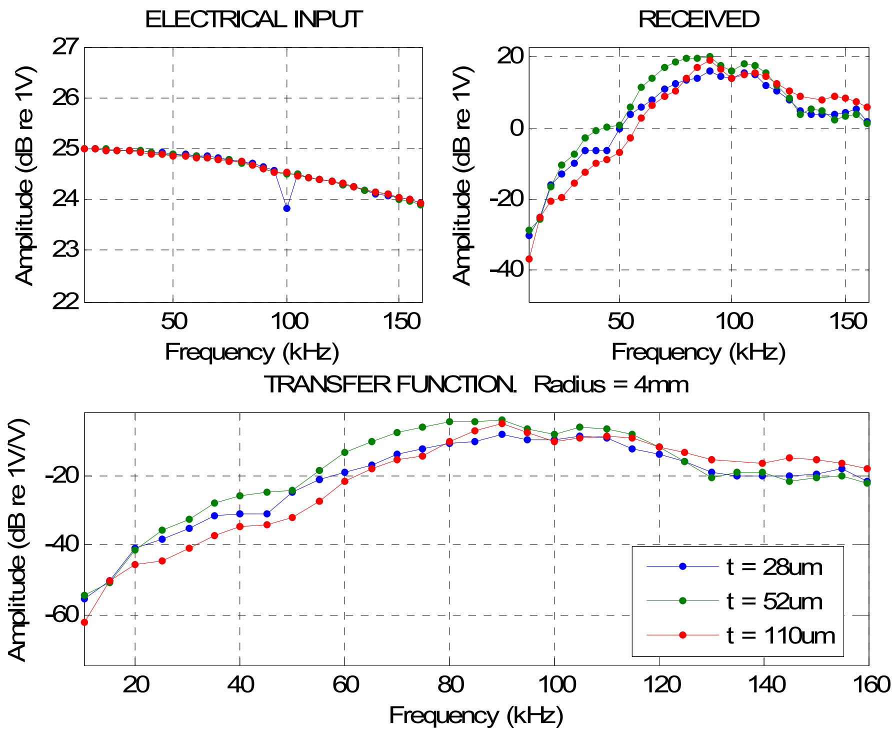

(c)

Figure 4.7. Experimental receiving transfer functions vs. frequency, for different thicknesses (28, 52 and 110 μm). (a) Radius = 2 mm, (b) Radius = 3 mm, and (c) Radius = 4 mm. Amplitude in dB (re 1 V/V). Frequency range: 10 kHz to 160 kHz.

4.1.2.3 Discussion

From Figure 4.6, it can be noticed that the transfer function amplitude depends on the active area radius, and as it increases, the amplitude increases, for the three different thicknesses, in all the frequency range. With respect to thickness, there is not a repetitive pattern that indicates how the system response depends on thickness for all the tests in Figure 4.7.

Figure 4.8 displays the experimental receiving behavior of the nine transducers in one graph, while Table 4.1 lists the amplitude transfer function mean for the nine transducers.

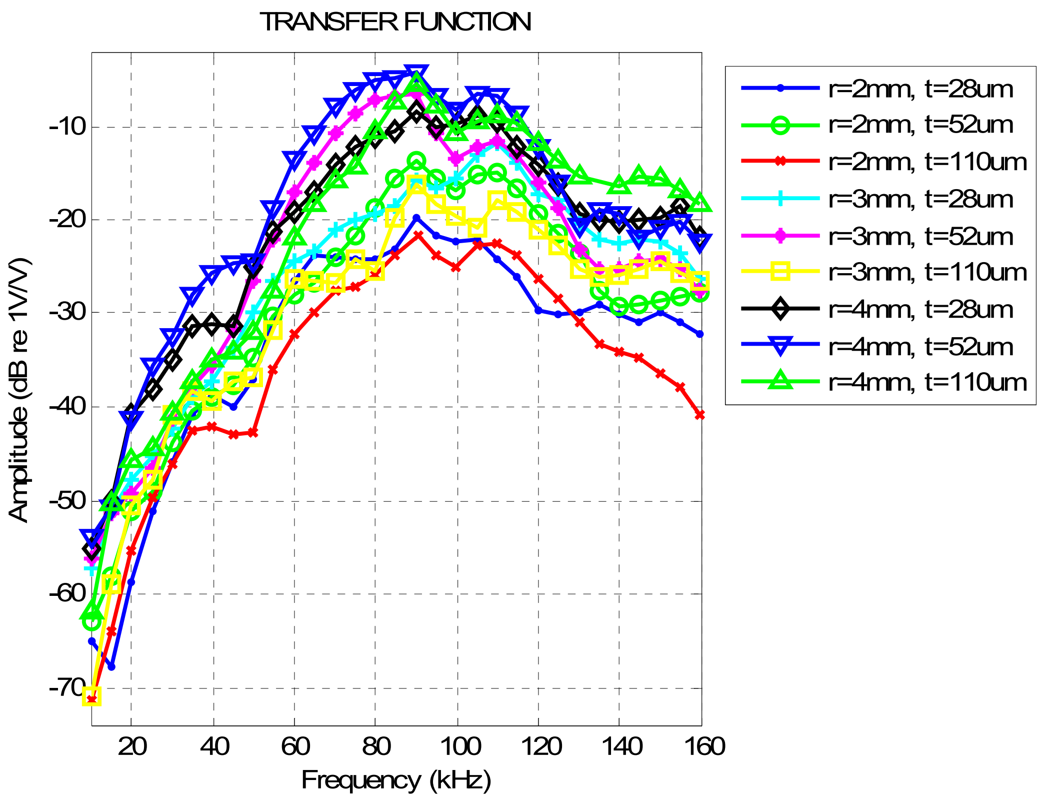

Figure 4.8. Experimental receiving transfer functions vs. frequency, for the 9 PVDF transducers constructed. Amplitude in dB (re 1 V/V). Frequency range: 10 kHz to 160 kHz.

Table 4.1. Experimental complete system transfer function mean for PVDF receiving from 10 kHz to 160 kHz.

PVDF TRANSDUCER		TRANSFER FUNCTION MEAN (dB re 1 V/V)
RADIUS (mm)	**THICKNESS (µm)**	
2	28	-33.2436
	52	-29.3464
	110	-35.5700
3	28	-26.3773
	52	-23.8781
	110	-30.2201
4	28	-21.6898
	52	-19.2596
	110	-22.1954

The transfer function amplitude behavior with respect to frequency is not flat. In general, the experimental amplitude increases with frequency until approximately 90 kHz, and then it start decreasing. However it is necessary to remember that the results presented here are for the complete system, including the Reson TC4033 as transmitter, therefore, to do a more precise analysis with respect to frequency, it would be necessary to compensate for the Reson and filters effect, which is made in next section.

4.1.3 PVDF COMPENSATED RECEIVING SENSITIVITY

The total system transfer function presented in the previous section, was found comparing the output and input voltage signals. Therefore, it includes the effects of the PVDF as a receiver, the Reson as a transmitter, the power amplifier, the water medium, the signal conditioning circuit and the acquisition system. In order to isolate the PVDF transfer function, compensation was applied in which the effects of the Reson as transmitter and the signal conditioning circuit are minimized. Although it is not possible to provide an exact measure of the PVDF receiving sensitivity with the method used, the interest of this research was to analyze the sensitivity trends with respect to frequency, active area and thickness, which can be accomplished by this method. The results are presented in the same form used for the previous section.

4.1.3.1 Receiving sensitivity vs. radius, with fixed thickness

This section shows the experimental receiving sensitivity of the nine transducers, divided in three groups. Each group has the same film thickness, while the radius varies. The frequency range for all the tests is from 10 kHz to 160 kHz. Compensation was applied to consider the Reson and signal conditioning circuit effects.

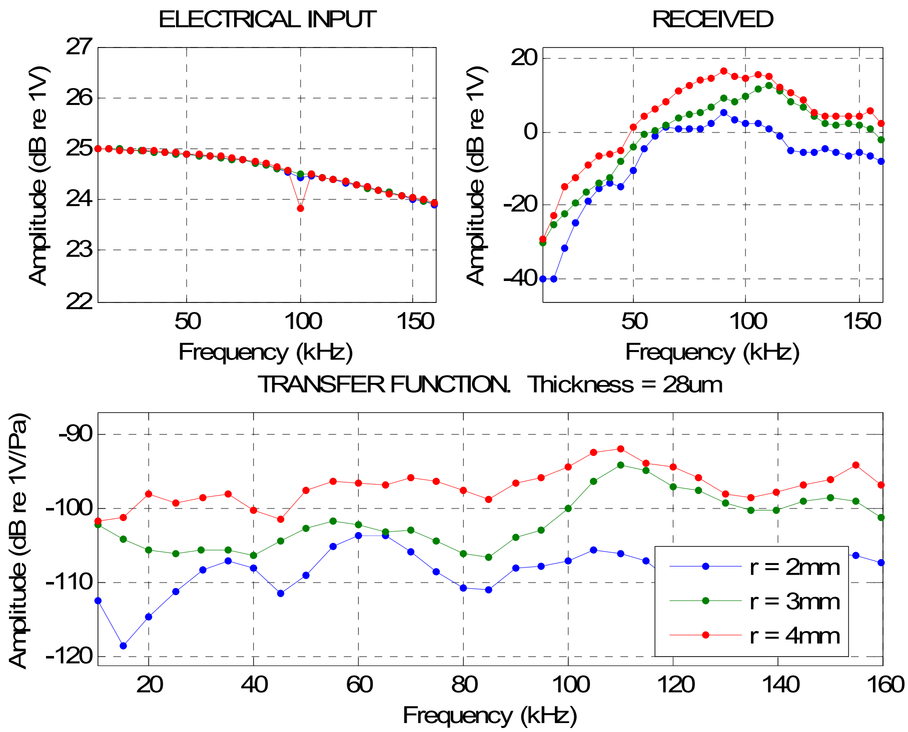

ELECTRICAL INPUT
RECEIVED
Amplitude (dB re 1V)
Frequency (kHz)
TRANSFER FUNCTION. Thickness = 28um
Amplitude (dB re 1V/Pa)
r = 2mm
r = 3mm
r = 4mm

(a)

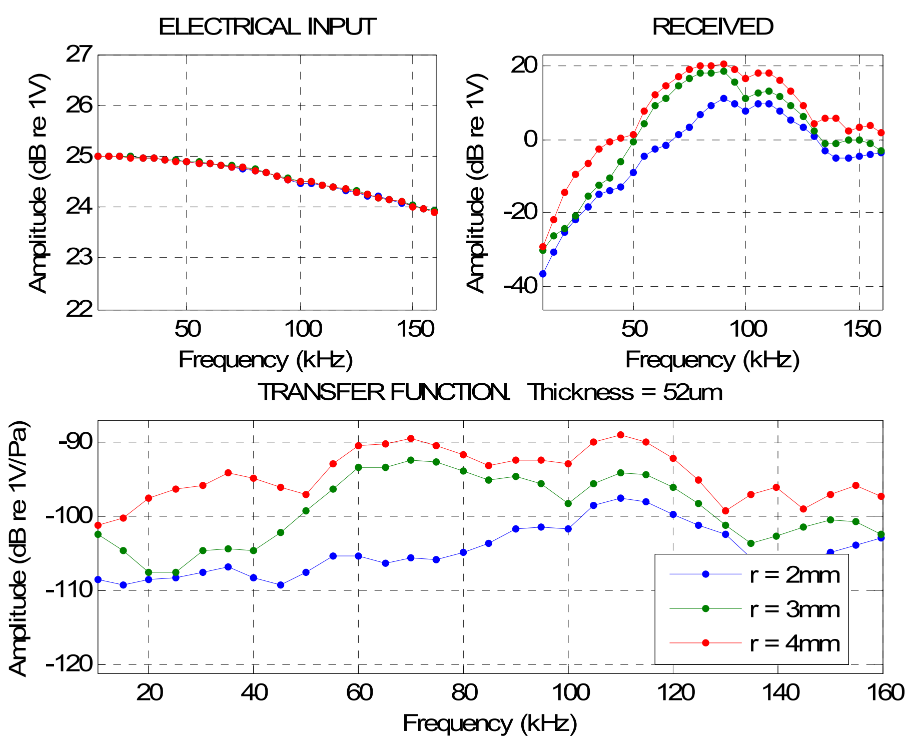

ELECTRICAL INPUT
RECEIVED
Amplitude (dB re 1V)
Frequency (kHz)
TRANSFER FUNCTION. Thickness = 52um
Amplitude (dB re 1V/Pa)
r = 2mm
r = 3mm
r = 4mm

(b)

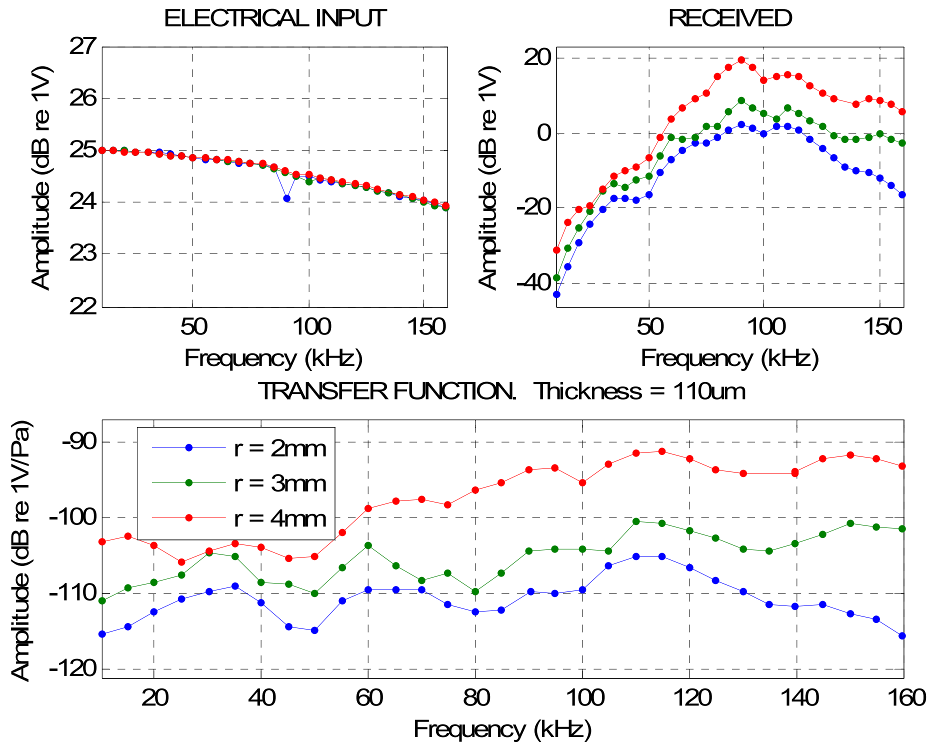

(c)

Figure 4.9. Experimental compensated receiving sensitivity vs. frequency, for different radiuses (2, 3 and 4 mm). (a) Thickness = 28 µm, (b) Thickness = 52 µm, and (c) Thickness = 110 µm. Amplitude in dB (re 1 V/Pa). Frequency range: 10 kHz to 160 kHz.

4.1.3.2 Receiving sensitivity vs. thickness, with fixed radius

Similar to the previous section, this section shows the experimental receiving sensitivity of the nine transducers, divided in three groups, but in this case, each group has the same active area radius, while the piezoelectric film thickness varies. The frequency range for all the tests is from 10 kHz to 160 kHz.

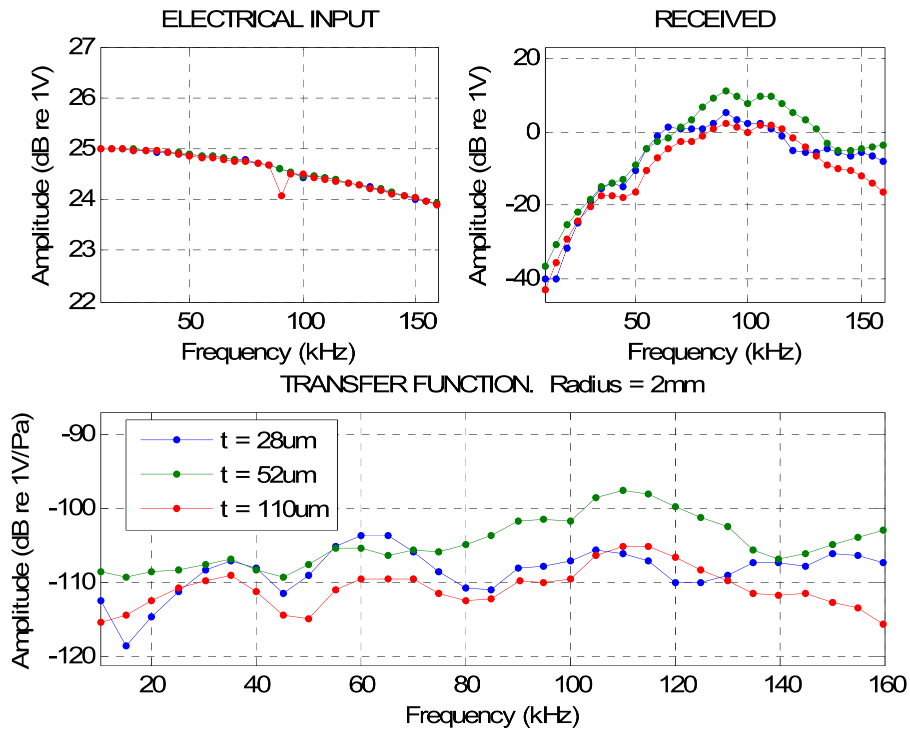
ELECTRICAL INPUT
RECEIVED
Amplitude (dB re 1V)
Frequency (kHz)
TRANSFER FUNCTION. Radius = 2mm
Amplitude (dB re 1V/Pa)
t = 28um
t = 52um
t = 110um
Frequency (kHz)

(a)

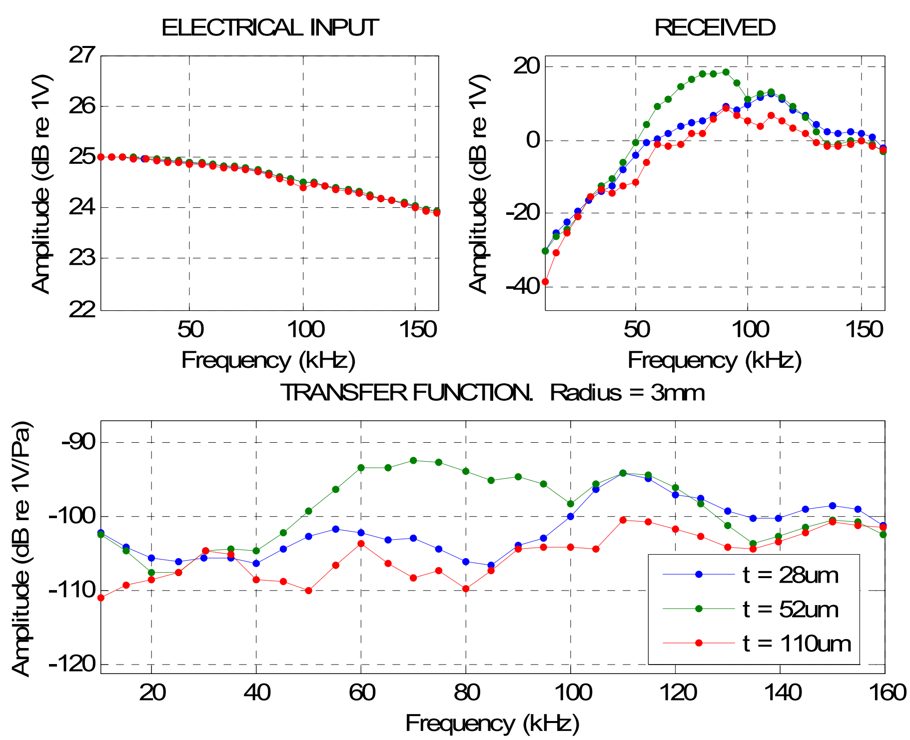
ELECTRICAL INPUT
RECEIVED
Amplitude (dB re 1V)
Frequency (kHz)
TRANSFER FUNCTION. Radius = 3mm
Amplitude (dB re 1V/Pa)
t = 28um
t = 52um
t = 110um
Frequency (kHz)

(b)

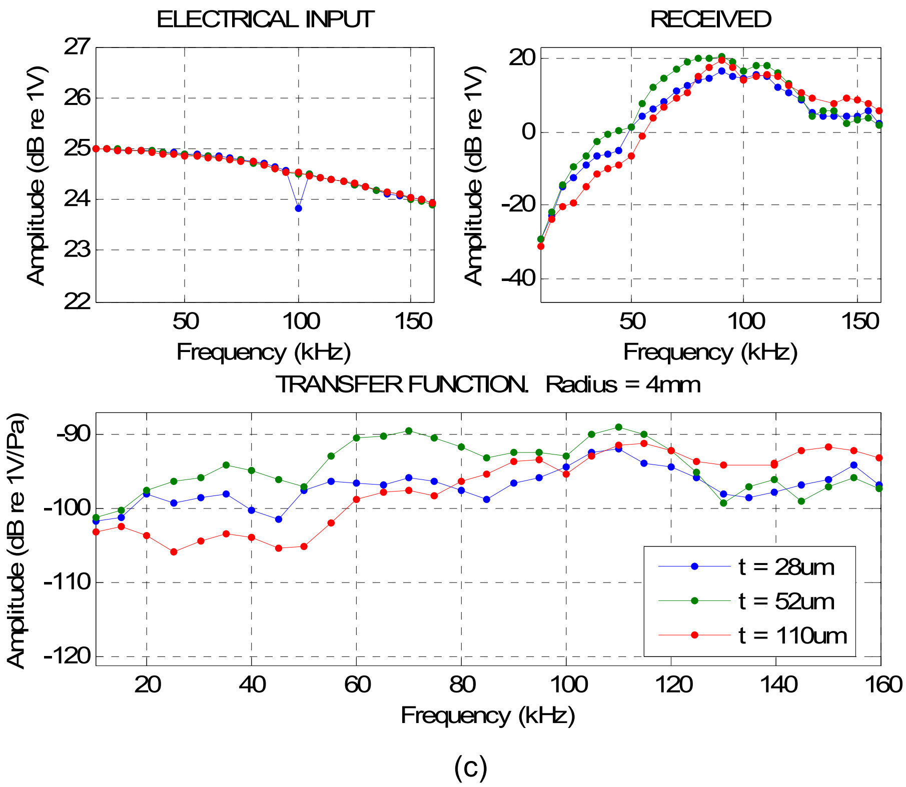

Figure 4.10. Experimental compensated receiving sensitivity vs. frequency, for different thicknesses (28, 52 and 110 μm). (a) Radius = 2 mm, (b) Radius = 3 mm, and (c) Radius = 4 mm. Amplitude in dB (re 1 V/Pa). Frequency range: 10 kHz to 160 kHz.

4.1.3.3 Discussion

As it was expected, it can be noticed from Figure 4.9 that the receiving sensitivity depends on the active area radius, and as it increases, the amplitude increases, for the three different thicknesses, in all the frequency range. With respect to thickness, the same observations made for Figure 4.7 apply to Figure 4.10, in which no clear tendency was identified.

Figure 4.11 displays the experimental receiving sensitivity of the nine transducers in one graph. The frequency range for all the tests is from 10 kHz to 160 kHz. Table 4.2 lists the sensitivity mean for the transducers.

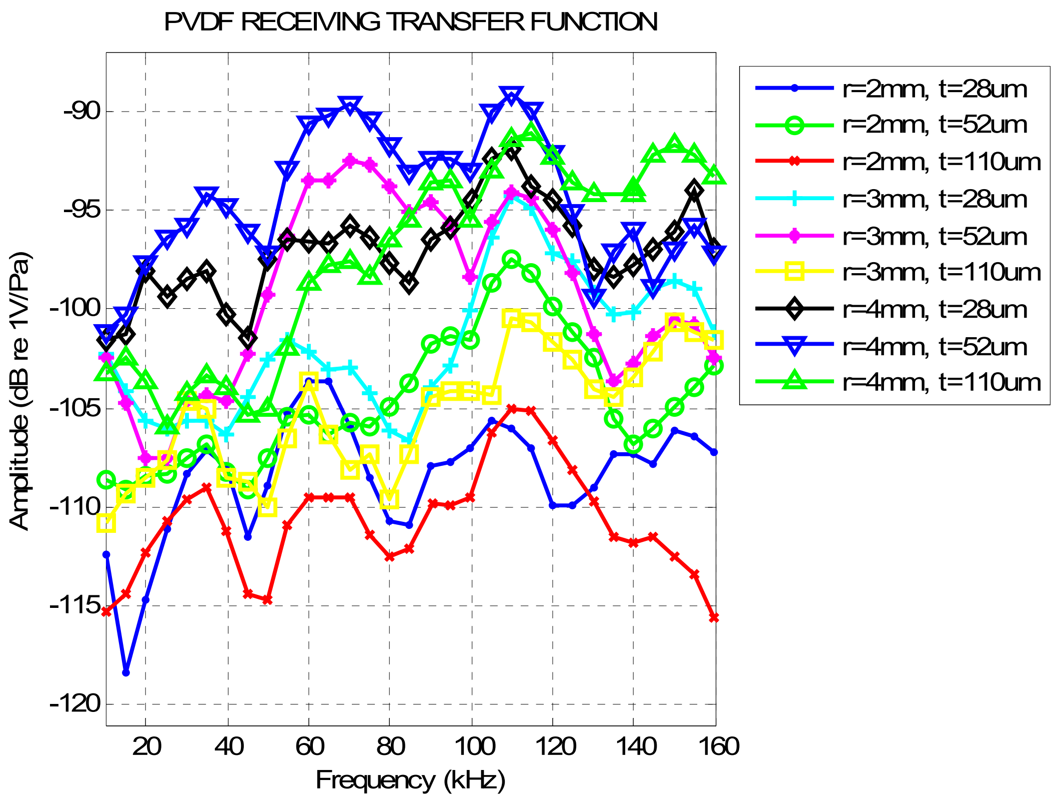

Figure 4.11. Experimental compensated receiving sensitivity vs. frequency, for the 9 PVDF transducers constructed. Amplitude in dB (re 1 V/Pa). Frequency range: 10 kHz to 160 kHz.

Table 4.2. Experimental PVDF receiving sensitivity mean from 10 kHz to 160 kHz.

PVDF TRANSDUCER		**SENSITIVITY MEAN (dB re 1 V/Pa)**
RADIUS (mm)	**THICKNESS (µm)**	
2	28	-108.4281
	52	-104.6299
	110	-110.7589
3	28	-101.7336
	52	-99.1768
	110	-105.2302
4	28	-97.0356
	52	-94.4446
	110	-97.4013

The compensated PVDF sensitivity presents a behavior less dependent on frequency than the one found for the total acoustic system transfer function, since the Reson effect has been eliminated. The maximum variation in sensitivity found for the nine transducers in all the frequency range was 14.9 dB, in contrast with the 56.4 dB variation from the total transfer function amplitude found in section 4.1.3.3.

Although the PVDF sensitivity was not constant with frequency for the nine transducers, there is not a marked tendency applicable to all the cases that clearly indicates a relation between sensitivity and frequency, except for an increment near 110 kHz.

4.1.4 PVDF TRANSMITTING - TOTAL SYSTEM TRANSFER FUNCTION

The nine PVDF transducers were examined as transmitters, applying the same voltage input to the transducer and recording the output voltage generated by the Reson TC4033 from the signal conditioning circuit. The following subsections present the results obtained for the whole system behavior, including the power amplifier, PVDF as transmitter, Reson as receiver, signal conditioning circuit and acquisition system. The results are presented in two different ways, to facilitate the analysis and identification of each variable influence.

4.1.4.1 Transmitting transfer function vs. radius, with fixed thickness

This section shows the experimental system behavior with the nine PVDF transducers as transmitters, divided in three groups. Each group has the same film thickness, while the radius varies. The frequency range for all the tests is from 10 kHz to 160 kHz.

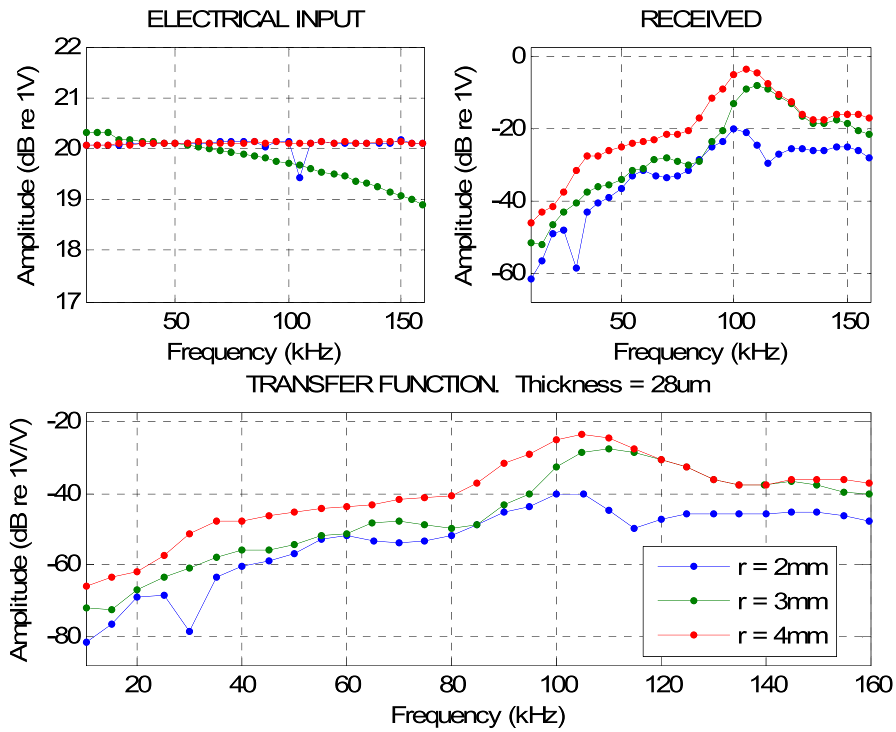
ELECTRICAL INPUT
RECEIVED
Amplitude (dB re 1V)
Frequency (kHz)
TRANSFER FUNCTION. Thickness = 28um
Amplitude (dB re 1V/V)
r = 2mm
r = 3mm
r = 4mm

(a)

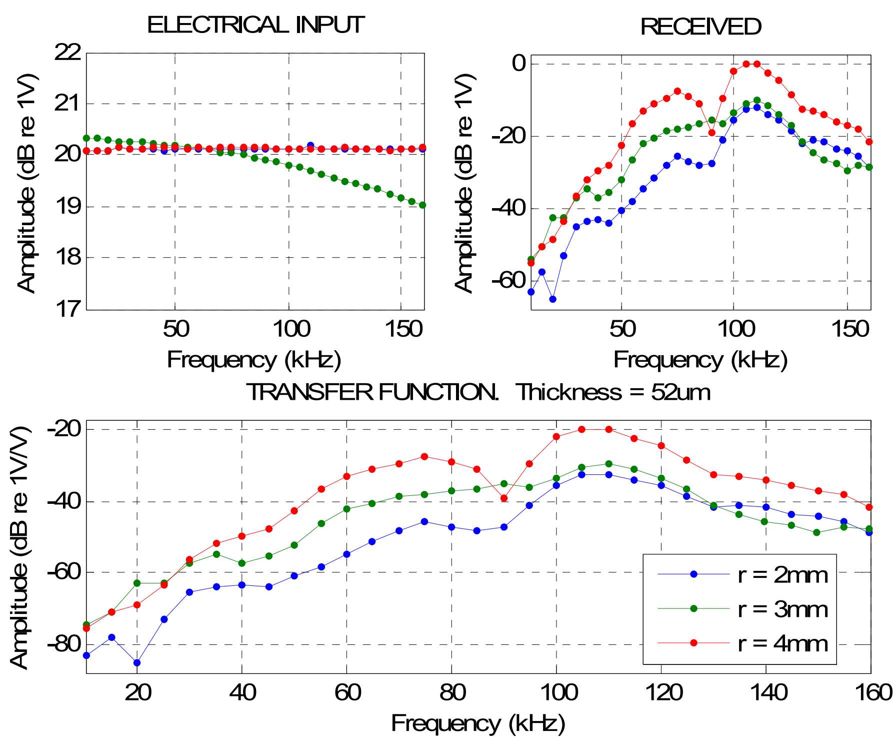
ELECTRICAL INPUT
RECEIVED
Amplitude (dB re 1V)
Frequency (kHz)
TRANSFER FUNCTION. Thickness = 52um
Amplitude (dB re 1V/V)
r = 2mm
r = 3mm
r = 4mm

(b)

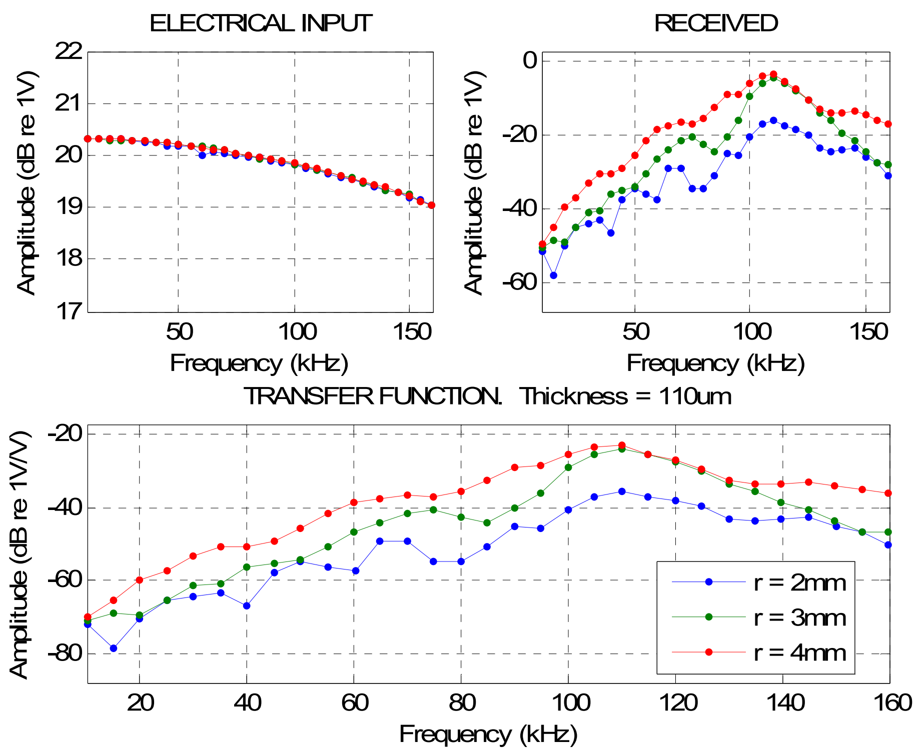

(c)

Figure 4.12. Experimental transmitting transfer functions vs. frequency, for different radiuses (2, 3 and 4 mm). (a) Thickness = 28 μm, (b) Thickness = 52 μm, and (c) Thickness = 110 μm. Amplitude in dB (re 1 V/V). Frequency range: 10 kHz to 160 kHz.

4.1.4.2 Transmitting transfer function vs. thickness, with fixed radius

Similar to the previous section, this section shows the system experimental behavior while using the nine PVDF transducers as transmitters. The results are divided in three groups. Each group contains the response of three transducers with the same active area radius, while the piezoelectric film thickness varies. The frequency range for all the tests is from 10 kHz to 160 kHz.

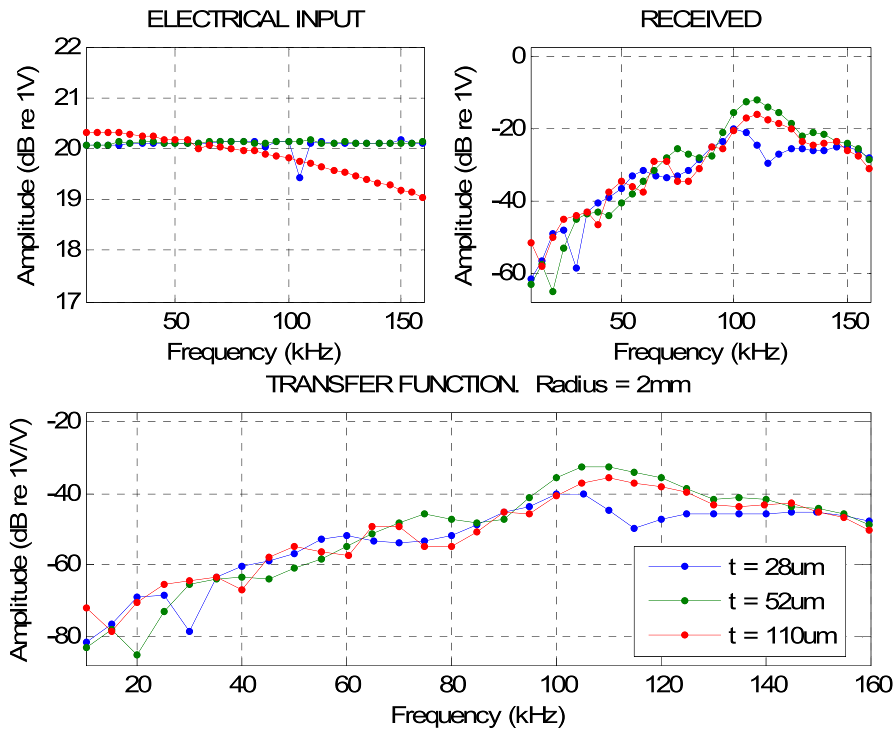
ELECTRICAL INPUT
RECEIVED
Amplitude (dB re 1V)
Frequency (kHz)
TRANSFER FUNCTION. Radius = 2mm
Amplitude (dB re 1V/V)
t = 28um
t = 52um
t = 110um

(a)

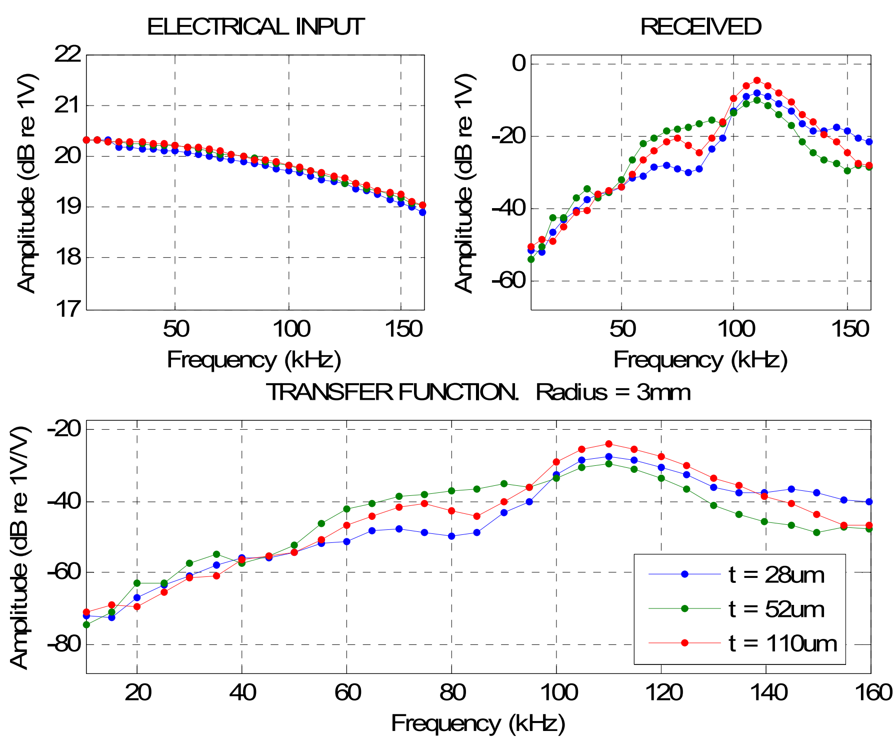
ELECTRICAL INPUT
RECEIVED
Amplitude (dB re 1V)
Frequency (kHz)
TRANSFER FUNCTION. Radius = 3mm
Amplitude (dB re 1V/V)
t = 28um
t = 52um
t = 110um

(b)

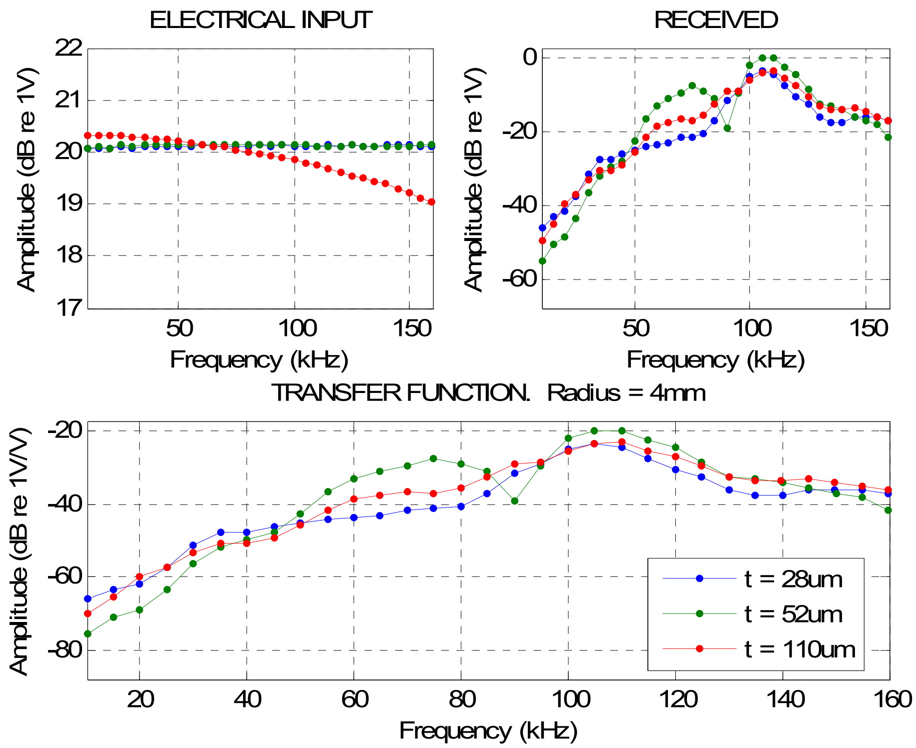

(c)

Figure 4.13. Experimental transmitting transfer functions vs. frequency, for different thicknesses (28, 52 and 110 μm). (a) Radius = 2 mm, (b) Radius = 3 mm, and (c) Radius = 4 mm. Amplitude in dB (re 1 V/V). Frequency range: 10 kHz to 160 kHz.

4.1.4.3 Discussion

From Figure 4.12, it can be noticed that the transfer function amplitude depends on the active area radius, and as it increases, the amplitude increases, for the three different thicknesses, in all the frequency range. With respect to thickness, no definite trend was observed, as seen in Figure 4.13, that allows to visually establish a clear relation between the film thickness and the transfer function amplitude. The amplitude appears to be approximately the same for the transducers with equal area, but different thicknesses, indicating that the thickness has not a noticeable influence in the transfer function amplitude.

Figure 4.14 displays in one graph the nine experimental system transfer functions obtained when the PVDF transducers were used as transmitters, while Table 4.3 lists the amplitude transfer functions means.

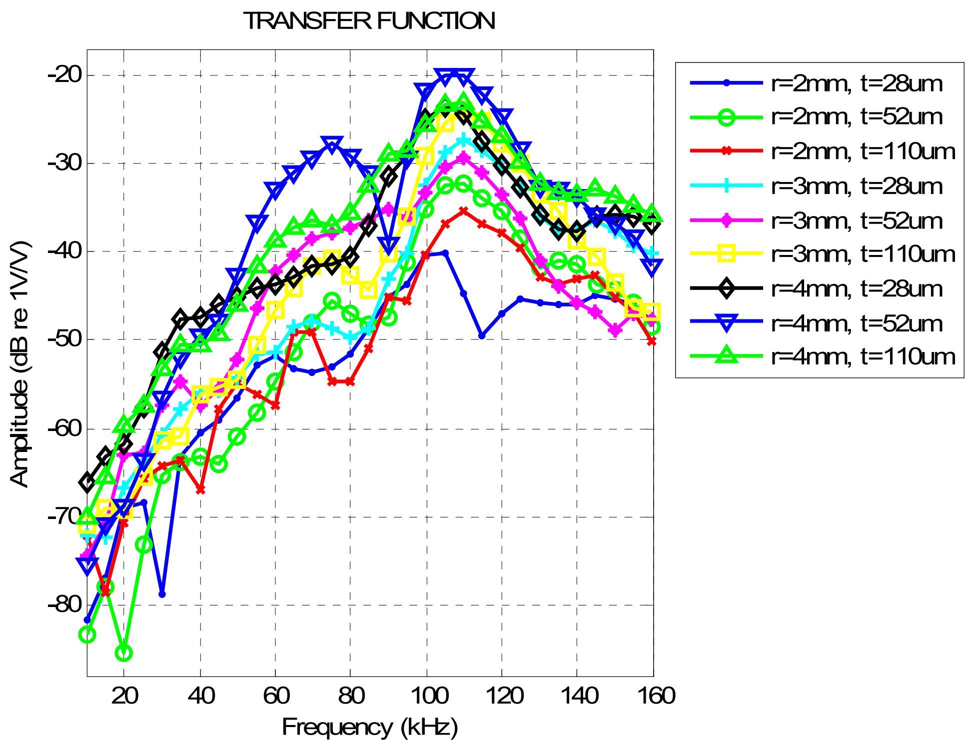

Figure 4.14. Experimental transmitting transfer functions vs. frequency, for the 9 PVDF transducers constructed. Amplitude in dB (re 1 V/V). Frequency range: 10 kHz to 160 kHz.

Table 4.3. Experimental complete system transfer function mean for PVDF transmitting from 10 kHz to 160 kHz.

PVDF TRANSDUCER		TRANSFER FUNCTION MEAN (dB re 1 V/V)
RADIUS (mm)	THICKNESS (µm)	
2	28	-53.4442
	52	-51.3851
	110	-51.5462
3	28	-46.2418
	52	-45.5807
	110	-45.0117
4	28	-40.5433
	52	-38.7640
	110	-38.9840

The transfer function amplitude behavior with respect to frequency is not flat. In general, the experimental amplitude increases with frequency until approximately 105 kHz, and then it decreases slowly. It is necessary to remember that the results presented here are for the complete system, including the Reson TC4033 as receiver; therefore, to do a more precise analysis with respect to frequency, it would be necessary to compensate for the Reson and filters effect, which is made in next section.

4.1.5 PVDF COMPENSATED TRANSMITTING SENSITIVITY

The total system transfer function presented in the previous section, was found comparing the output and input voltage signals. Therefore, it includes the effects of the PVDF as a transmitter, the Reson as a receiver, the power amplifier, the water medium, the signal conditioning circuit and the acquisition system. In order to isolate the PVDF transfer function, compensation was applied in which the effects of the Reson as receiver and the signal conditioning circuit are minimized. Although it is not possible to provide an exact measure of the PVDF transmitting sensitivity with the method used, the interest of this research was to analyze the sensitivity trends with respect to frequency, active area and thickness, which can be accomplished by this method. The results are presented in the same form used for the previous section.

4.1.5.1 Transmitting sensitivity vs. radius, with fixed thickness

This section shows the experimental transmitting sensitivity of the nine transducers, divided in three groups. Each group has the same film thickness, while the radius varies. The frequency range for all the tests is from 10 kHz to 160 kHz. Compensation was applied to consider the Reson and signal conditioning circuit effects.

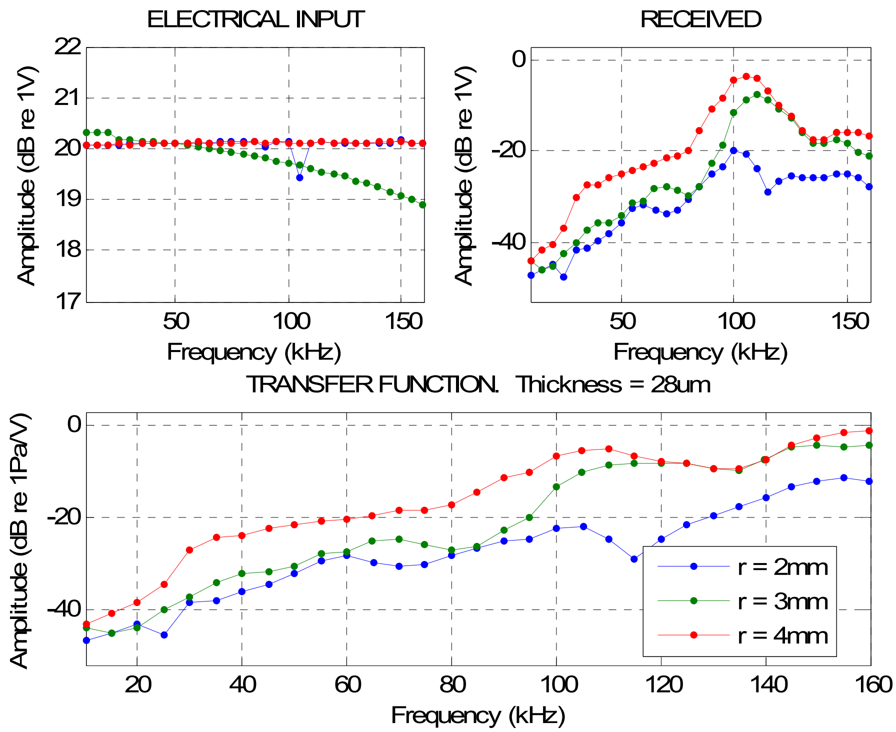

ELECTRICAL INPUT
RECEIVED
Amplitude (dB re 1V)
Frequency (kHz)
TRANSFER FUNCTION. Thickness = 28um
Amplitude (dB re 1Pa/V)
r = 2mm
r = 3mm
r = 4mm

(a)

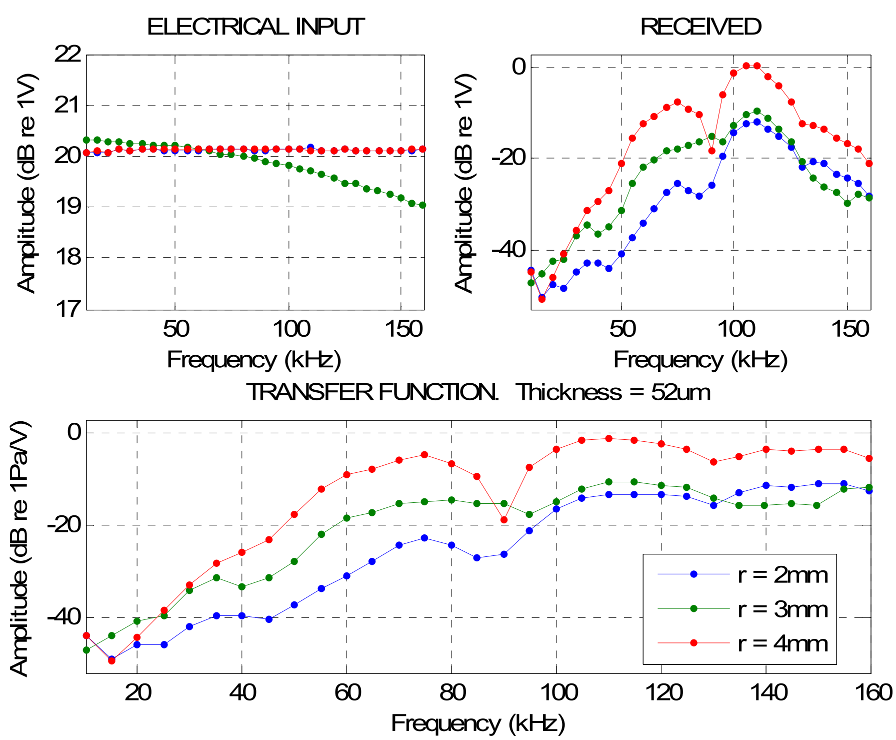

ELECTRICAL INPUT
RECEIVED
Amplitude (dB re 1V)
Frequency (kHz)
TRANSFER FUNCTION. Thickness = 52um
Amplitude (dB re 1Pa/V)
r = 2mm
r = 3mm
r = 4mm

(b)

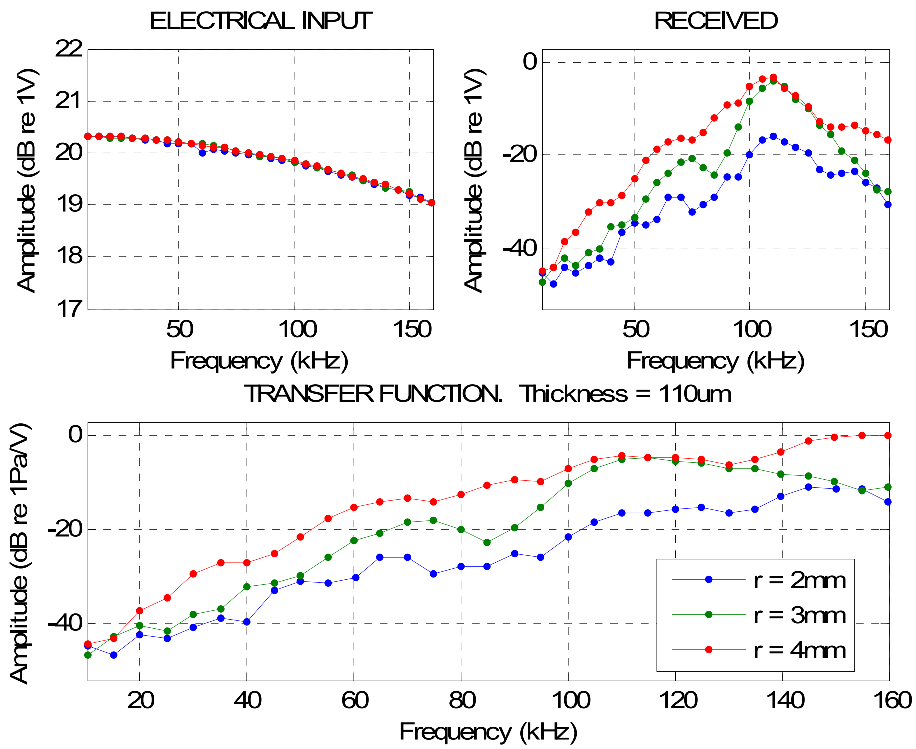

(c)

Figure 4.15. Experimental compensated transmitting sensitivity as function of frequency, for the transducers with different radiuses (2, 3 and 4 mm). (a) Thickness = 28 μm, (b) Thickness = 52 μm, and (c) Thickness = 110 μm. Amplitude in dB (re 1 Pa/V). Frequency range: 10 kHz to 160 kHz.

4.1.5.2 Transmitting sensitivity vs. thickness, with fixed radius

Similar to the previous section, this section shows the experimental transmitting sensitivity of the nine PVDF transducers. The results are divided in three groups, but in this case, each group has the same active area radius, while the piezoelectric film thickness varies. The frequency range for all the tests is from 10 kHz to 160 kHz.

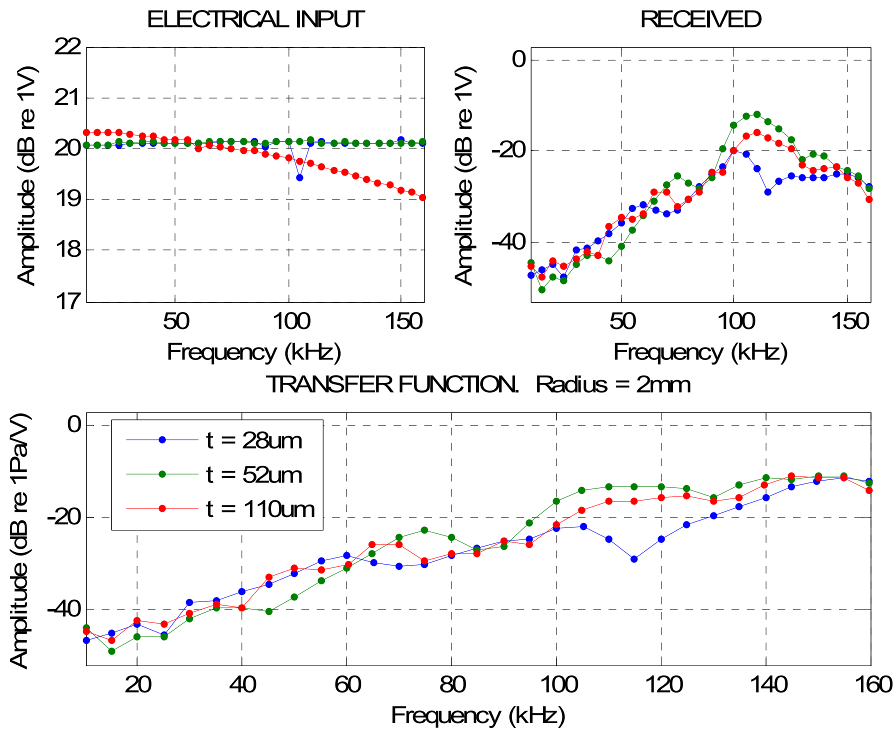

ELECTRICAL INPUT
RECEIVED
Amplitude (dB re 1V)
Frequency (kHz)
TRANSFER FUNCTION. Radius = 2mm
Amplitude (dB re 1Pa/V)
t = 28um
t = 52um
t = 110um

(a)

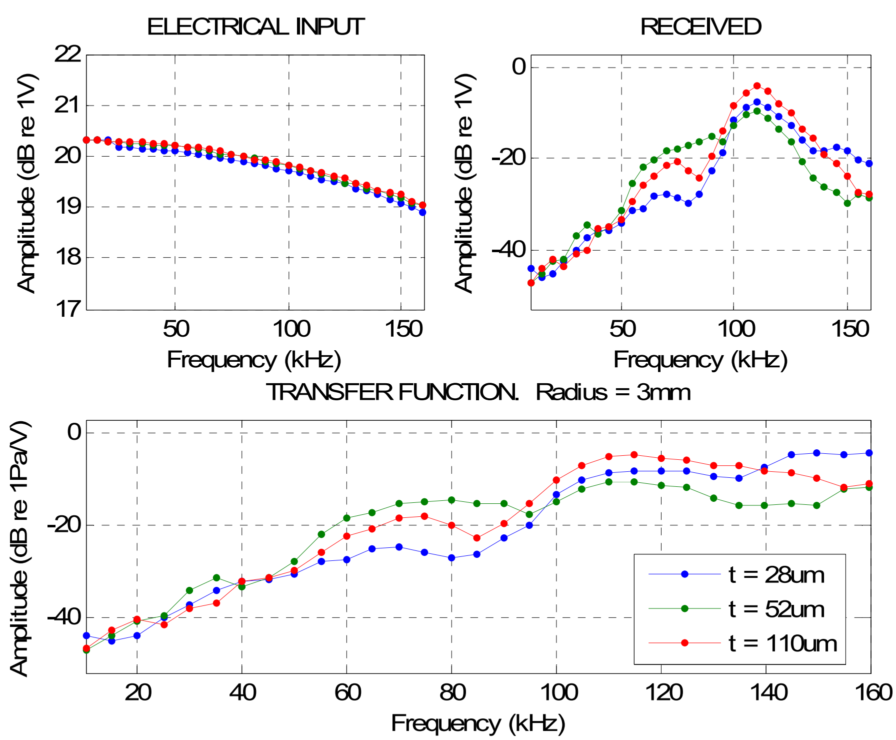

ELECTRICAL INPUT
RECEIVED
Amplitude (dB re 1V)
Frequency (kHz)
TRANSFER FUNCTION. Radius = 3mm
Amplitude (dB re 1Pa/V)
t = 28um
t = 52um
t = 110um

(b)

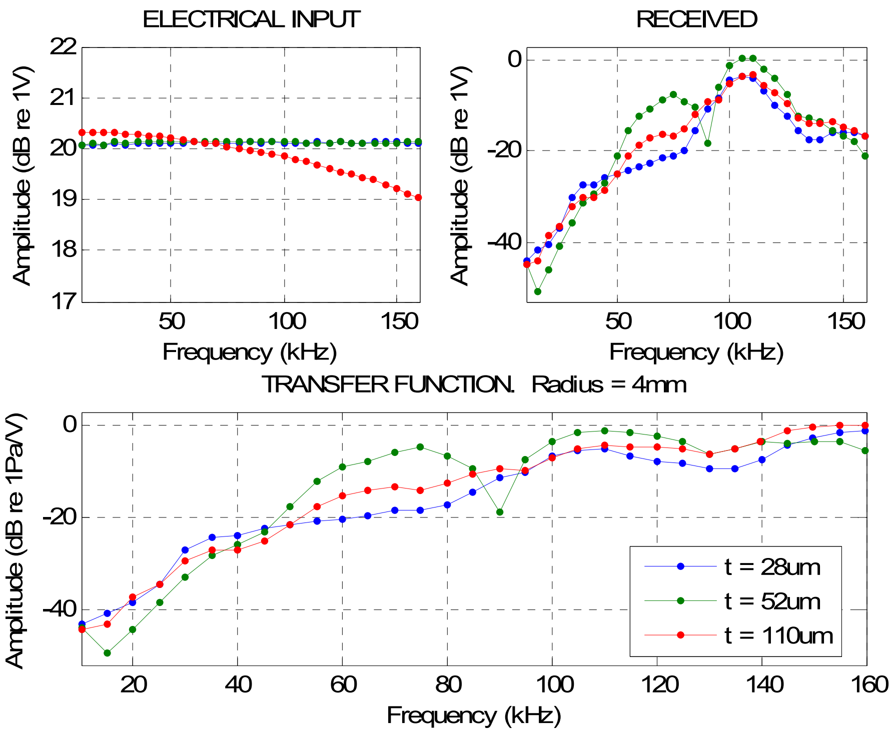

(c)

Figure 4.16. Experimental compensated transmitting sensitivity as function of frequency, for the transducers with different thicknesses (28, 52 and 110 μm). (a) Radius = 2 mm, (b) Radius = 3 mm, and (c) Radius = 4 mm. Amplitude in dB (re 1 Pa/V). Frequency range: 10 kHz to 160 kHz.

4.1.5.3 Discussion

As it was expected, it can be noticed from Figure 4.15 that the transmitting sensitivity depends on the active area radius, and as it increases, the amplitude increases, for the three different thicknesses, in all the frequency range. With respect to thickness, the same observations made for Figure 4.13, apply to Figure 4.16, in which the transmitting sensitivity does not appear to be affected by the piezofilm thickness.

Figure 4.17 displays in one graph, the nine experimental transmitting sensitivities obtained for the PVDF transducers, while Table 4.4 lists the transmitting sensitivities means for the nine transducers.

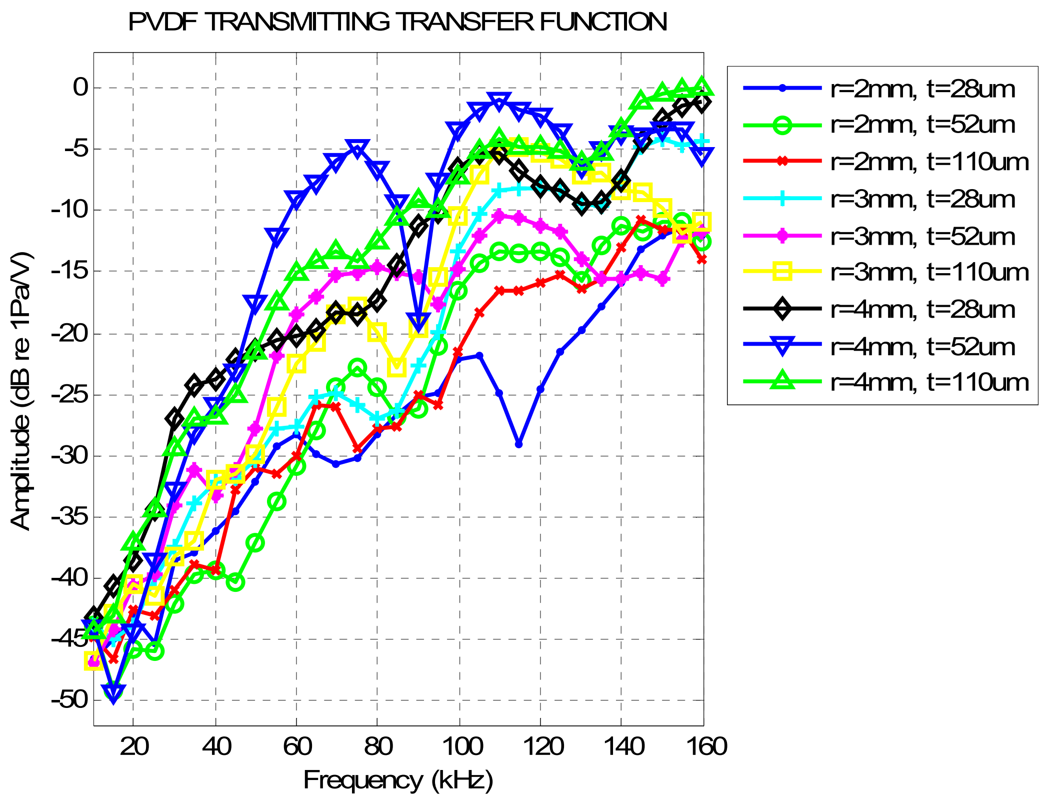

Figure 4.17. Experimental compensated transmitting sensitivity vs. frequency, for the 9 PVDF transducers constructed. Amplitude in dB (re 1 V/V). Frequency range: 10 kHz to 160 kHz.

Table 4.4. Experimental PVDF transmitting sensitivity mean from 10 kHz to 160 kHz.

PVDF TRANSDUCER		SENSITIVITY MEAN (dB re 1 Pa/V)
RADIUS (mm)	THICKNESS (µm)	
2	28	-27.7129
	52	-25.5591
	110	-26.0154
3	28	-21.5123
	52	-20.9618
	110	-20.1674
4	28	-16.1949
	52	-13.8721
	110	-14.6060

The compensated transmitting sensitivity behavior is proportional to the frequency, increasing the magnitude when the frequency increases. This behavior is maintained for the complete frequency range of interest (from 10 kHz to 160 kHz), although the increment rate diminishes with frequency.

4.2 SIMULATIONS RESULTS AND DISCUSSION

4.2.1 RECEIVING SENSITIVITY

The transducer model described in section 3.2.1 (page 53) was simulated using MATLAB, in order to observe the transducer receiving sensitivity as function of frequency, transducer radius, film thickness and electrical load. First, the sensitivity was simulated for the nine implemented transducers, using the combination of changing the three radiuses (2, 3 and 4 mm) and three thicknesses (28, 52 and 110 µm).

The transducer's sensitivity can be obtained from the open circuit sensitivity because it depends only on the film characteristics and the transducer's geometry. The closed circuit sensitivity (composed of the transducer, cable and electrical load) was simulated too. Both sensitivities are presented, allowing distinguishing the effect of the electrical circuit.

4.2.1.1 Modifying Radius and Thickness

The open circuit and closed circuit sensitivities were simulated for the nine transducers in the frequency range of interest, from 1 kHz to 160 kHz. Then, to verify the resonance behavior, the simulations were performed in the frequency range from 1 kHz to 24 MHz.

4.2.1.1.1 Open Circuit

Figure 4.18 (a) shows the open circuit sensitivity of the nine PVDF transducers, from 1 kHz to 160 kHz, while Table 4.5 lists the sensitivities' average for the transducers. As it can be seen from Figure 4.18 (a), the sensitivity is completely flat, having a maximum variation of $7.3 \cdot 10^{-3}$ dB. Since the range is so small, representing less than the 0.008% of the mean for all the cases, the sensitivity can be considered constant in the frequency range from 1 kHz to 160 kHz.

Table 4.5. Simulated open circuit receiving sensitivity mean from 1 to 160 kHz.

PVDF TRANSDUCER		SENSITIVITY MEAN (dB re 1 V/Pa)
RADIUS (mm)	THICKNESS (μm)	
2	28	-104.7326
	52	-99.3553
	110	-92.8456
3	28	-102.0547
	52	-96.6774
	110	-90.1677
4	28	-100.5432
	52	-95.1659
	110	-88.6562

As it was expected, the sensitivity increases as the area and the thickness increase. However, note that the thickness variations have more influence than the area variations, since the sensitivity is greater for the transducers with greater thickness, independent from their radiuses.

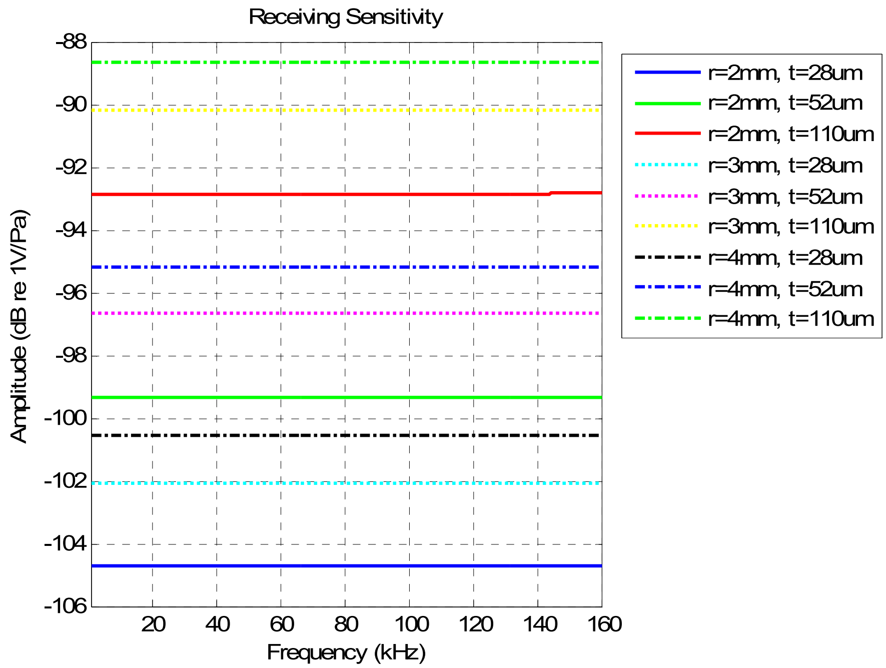

(a)

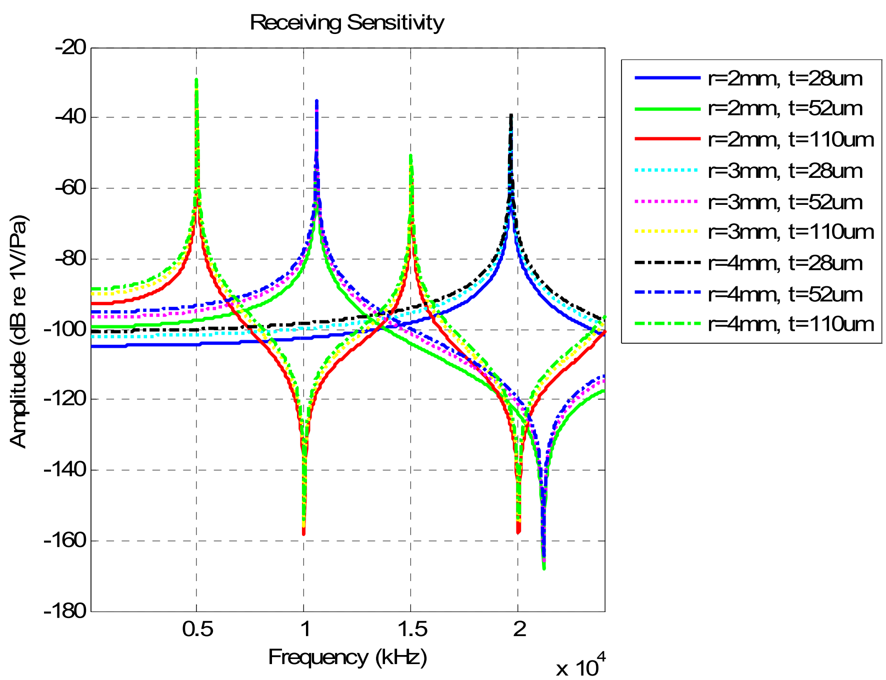

(b)

Figure 4.18. Simulated open circuit receiving sensitivity as function of frequency, for the 9 PVDF transducers constructed. Amplitude in dB (re 1 V/Pa). (a) Frequency range: 1 kHz to 160 kHz. (b) Frequency range: 1 kHz to 24 MHz.

Figure 4.18 (b) shows the open circuit sensitivity of the nine PVDF transducers, from 1 kHz to 25 MHz. At high frequencies, the sensitivity behavior is not flat. It presents a resonance behavior at a specific frequency for each thickness. However, several peaks appear in the graphic for one thickness. It is necessary to remember that the model used is valid only for frequencies lower than the resonance frequency established by $\lambda/4$, therefore, only the first increasing peak represents the resonance, while the others are just integer multiples of the first one, resulting from the mathematical model. From the nine transducers, there are only three resonance frequencies, which are defined by the film thickness: the thicker the film, the lower the resonance frequency, although the sensitivity amplitude increases. The active area does not affect this behavior.

4.2.1.1.2 Closed Circuit

Figure 4.19 (a) shows the closed circuit sensitivity of the nine PVDF transducers, from 1 kHz to 160 kHz, using the cable and electrical loading impedances, while Table 4.6 lists the sensitivities' average and range for the transducers. As it can be seen from the figure and the table, the response is completely flat, having a maximum variation of 18×10^{-3} dB. Since the range is so small, representing less than the 0.016% of the mean for all the cases, the closed circuit sensitivity can be considered constant in the frequency range from 1 kHz to 160 kHz.

Table 4.6. Simulated closed circuit receiving sensitivity mean from 1 to 160 kHz.

PVDF TRANSDUCER		SENSITIVITY MEAN (dB re 1 V/Pa)
RADIUS (mm)	THICKNESS (μm)	
2	28	-113.7162
	52	-112.1592
	110	-111.0397
3	28	-108.4858
	52	-106.3261
	110	-104.6677
4	28	-105.3252
	52	-102.6372
	110	-100.4427

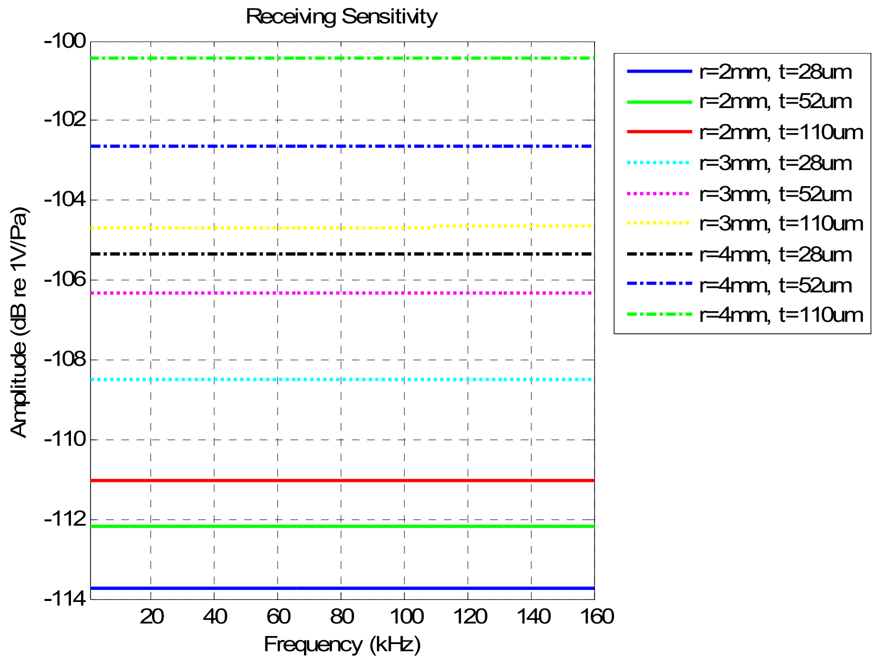

(a)

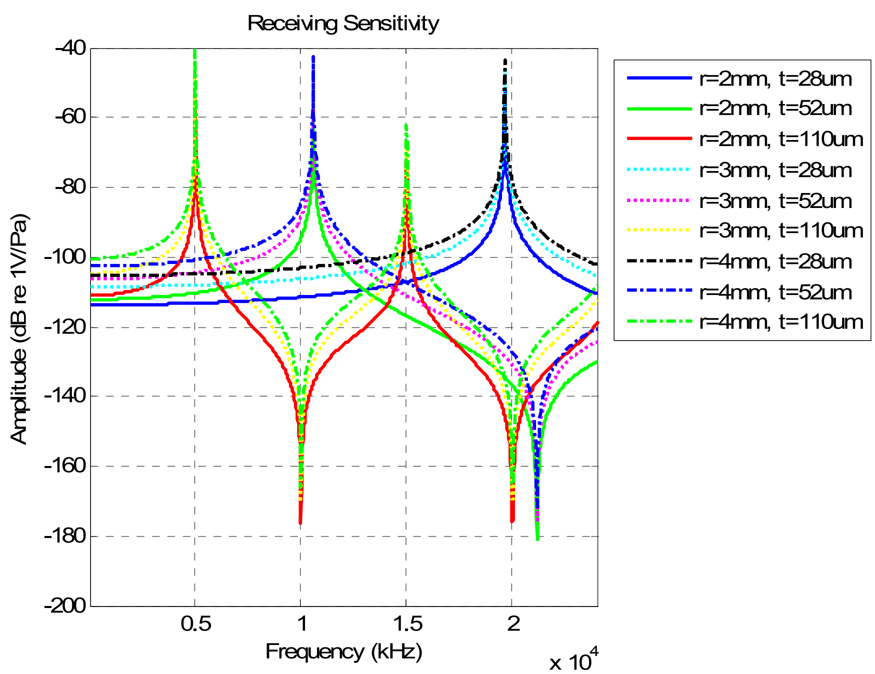

(b)

Figure 4.19. Simulated closed circuit receiving sensitivity as function of frequency, for the 9 PVDF transducers constructed. Amplitude in dB (re 1 V/Pa). (a) Frequency range: 1 kHz to 160 kHz. (b) Frequency range: 1 kHz to 24 MHz.

As seen in Figure 4.19 (a) for low frequencies, the sensitivity increases as the area and the thickness increase. However, opposite to the open circuit sensitivity case, the active area variations have more influence than the thickness variations, since the transducers with the greater sensitivities are the ones with the greater area. This behavior can be attributed to the load impedance impact (cable and instrumentation amplifier), which diminishes the piezoelectric film capacitance effect.

Figure 4.19 (b) shows the closed circuit sensitivity of the nine PVDF transducers, from 1 kHz to 25 MHz. As in the open circuit case, at high frequencies the sensitivity behavior is not flat with respect to frequency and presents a resonance frequency that depends only on the piezoelectric film thickness. Although several peaks appear in the graphic for the same thickness, only the first one is real since the model used is valid only for frequencies lower than the resonance frequency established by $\lambda/4$. From the nine transducers, there are only three resonance frequencies, which are defined by the film thickness: the thicker the film, the lower the resonance frequency, although the sensitivity amplitude increases somewhat. The active area does not affect this behavior, just the starting amplitude at low frequencies.

However, despite of these resonant behaviors, there is a flat response frequency range for both cases, open and closed circuit, at frequencies well below the resonance frequency. In order to confirm this statement, a simulation was performed with the 9 transducers in closed circuit, from 1 kHz to 500 kHz, and is presented in Figure 4.20. As seen from the figure, the response is completely flat, having a maximum variation of 82.5×10^{-3} dB. Since the range is so small, representing less than the 0.08% of the mean for all the cases, the closed circuit sensitivity can be considered constant in the frequency range from 1 kHz to 160 kHz for the three thicknesses used (28, 52 and 110 μm).

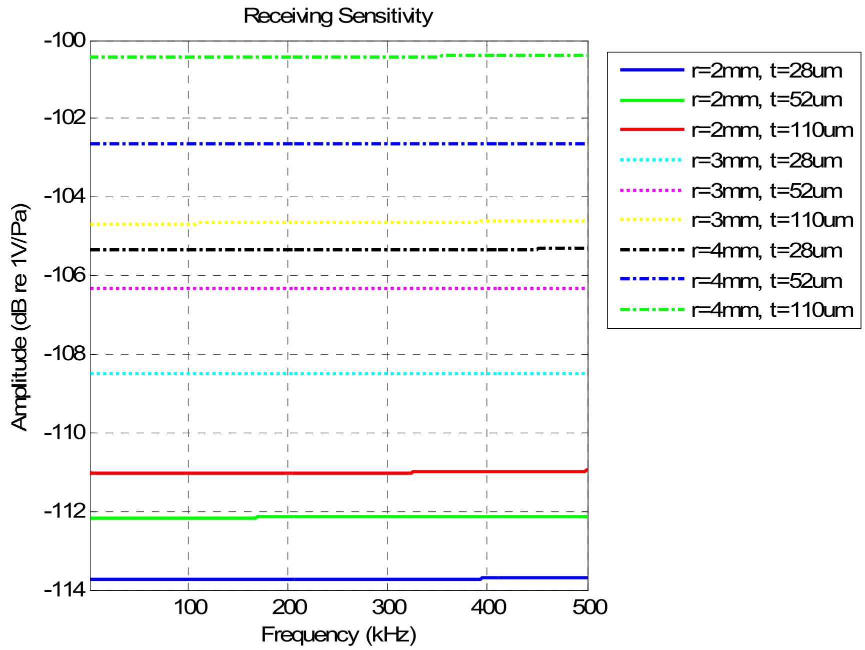

Figure 4.20. Simulated closed circuit receiving sensitivity as function of frequency, for the 9 PVDF transducers constructed. Amplitude in dB (re 1 V/Pa). Frequency range: 1 kHz to 500 kHz.

4.2.1.2 Receiving sensitivity as function of Radius

As it was observed, the receiving sensitivity can be modified by changing the active area radius. In order to allow an analysis on how these changes affect the transducer performance, a simulation was realized in which the radius was varied from 1 to 100 mm in a continuous form. This range was selected arbitrarily, for convenience.

From the previous figures it was observed that the transducers have a completely flat frequency response, as long as the frequency range is well below the resonance frequency. Therefore, a unique average sensitivity can be calculated for the frequency range of interest, given a specific radius and thickness, by calculating the sensitivity mean. In that form, a constant value was obtained for each transducer configuration, instead of a sequence as function of frequency. Subsequently, the radius was changed continuously from 1 to 100 mm and the sensitivity mean was calculated for each value, in the frequency range of 1 kHz to 160 kHz. This was repeated for three different thicknesses (28, 52 and 110 µm). The results are presented in Figure 4.21 (a) for open circuit, and Figure 4.21 (b) for closed circuit.

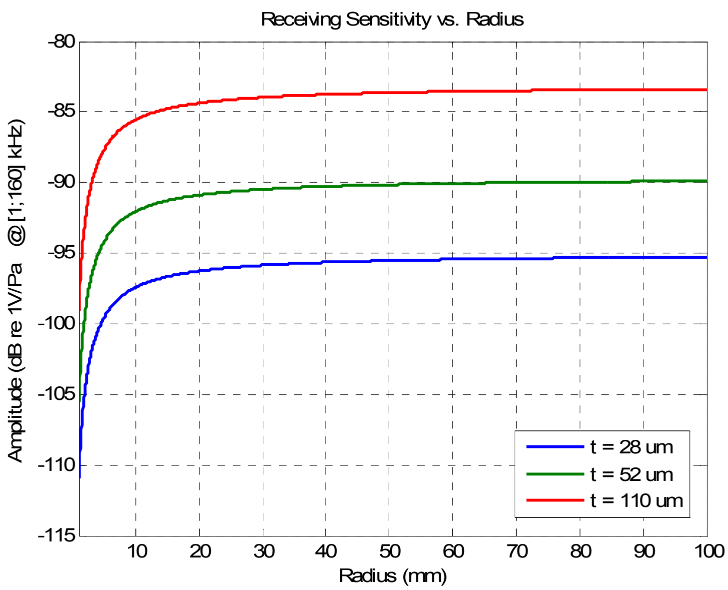

(a)

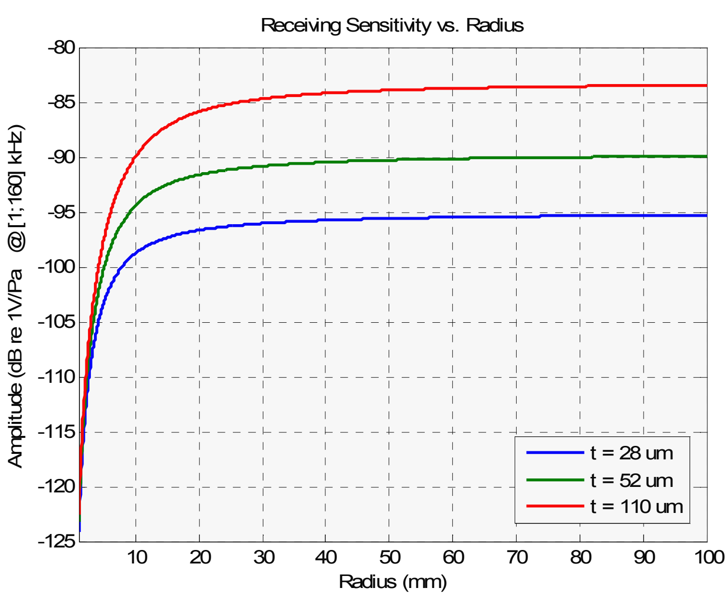

(b)

Figure 4.21. Simulated receiving sensitivity average as function of radius (from 1 to 100 mm), for 3 different thicknesses (25, 52 and 110 µm). Amplitude in dB (re 1 V/Pa). Frequency range: 1 kHz to 160 kHz. (a) Open circuit. (b) Closed circuit.

Although the sensitivity increases with the radius, this is valid only for small radiuses. The sensitivity slowly tends to stabilize and increasing the radius will not produce any changes on the sensitivity, for open and closed circuit, at least if the frequency range is maintained constant. This can be demonstrated with Figure 4.22, where the radius was varied from 1 mm to 1m.

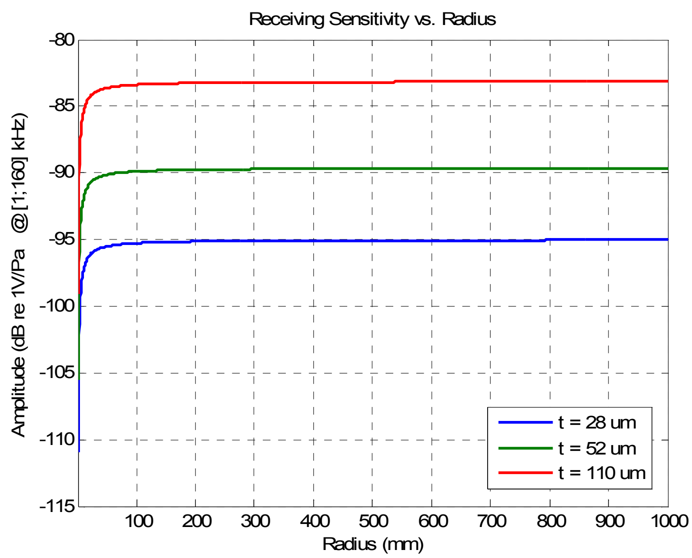

(a)

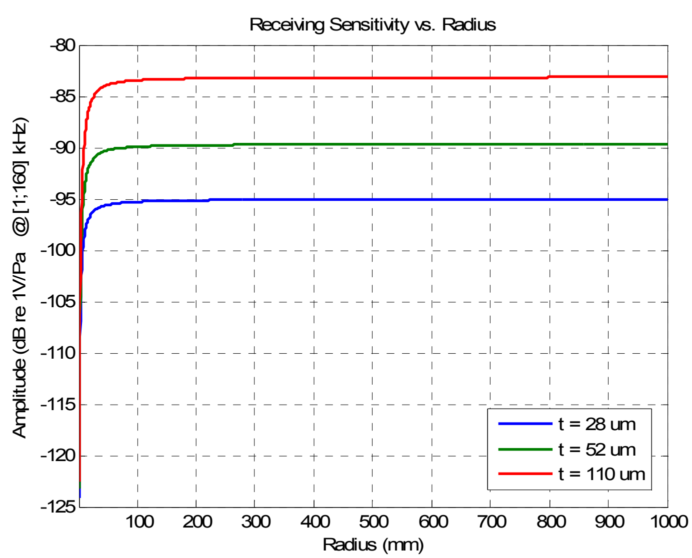

(b)

Figure 4.22. Simulated receiving sensitivity average as function of radius (from 1 mm to 1 m), for 3 different thicknesses (25, 52 and 110 μm). Amplitude in dB (re 1 V/Pa). Frequency range: 1 kHz to 160 kHz. (a) Open Circuit. (b) Closed Circuit.

4.2.1.3 Receiving sensitivity as function of Thickness

The receiving sensitivity can also be modified by changing the piezoelectric film thickness. In order to allow an analysis on how these changes affect the transducer performance, a simulation was realized in which the thickness was varied from 3.4 to 340 μm in a continuous form. The maximum thickness used was selected in order to maintain the frequency range (1 kHz to 160 kHz) well below the resonance frequency, which is given by the speed of sound in the piezoelectric film, over four times the film thickness. This condition guaranties the flat frequency behavior required to consider the sensitivity as independent of frequency. The resonance frequency must be at least 10 times the maximum frequency to be tested, which was 160 kHz. Then, for a resonance frequency of at least 1.6 MHz, the corresponding maximum PVDF film thickness is 343.75 μm.

Once the flat frequency response was guarantied, the sensitivity mean was calculated for the frequency range of interest, given a specific radius and thickness. In that form, a constant value was obtained for each transducer specification, instead of a sequence as function of frequency. The thickness was changed continuously from 3.4 to 340 μm and the sensitivity mean was calculated for each value, in the frequency range of 1 kHz to 160 kHz. This was repeated for three different active area radiuses (2, 3 and 4 mm). The results are presented in Figure 4.23 (a) for open circuit, and Figure 4.23 (b) for closed circuit.

The receiving sensitivity depends on the piezoelectric film thickness for both cases, open and closed circuit, increasing as the thickness increases. However, for the open circuit, its influence is categorically more marked than for the closed circuit, as it can be seen from the graphics. For the open circuit case, the sensitivity increases 40 dB from its lower value, at thickness = 3.4 μm, to its highest, at thickness = 340 μm. This range is the same for all the radiuses. In contrast, for the closed circuit case, the sensitivity increment is different for each radius, but in all cases is almost less than a half than with the open circuit case.

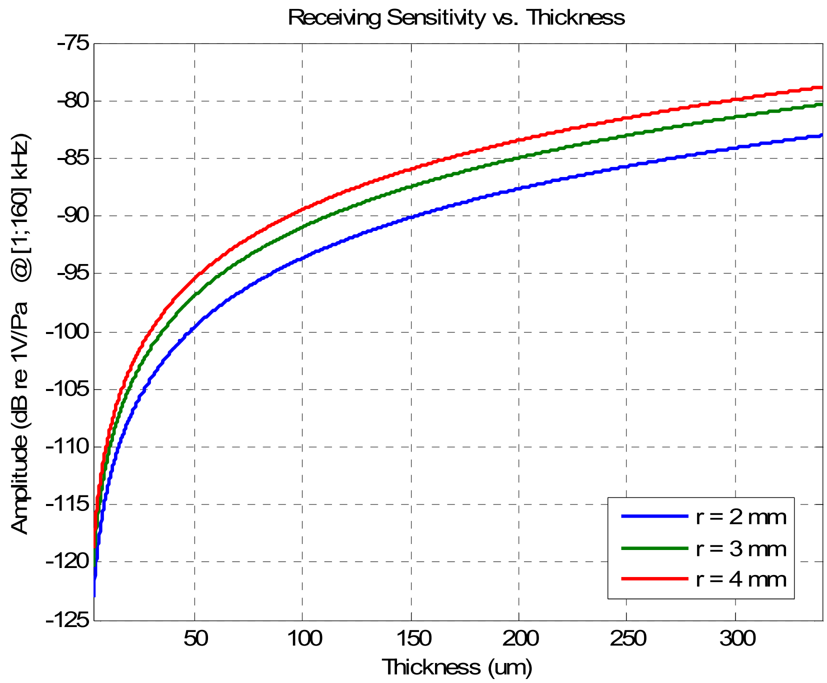

(a)

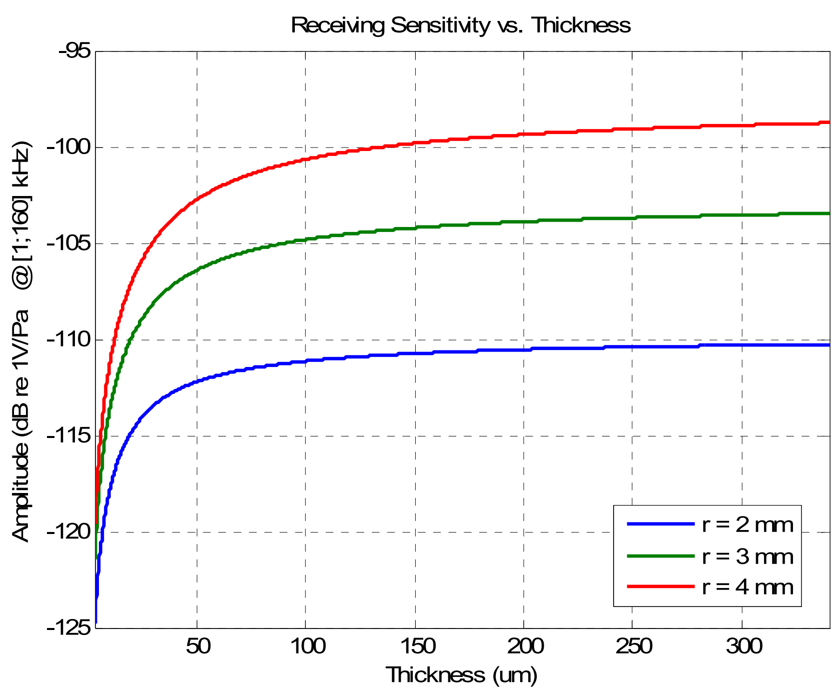

(b)

Figure 4.23. Simulated receiving sensitivity average as function of thickness (from 3.4 to 340 μm), for 3 different radiuses (2, 3 and 4 mm). Amplitude in dB (re 1 V/Pa). Frequency range: 1 kHz to 160 kHz. (a) Open circuit. (b) Closed circuit.

Since in this simulation the maximum thickness allowed to have flat frequency response was used, it does not make sense to extend the thickness range to see if the sensitivity increases indefinitely. However, from the previous simulations presented in this chapter, it can be deducted that the sensitivity will increase with thickness, as long as the resonance frequency is not reached.

4.2.1.4 Modifying the resistive load in Closed Circuit

In order to verify how the closed circuit model predicts the influence of the resistive electrical load on the receiving sensitivity, it was calculated for a transducer with a 3 mm active area radius and a thickness of 52 μm. The input resistance, connected in parallel to the transducer cable terminals and the instrumentation amplifier, was changed among 0.1, 1, 10 and 100 MΩ, and the sensitivity was calculated for the frequency range from 1 kHz to 160 kHz.

From Figure 4.24 (a), it was observed that this resistance only affects the low frequency sensitivity behavior. Then, the sensitivity was calculated for the partial frequency range from 1 kHz to 20 kHz, and is presented in Figure 4.24 (b). The effect of this resistance can be understood as a RC high pass filter, formed with the piezo film and cable capacitances.

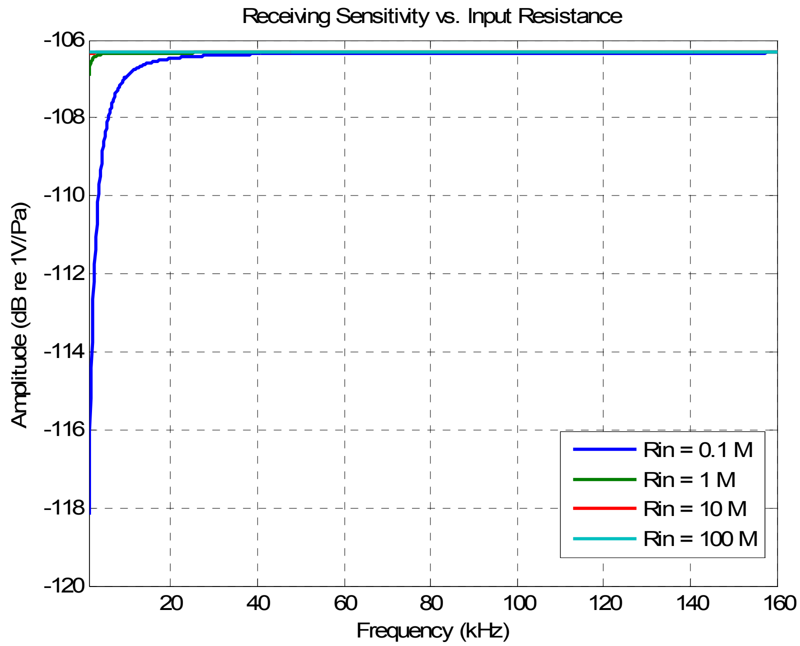

(a)

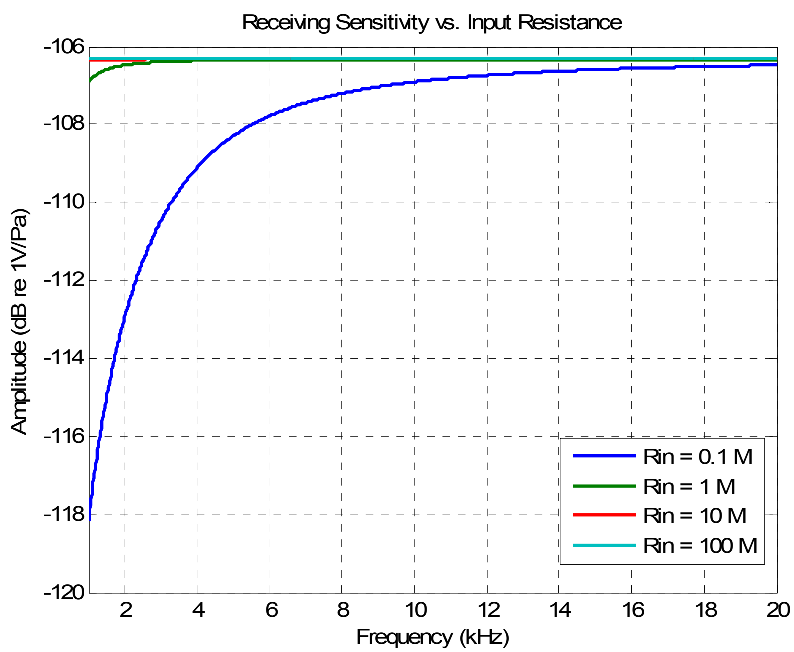

(b)

Figure 4.24. Simulated receiving sensitivity for a PVDF transducer modifying the signal conditioning circuit input resistance (0.1, 1, 10 and 100 MΩ). Amplitude in dB (re 1 V/Pa). (a) Frequency range: 1 kHz to 160 kHz. (b) Frequency range: 1 kHz to 20 kHz.

4.2.2 TRANSMITTING SENSITIVITY

The transducer model described in section 3.2.2 (page 56) was simulated using MATLAB, in order to observe the transducer's transmitting sensitivity as a function of frequency, transducer radius and film thickness. The sensitivity is simulated for the nine implemented transducers, using the combination of changing the three radiuses (2, 3 and 4 mm) and three thicknesses (28, 52 and 110 µm), and the results are presented in Figure 4.25. The frequency range used was from 1 kHz to 160 kHz.

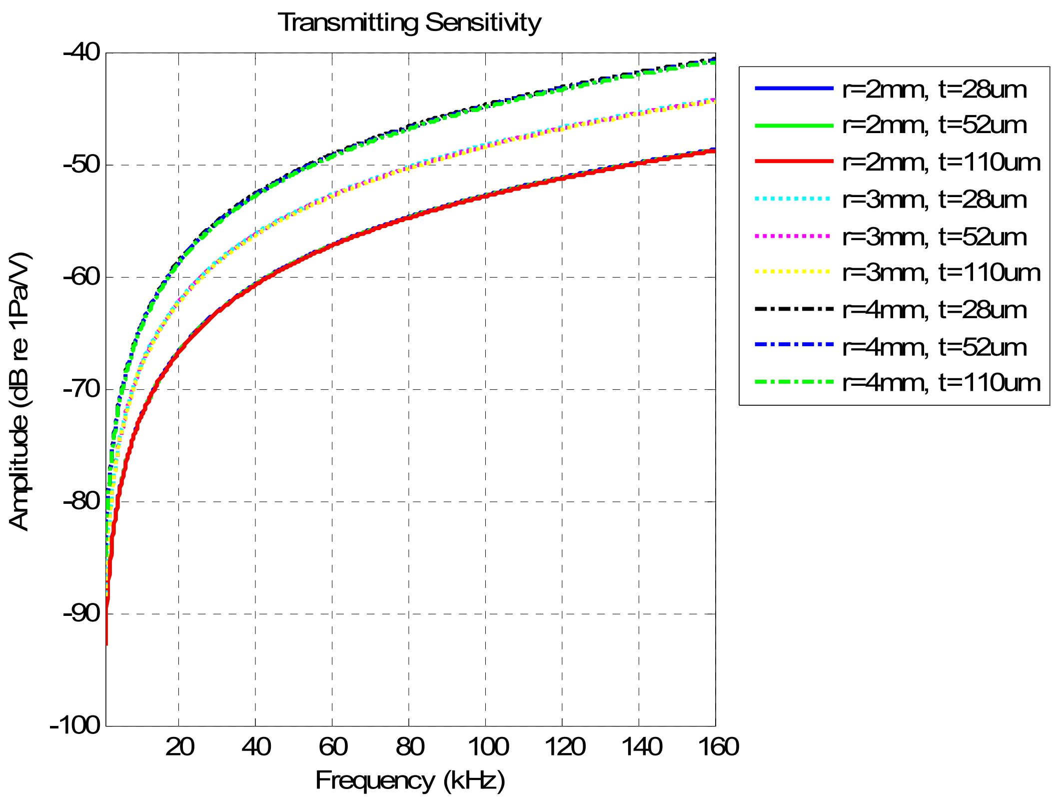

Figure 4.25. Simulated transmitting sensitivity as function of frequency, for the 9 PVDF transducers constructed. Amplitude in dB (re 1Pa/V). Frequency range: 1 kHz to 160 kHz.

In contrast with the receiving sensitivity, the PVDF transducers transmitting sensitivity is not flat, and it increases with increasing frequency. Besides, the transmitting sensitivity depends almost exclusively on the transducer active area, increasing as the radius increases. Respect to the piezoelectric film thickness, it does not affect considerably the transmitting sensitivity.

Table 4.7. Simulated transmitting sensitivity mean from 1 to 160 kHz.

PVDF TRANSDUCER		**SENSITIVITY MEAN (dB re 1 Pa/V)**
RADIUS (mm)	**THICKNESS (µm)**	
2	28	-57.1543
	52	-57.2018
	110	-57.2343
3	28	-52.6876
	52	-52.7690
	110	-52.8327
4	28	-49.1041
	52	-49.2084
	110	-49.3015

Table 4.7 lists the simulated transmitting sensitivity mean for the nine PVDF transducers. For all the transducers, the sensitivities increase approximately 44 dB from its lower value, at frequency = 1 kHz, to its highest, at frequency = 160 kHz, although the maximum and minimum sensitivity values change from one transducer to another. This range represents the transducer sensitivity increment due to the increment in frequency.

On the other hand, keeping the radius constant, the transmitting sensitivity variation obtained from the greater thickness (110 µm) to the minimum (28 µm), was of 0.08 dB for the transducers with radius = 2 mm, 0.15 dB for the transducers with radius = 3 mm, and 0.20 dB for the transducers with radius = 4 mm, confirming that the thickness influence on the transmitting sensitivity is very limited. Therefore, for transmitting applications, the transducer radius is the design parameter that affects the response the most.

Although these results are consistent with the theory, it could be possible that the model used underestimated the piezofilm thickness effects, since it was created for piezoelectric crystals, which are thicker than piezo films, and are normally employed at higher frequencies, near their resonance frequency.

4.3 COMPARISON BETWEEN EXPERIMENTAL AND SIMULATION RESULTS

In this section, the experimental results are compared with the simulations and the trends noticed from the experimental data are analyzed based on the results expected from the theoretical models.

4.3.1 PVDF RECEIVING BEHAVIOR

The experimental data showed that the total system transfer function (section 4.1.2) and the PVDF receiving sensitivity (section 4.1.3) depend on the active area radius, and as it increases, the amplitude increases, for the three different thicknesses, in all the frequency range. This behavior is in good agreement with the response projected by the model simulated, were PVDF receiving sensitivity was found to be proportional to the active area radius.

With respect to thickness, no definite trend was observed that allows to visually establish a clear relation between the film thickness and the transfer functions for the complete system or the PVDF sensitivity. This behavior was not expected based on the simulation results, since the simulated data showed a slightly amplitude increase with the thickness increase. However, since the sensitivity differences for transducers with the same area varying the thickness, was found to be small in simulations, the experimental results can still be considered consistent.

Additionally, it is necessary to consider that PVDF films are mechanically drawn to provide a microstructure suitable for strong piezoelectricity, and thicker PVDF films tend to be of poor quality with a tendency to undergo dielectric breakdown during the polarization stage [20]. Because of this, it is possible that the thicker films used had lower quality than the thinner, and consequently do not provide the best response.

Figure 4.26 displays the simulated and experimental receiving behavior of the nine transducers in one graph.

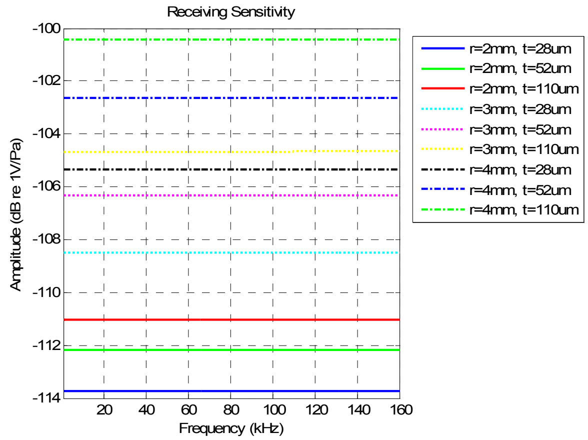

(a)

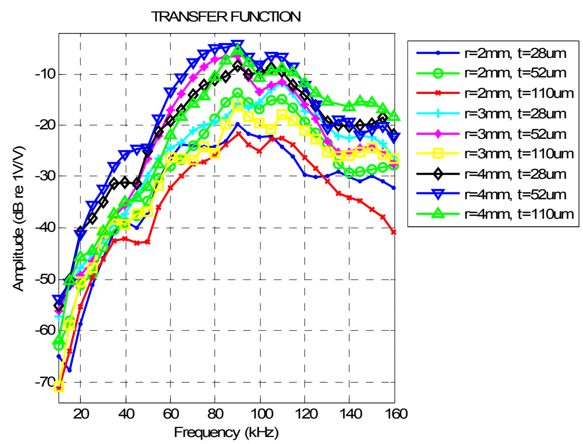

(b)

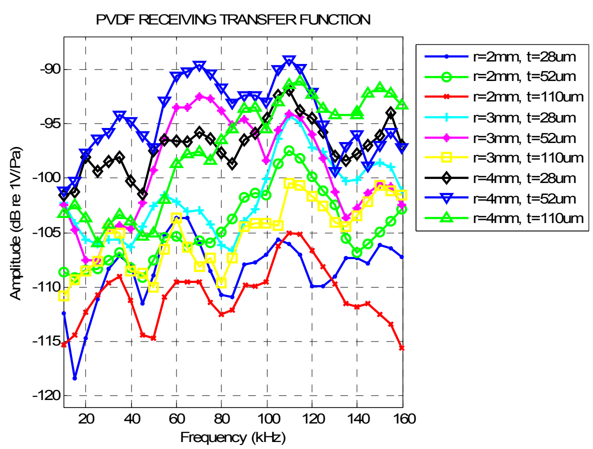

(c)

Figure 4.26. Receiving behavior as function of frequency, for the 9 PVDF transducers constructed. (a) Simulated closed circuit sensitivity. Amplitude in dB (re 1 V/Pa). (b) Experimental total system transfer function. Amplitude in dB (re 1 V/V). (c) Experimental compensated sensitivity. Amplitude in dB (re 1 V/Pa).

As seen in Figure 4.26 (a), the simulated receiving sensitivity has a completely flat frequency behavior. However, the total system transfer function seen in Figure 4.26 (b) is highly dependent on frequency. Its amplitude increases with frequency until approximately 90 kHz, and then it starts decreasing. This behavior is consistent with the expected since the complete system includes the Reson TC4033 as a transmitter, which transmitting sensitivity increases with frequency until resonance at 90 kHz, and then starts decreasing, as shown in Figure 3.30 (b).

Alternatively, in an attempt to minimize the frequency effects caused by the Reson as transmitter and the signal conditioning circuit, a transfer function compensation was applied resulting in the PVDF receiving sensitivity shown in Figure 4.26 (c). Although the compensated PVDF sensitivity presents a behavior less dependent on frequency than the one found for the total acoustic system transfer function, it is not completely flat as it was expected. However, there is not a marked tendency applicable to all the cases that clearly indicates a relation between sensitivity and frequency, except for an increment near 110 kHz.

This behavior can be caused by an inaccuracy in the function used to approximate the Reson transmitting sensitivity. Besides, the model used does not consider the effects caused by the conductive tape used to attach the PVDF film to the copper board. This additional layer could be affecting the transducer frequency response.

4.3.2 PVDF TRANSMITTING BEHAVIOR

The experimental data showed that, similar to the receiving behavior, the total system transfer function (section 4.1.4) and the PVDF transmitting sensitivity (section 4.1.5) depend on the active area radius, and as it increases, the amplitude increases, for the three different thicknesses, in all the frequency range. This behavior is in good agreement with the response projected by the model simulated, were PVDF transmitting sensitivity was found to be proportional to the active area radius.

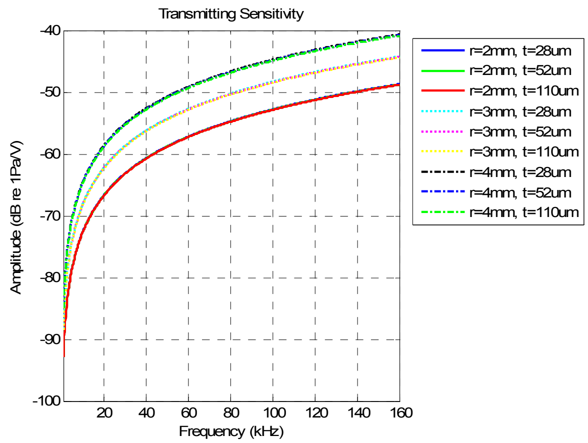

(a)

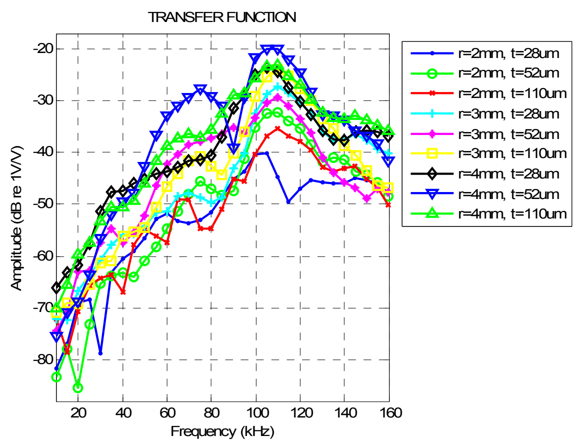

(b)

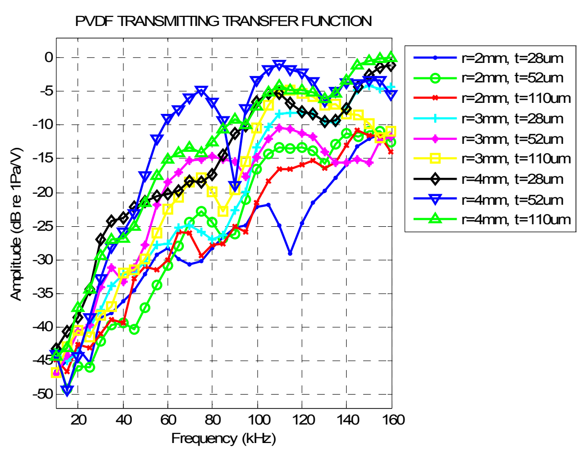

(c)

Figure 4.27. Transmitting behavior as function of frequency, for the 9 PVDF transducers constructed. (a) Simulated closed circuit sensitivity. Amplitude in dB (re 1 Pa/V). (b) Experimental total system transfer function. Amplitude in dB (re 1 V/V). (c) Experimental compensated sensitivity. Amplitude in dB (re 1 Pa/V).

The experimental transfer functions amplitude appears to be approximately the same for the transducers with equal area, but different thicknesses, indicating that the thickness has not a noticeable influence in the transfer function amplitude. Therefore, the experimental results agree with the simulation results, since the sensitivity differences for transducers with the same area varying the thickness, was found to be almost null in simulations (section 4.2.2).

With respect to frequency, the simulations demonstrated a transmitting sensitivity permanently increasing with frequency for the range of interest, as seen in Figure 4.27 (a). The total system transfer function seen in Figure 4.27 (b) is highly dependent on frequency. Its amplitude increases with frequency until approximately 105 kHz, and then it decreases slowly. This behavior is consistent with the expected since the complete system includes the Reson TC4033 as a receiver, which receiving sensitivity increases with frequency until resonance at 105 kHz, and then starts decreasing, as shown in Figure 3.30 (a).

Alternatively, in an attempt to minimize the frequency effects caused by the Reson as receiver and the signal conditioning circuit, a transfer function compensation was applied resulting in the PVDF transmitting sensitivity shown in Figure 4.27 (c). The compensated sensitivity is proportional to the frequency, increasing the magnitude when the frequency increases, but with a higher rate for low frequencies, in the same way observed for the simulated sensitivity. The maximum experimental increment in sensitivity for all the frequency range is approximately 48.4 dB, and the minimum is 33.6 dB, values that are close to the sensitivity increase of 44 dB found in the simulations. Therefore, the compensated transmitting sensitivity frequency behavior experimentally found is in good agreement with the response projected by the model simulated.

5 CONCLUSIONS AND RECOMMENDATIONS

Nine different PVDF transducers were developed to be used as receivers and transmitters in underwater applications, such as acoustic reflectometry studies. The nine transducers were created through the combination of three different PVDF film thicknesses (28, 52 and 110 µm) and three circular active areas (with radius 2, 3 and 4 mm). They represent a novel transducer concept because of their working range, from 10 kHz to 160 kHz, and their physical construction, easily shaped to customized applications.

The PVDF transducers receiving and transmitting behavior was studied through computer simulations and experimental tests, with respect to three main parameters: frequency, active area and film thickness.

Modeling only the transducer, without any electrical load connected to it, the open circuit receiving sensitivity was simulated. Under these conditions, the sensitivity is proportional to the active area and thickness. This means that the open circuit receiving sensitivity increases as any of the two (or both) mentioned parameters increase. However, the effect of film thickness on sensitivity is much larger than the effects from changing active area. For our specific case, the thickness changes (from 28 µm to 110 µm) generate a sensitivity increase of 11.9 dB, which is almost three times the increase generated by changing the active area (from radius 2 mm to 4 mm). Although this information is useful to better understand the transducer behavior, it is impossible to make a comparison with experimental data, since the voltage acquisition will always generate an electrical load to the transducer.

The closed circuit receiving sensitivity was modeled and simulated, concluding that the electrical load connected to the transducer plays a decisive role in the transducer's sensitivity performance. Although for this case the sensitivity also increases with increasing the active area or the thickness, the relation between the parameters impact is inverse from the encountered for the open circuit case. The closed circuit receiving sensitivity is affected more by changes in area, than by changes in thickness, at least for frequencies well below the resonance frequency.

For our specific case, the active area changes (from radius 2 mm to 4 mm) generate a sensitivity increase of approximately 2.5 times the increase generated by changing the thickness (from 28 μm to 110 μm). This behavior can be explained because of the electrical load capacitive component, given by the cable capacitance (C_{cable}) connected in parallel with the instrumentation amplifier input capacitance, which in this case is almost despicable compared with C_{cable}. The PVDF transducer capacitance depends on the piezofilm thickness and area. However, since C_{cable} is larger than the transducers' capacitance (C_{PVDF}), the variations in C_{PVDF} due to thickness changes, do not longer affect considerably the sensitivity behavior. However, as it was expected, the resonance frequency is not affected because it depends on the piezofilm thickness, not its capacitance. Therefore, the cable used to connect the transducers considerably impacts the receiving sensitivity.

On the other hand, the resistive load component affects the closed circuit receiving sensitivity frequency response since it will form a RC high-pass filter with the transducer, where the cut-off frequency is inversely proportional to the resistance. The input resistance should be selected as high as possible, but being careful that undesired low frequency noise does not saturate the pre-amplifier. This noise can include the voltage generated by the PVDF pyroelectric properties. In applications where temperature changes are a concern, this resistance should be carefully selected. In general, it is advisable to use an external resistance connected in parallel with the transducer's output, since the instrumentation amplifier input resistance is generally very large.

The constructed PVDF transducers were tested using amplitude modulated Hanning pulses with a duration of 200 μs, shifting the carrier frequency from 10 kHz to 160 kHz, at intervals of 5 kHz. To characterize the receiving sensitivity, the pulses were sent with a Reson TC4033 transducer, and received with the PVDF transducers. After processing the signals acquired, the experimental results showed an evident tendency for the receiving sensitivity, increasing as the active area increased. This result coincides with the trends obtained from the model. With respect to thickness, it was not possible to detect, from the experimental results, a clear relation between the receiving sensitivity and the piezofilm thickness, although based on the simulations, small increments were expected when incrementing thickness. This can be explained considering that there are reports in the literature which indicate that due to the fabrication process of PVDF films, the piezoelectric characteristics and quality can be reduced for thicker films,

From the simulations, the receiving sensitivity was found to be almost constant with respect to frequency, as long as the transducers are operated well below the resonance frequency. Considering the PVDF thicknesses used (28, 52 and 110 μm), the resonance frequencies should be at 19.6 MHz, 10.6 MHz and 5 MHz, respectively, which are much larger than the maximum carrier frequency tested (160 kHz). The PVDF receiving sensitivity experimentally obtained presents a behavior less dependent on frequency than the one found for the total acoustic system transfer function, but it is not completely flat as it was expected. However, there is not a marked tendency applicable to all the cases that clearly indicates a relation between sensitivity and frequency. This behavior can be caused by an inaccuracy in the function used to approximate the Reson transmitting sensitivity, and additionally, there are factors that are not been considered in the model and, despite all efforts to be minimized, could be affecting the measurements, such as reflections, noise and adhesive layers.

The PVDF transducers were modeled as transmitters too, using the KLM model. A computer simulation was implemented to predict the transmitting sensitivity behavior with respect to frequency, piezofilm thickness and active area. The simulations reveal that the transmitting sensitivity increases, as the transducer active area increases, but the piezofilm thickness does not have an appreciable influence over the sensitivity in the frequency range of interest (from 10 kHz to 160 kHz).

The constructed PVDF transducers were tested as transmitters using the same amplitude modulated Hanning pulses, shifting the carrier frequency from 10 kHz to 160 kHz, at intervals of 5 kHz. To characterize the transmitting sensitivity, the pulses were sent with the PVDF transducers and received with a Reson TC4033 hydrophone. After processing the acquired signals, the experimental results showed an evident trend for the transmitting sensitivity, increasing as the active area increased. For thickness, there was not any detectable trend that relates the transmitting sensitivity to the thickness. These results are in good agreement with the behavior expected based on the simulations.

With respect to frequency, the PVDF transducers increase their transmitting sensitivity as the frequency increases, at least for the frequency range of interest. This was found to be true for both, the simulations and the experimental results. The sensitivity increase due to the changes of frequency (from 10 kHz to 160 kHz) for the simulation was 44 dB, while the experimental sensitivity increase mean for the nine transducers implemented, using the same frequency range was approximately 40.5 dB, which is close to what was expected. It can be concluded that the model used appropriately projects the transducer transmitting response for frequencies well below the resonance frequency.

During the research, different construction methods and techniques were used to implement the PVDF transducers. It was found that the electrodes connection is the most critical part in the physical design, since the electrode contacts must not damage the piezofilm and can introduce noise if they are not isolated, specially the positive electrode. Besides, since the transducer is based on a thin film, the size is very much determined by the external connections design. It was concluded that the last construction method used, attaching the PVDF film to a pre-engraved conductive base, is suitable and provides an excellent method to connect the electrodes without affecting the piezofilm physical properties. In addition, several water proof cases were tested, concluding that the case molded with epoxy material offers the most advantages. The main asset of this kind of case is that it can be easily shaped to satisfy any specific application requirements, without the necessity of changing the transducer core. It could be molded to attach the transducer to a determined space geometry, for example a tube wall.

5.1 RECOMMENDATIONS

The transducers developed open a wide range of new possibilities to be explored as future work. It would be useful to establish how the transducers sensitivity is related with other physical parameters such as active area shape, backing materials, adhesive materials, etc. Besides, the experiments could be expanded to higher frequencies in order to verify the resonance behavior predicted by the theory, and how the different parameters affect the sensitivity at high frequencies. The effects of changing distance and angle between the transmitter and receiver could be studied, and it is recommended to perform the experiments in an anechoic tank, which would help to improve the quality of the measurements and enable the execution of different tests. In addition, considering the problems encountered in this and other researches with thicker PVDF films, it would be interesting to develop similar hydrophones as the ones described here, but using multilayer laminated PVDF membranes.

Finally, although the transducers created are relatively small (from approximately 8 mm diameter, to 12 mm), the same construction techniques used in this research could be used to build smaller transducers, but it would be necessary to eliminate some of the manual processes, and replace them for more specialized processes, specially the electrode printing. The cable selection would be an important factor too, not only because of its electrical characteristics, but for its size.

6 REFERENCES

1. http://www.who.int/cardiovascular_diseases/en/.

2. http://www.americanheart.org.

3. http://www.worldheart.org/.

4. D.B. Sharp, *Acoustic Pulse Reflectometry for the Non - Invasive Monitoring of Ducts*, Open University, Faculty of Technology, Milton Keynes: UK. p. 1 - 6.

5. M.M. Sondhi and B. Gopinath, *Determination of vocal - tract shape from impulse response at the lips.* Journal of Acoustic Soc. Am., 1971. **49**(6): p. 1867 - 1873.

6. A.C. Jackson, J.P. Butler, E.J. Millet, F.G. Hoppin, and S.V. Dawson, *Airway geometry by analysis of acoustic pulse response measurements.* Journal of Applied Physiology, 1977. **43**(3): p. 523 - 536.

7. J.J. Fredberg, G.M. Glass, M.E. Wohl, and H.L. Dorkin, *Airway area by acoustic reflections measured at the mouth.* Journal of Applied Physiology, 1980. **48**(5): p. 749 - 758.

8. A.H. Benade and J.H. Smith, *Brass wind instrument impulse response measurements.* Journal of Acoustic Soc. Am., 1981. **70**(22).

9. R.D. Ayers, L.J. Eliason, and M.M. Salem, *Multiple reflections in simple bore shapes.* Journal of Acoustic Soc. Am., 1985. **77**(90).

10. R.D. Ayers, L.J. Eliason, and M.M. Salem, *An acoustic pulse generator for wind instrument bores.* Journal of Acoustic Soc. Am., 1985. **77**(89).

11. D.B. Sharp, *Acoustic pulse reflectometry for the measurement of musical wind instruments*. 1996, University of Edinburgh.

12. D.B. Sharp, D.M. Campbell, and A. Myers, *Input Impedance Measurements on wind Instruments using Pulse Reflectometry*, in *Department of Physics*, University of Edinburgh. p. 1 - 4.

13. D.T. Raphael, *Acoustic Reflectometry Profiles of Endotracheal and Esophageal Intubation.* Anesthesiology, 2000. **92**(5): p. 1293 - 1299.

14. D.T. Raphael, M. Benbassat, D. Arnaudov, A. Bohorquez, and B. Nasseri, *Validation Study of Two-microphone Acoustic Reflectometry for Determination of Breathing Tube Placement in 200 Adult Patients.* Anesthesiology, 2002. **97**(6): p. 1371-1377.

15. B. Louis, R. Fodil, S. Jaber, J. Pigeot, P.H. Jarreau, F. Lofaso, and D. Isabey, *Dual assessment of airway area profile and respiratory input impedance from a single transient wave.* Journal of Applied Physiology, 2001. **90**: p. 630 - 637.

16. E.J. Juan and G. Wodicka, *Miniature Acoustic Guidance System for Endotracheal tubes*, in *PhD Thesis in Electrical Engineering*. 2001, Purdue University.

17. S. Bryan and R. Darke, *Use of Acoustic Reflectometry for Home Monitoring of Otitis Media in a High-Risk Pediatric Population.* The Permanent Journal, 2003. **7**(3).

18. S.L. Ordoñez, *Guidance and Monitoring of Liquid - Filled Tubes Using Time Domain Acoustic Reflectometry*, in *M.S. Thesis in Electrical Engineering*. 2005, University of Puerto Rico: Mayagüez, Puerto Rico. p. 133.

19. H.M. Figueroa, *Estimation of Vessel Wall Compliance Using Acoustic Reflectometry*, in *M.S. Thesis in Electrical Engineering*. 2006, University of Puerto Rico: Mayaguez, Puerto Rico. p. 135.

20. S. Robinson, R.C. Preston, M. Smith, and C. Millar, *PVDF Reference Hydrophone Development in the UK - From Fabrication and Lamination to Use as Secondary Standards.* IEEE Transactions on Ultrasonics, Ferroelectrics, and Frequency Control, 2000. **47**(6): p. 1336 - 1344.

21. F.S. Foster, K.A. Harasiewiez, and M.D. Shcar., *A History of Medical and Biological Imaging with Polyvinylidene Fluoride (PVDF) Transducers.* IEEE Transactions on Ultrasonics, Ferroelectrics, and Frequency Control, 2000. **47**(6): p. 1363 - 1371.

22. F.S. Foster, K.A. Harasiewiez, and C.J. Pavlin, *Advances in ultrasound biomicroscopy.* Journal of Ultrasound Med. Biol., 2000. **26**: p. 1-27.

23. W. Galbraith and G. Hayward, *Development of a PVDF Membrane Hydrophone for use in Air-Coupled Ultrasonic Transducer Calibration.* IEEE Transactions on Ultrasonics, Ferroelectrics, and Frequency Control, 1998. **45**(6): p. 1549 - 1558.

24. B. Granz, *PVDF Hydrophone for the Measurement of Shock Waves.* IEEE Transactions on Electrical Insulation, 1989. **24**(3): p. 400-403.

25. D. Cathignol. *PVDF Hydrophone with Liquid Electrodes for Shock Wave Measurements*. in *IEEE Ultrasonics Symposium*. 1990.

26. J.P. Zheng. *Dielectric Properties of PVDF Films and Polymer Laminates with PVDF for Energy Storage Applications*. in *6th International Conference on Properties and Applications of Dielectric Materials*. 2000. Xi'an, China: Xi'an Jiaotong University.

27. P. Lum, M. Greenstein, C. Grossman, and T.L. Szabo, *High-Frequency Membrane Hydrophone.* IEEE Transactions on Ultrasonics, Ferroelectrics, and Frequency Control, 1996. **43**(4): p. 536-544.

28. M. Platte, *A polyvinylidene fluoride needle hydrophone for ultrasonic applications.* Ultrasonics, 1985: p. 113-118.

29. P.A. Lewin, G. Lypacewicz, R. Bautista, and V. Devaraju, *Sensitivity of ultrasonic hydrophone probes below 1 MHz.* Ultrasonics, 2000. **38**: p. 135-139.

30. K.C. Shotton, D.R. Bacon, and R.M. Quilliam, *A PVDF membrane hydrophone for operation in the range of 0.5 MHz to 15 MHz.* Ultrasonics, 1980: p. 123-126.

31. Y. Yiquan, S. Binwen, and L. Zongjie, *A New Multilayer Planar PVDF Standard Hydrophone and its Applications.* IEEE Transactions on Ultrasonics, Ferroelectrics, and Frequency Control, 1995. **42**(5): p. 958-965.

32. D.R. Fox, *A Low-Density Extended Acoustic Sensor for Low-Frequency Arrays.* IEEE Journal of Oceanic Engineering, 1988. **13**(4): p. 291-295.

33. P.A. Lewin and M.E. Shafer, *Wide-Band Piezoelectric Polymer Acoustic Sources.* IEEE Transactions on Ultrasonics, Ferroelectrics, and Frequency Control, 1988. **35**(2): p. 175 - 184.

34. www.reson.com.

35. www.dolphinear.com.

36. www.cetaceanresearch.com.

37. www.afabsound.com/products.htm.

38. www.chelsea.co.uk, Chelsea Technologies Group.

39. www.force.dk, Force Technology.

40. R. Pecha, www.rp-acoustics.de.

41. Y. Roh, V.V. Varadan, and V.K. Varadan, *Characterization of All the Elastic, Dielectric, and Piezoelectric Constants of Uniaxially Oriented Poled PVDF Films.* IEEE Transactions on Ultrasonics, Ferroelectrics, and Frequency Control, 2002. **9**(6): p. 836 - 847.

42. I. Measurements Specialties, *Piezo Film Sensors. Technical Manual*. 1999: Norristown, PA.

43. M. Castillo, P. Acevedo, and E. Moreno, *KLM model for lossy piezoelectric transducers.* Ultrasonics, 2003. **41**: p. 671-679.

44. S. Sherrit, S.P. Leary, B.P. Dolgin, and Y. Bar-Cohen. *Comparison of the Mason and the KLM Equivalent Circuits for Piezoelectric Resonators in the Thickness Mode*. in *IEEE Ultrasonics Symposium*. 1999.

45. T.A. Bigelow, *Experimental Evaluation of Nonlinear Indices for Ultrasound Transducer Characterizations*, in *Electrical Engineering Department*. 2001, University of Illinois: Urbana, IL. p. 150.

46. R.G. Swartz and J.D. Plummer, *Integrated Silicon-PVF2 Acoustic Transducer Arrays.* IEEE Transactions on Electronic Devices, 1979. **26**(12): p. 1921-1932.

47. C. Koch and W. Molkenstruck, *Primary Calibration of Hydrophones with Extended Frequency Range 1 to 70 MHz Using Optical Interferometry.* IEEE Transactions on Ultrasonics, Ferroelectrics, and Frequency Control, 1999. **46**(5): p. 1303-1315.

48. P.E. Bloomfield. *Dielectric and Piezoelectric Properties of Stacked and Plated PVDF, P(VDF/TeFE), P(VDF/TrFE) and Ceramic/Rubber Composite Thick Films*. in *Ninth IEEE International Symposium of Applications in Ferroelectrics*. 1995.

49. H.W. Joo, C.H. Lee, and H.K. Jung, *Identification of the piezoelectric material coefficients using the finite element method with an asymptotic waveform evaluation.* Ultrasonics, 2004. **43**: p. 13-19.

50. K.W. Kwok, H.L. Wah-Chan, and C.L. Choy, *Evaluation of the Material Parameters of Piezoelectric Materials by Various Methods.* IEEE Transactions on Ultrasonics, Ferroelectrics, and Frequency Control, 1997. **44**(4): p. 733 - 742.

51. P.E. Bloomfield, W.J. Lo, and P.A. Lewin, *Experimental Study of the Acoustical Properties of Polymers Utilized to Construct PVDF Ultrasonic Transducers and*

the Acousto-Electric Properties of PVDF and P(VDF/TrFE) Films. IEEE Transactions on Ultrasonics, Ferroelectrics, and Frequency Control, 2000. **47**(6): p. 1397-1405.

52. P.N. Gélat, R.C. Preston, and A. Hurrel, *A theoretical model describing the transfer characteristics of a membrane hydrophone and validation.* Ultrasonics, 2005. **43**: p. 331 - 341.

53. L.E. Kinsler, A.R. Frey, A.B. Coppens, and J.V. Sanders, *Fundamentals of Acoustics*. Third ed, ed. I. John Wiley & Sons. 1982, New York.

54. D.T. Blackstock, *Radiation from a Baffled Piston*, in *Fundamentals of Physical Acoustics*, I. John Wiley & Sons, Editor. 2000, Wiley-Interscience Publication: New York.

55. IEC, *Measurement and Characterization of Ultrasonic Fields using Hydrophones in the Frequency Range 0.5 MHz to 15 MHz*. 1991.

56. AIUM/NEMA, *Acoustic Output Measurement and Labeling Standard for Diagnostic Ultrasound Equipment*. 1992.

57. T. Kugelstadt, *Chapter 16. Active Filter Design Techniques*, in *Op Amps for Everyone*. 2001, Texas Instruments: Dallas, TX. p. 16.1-16.64.

58. www.ti.com, Texas Instruments.

59. www.national.com, National Semiconductors.